

**Exploration of In-Situ Diagnosis Methods for the  
Evaluation of Mechanical and Magnetic Performance  
of Hard Disk Drives**

ZHU JIN

**NATIONAL UNIVERSITY OF SINGAPORE**

**2005**

**Exploration of In-Situ Diagnosis Methods for the  
Evaluation of Mechanical and Magnetic Performance  
of Hard Disk Drives**

**ZHU JIN**

**(B.Eng (hons). HUST, P.R.China)**

**A THESIS SUBMITTED  
FOR THE DEGREE OF MASTER OF ENGINEERING  
DEPARTMENT OF ELECTRICAL AND COMPUTER ENGINEERING  
NATIONAL UNIVERSITY OF SINGAPORE**

**2005**

## **Acknowledgments**

Here I would like to thank for those who have accompanied me and helped me through this Master thesis work. Firstly, I would like to express my most sincere gratitude for my supervisor, Dr. Liu Bo, for his unselfish guidance, constructive advices and warmest encouragement in the past two years; His keen observation and strict research attitude contributed a great deal to the research work. I would also wish to thank Prof. Li Le-Wei, for his generous support and guidance to my research and thesis work.

Secondly, I would like to appreciate Ms. Zhang Wei, who has given me a lot of suggestions and help during my experimental work and methodology explorations. She always brought up some new ideas for experimental set up and data analysis, which helps me a lot in understanding more about the measurement methodology.

Thanks are also given to my friends, Ms. Liu Jin, Mr. Li Hui, Ms. Xiao Peiying, Ms. Ye Huanyi, Ms. Kek Eeling, Ms. Jiang Ying, Ms. Zhou Yipin, Mr. Han Yufei, and so on, for providing friendship and companionship through those happy and sad time.

Last but not least, I would like to thank my parents and my brother, who always encourage me and support me to pursue more colorful and fruitful life. Without their love, I could not have studied and lived in Singapore which is so far away from my hometown. Also thanks people who love me and people I love, thanks for those happy time in National University of Singapore.

# Contents

<b>ACKNOWLEDGMENTS</b>	<b>I</b>
<b>CONTENTS</b>	<b>II</b>
<b>SUMMARY</b>	<b>VI</b>
<b>NOMENCLATURE</b>	<b>IX</b>
<b>LIST OF FIGURES</b>	<b>XI</b>
<b>LIST OF TABLES</b>	<b>XIV</b>
<b>CHAPTER 1 INTRODUCTION</b>	<b>1</b>
1.1 OVERVIEW OF DIGITAL MAGNETIC INFORMATION STORAGE.....	2
<i>1.1.1 Evolution of Magnetic Hard Disk Drive.....</i>	<i>2</i>
<i>1.1.2 Technology Trends and Challenges.....</i>	<i>5</i>
1.2 CONSTRUCTION OF HARD DISK DRIVE AND HEAD-MEDIA INTERFACE CHARACTERIZATION .....	6
1.3 RESEARCH OBJECTIVES.....	10
1.4 THESIS STRUCTURE.....	12
<b>CHAPTER 2 FLYING HEIGHT MEASUREMENT METHODS AT DISK DRIVE LEVEL</b>	<b>14</b>
2.1 DRIVE LEVEL FLYING HEIGHT EVALUATION CRITERIA .....	15
2.2 WRITING-PROCESS BASED FLYING HEIGHT MEASUREMENT TECHNIQUES .....	15
<i>2.2.1 Carrier Erasure Current Method.....</i>	<i>16</i>
<i>2.2.2 Scanning Carrier Current Method for In-Situ Flying Height Measurement</i>	<i>18</i>
2.3 ART OF READING-PROCESS BASED IN-SITU FLYING HEIGHT TESTING METHODS .....	20
<i>2.3.1 Readback Signal Modulation Technique .....</i>	<i>21</i>

2.3.2 <i>PW50 Method for Flying Height measurement</i> .....	23
2.3.3 <i>Thermal Method</i> .....	26
2.3.4 <i>Harmonic Ratio Method for Flying Height measurement</i> .....	29
2.4 SUMMARY OF IN-SITU FLYING HEIGHT TESTING TECHNIQUES.....	32
<b>CHAPTER 3 A NEW APPROACH FOR DRIVE LEVEL FLYING HEIGHT ANALYSIS</b>	<b>34</b>
3.1 FUNDAMENTAL PHYSICS FOR READING PROCESS .....	34
3.1.1 <i>Frequency Domain Expressions of the Generalized Readback Voltage of Multiple Transitions</i> .....	36
3.1.2 <i>Spectral Analysis of Square Wave Recording</i> .....	37
3.1.3 <i>Spectral Analysis of Playback Signal of Pattern “111100”</i> .....	38
3.2 EVALUATION OF HARMONIC RATIO FLYING HEIGHT METHOD.....	40
3.2.1 <i>Influencing Factors for Harmonic Ratio Method</i> .....	41
3.2.1.1 Measurement Sensitivity.....	41
3.2.1.2 Measurement Precision .....	42
3.2.1.3 Measurement Errors.....	44
3.2.2 <i>Flying Height Error Function</i> .....	45
3.2.2.1 Variance of System Parameters and Its Effect on Flying Height Measurement.....	47
3.2.2.2 Noise Effect on Flying Height measurement.....	48
3.3 METHODOLOGY OF HARMONIC BURST METHOD .....	52
3.3.1 <i>Principles of Harmonic burst Method</i> .....	52
3.3.2 <i>Principle for Selection of Channel Density of Flying Height Measurement for Harmonic burst Method</i> .....	53
3.3.2.1 Minimization of Flying Height Error with Proper Selection of Channel Density and Frequency Ratio $\alpha$ .....	54

3.3.2.2 Nonlinearities Effect in Flying Height Measurement Process.....	57
3.4 SUMMARY .....	58
<b>CHAPTER 4 EMBODIMENTS OF HARMONIC BURST METHOD ON HARD DISK DRIVE</b>	<b>60</b>
4.1 SERVO MECHANISM ON HARD DISK DRIVE .....	60
4.2 TWO EMBODIMENTS OF HARMONIC BURST METHOD ON HARD DISK DRIVES ....	63
4.3 BLOCK LENGTH SELECTION AND FILTER APPLICATION .....	65
4.3.1 <i>Characteristic Resonance Frequencies in Hard Disk Drive</i> .....	66
4.3.2 <i>Selection of the Block Length</i> .....	68
4.3.3 <i>Bandwidth Effect of Spectrum analyzer</i> .....	69
4.3.4 <i>Software-based Wide Bandwidth Filter</i> .....	73
4.4 SUMMARY .....	76
<b>CHAPTER 5 DRIVE LEVEL SLIDER FLYING STABILITY ANALYSIS</b>	<b>77</b>
5.1 EXPERIMENTAL SETUP .....	77
5.1.1 <i>Hardware Setup</i> .....	77
5.1.2 <i>Software Setup for Flying Height Measurement</i> .....	78
5.1.2.1 <i>Software Setup for Component-Level Testing on Spinstand</i> .....	79
5.1.2.2 <i>Drive-Level Testing Software</i> .....	82
5.2 TESTING FREQUENCY SELECTION FOR HARMONIC BURST METHOD .....	83
5.3 COMPONENT-LEVEL FLYING HEIGHT STABILITY ANALYSIS .....	87
5.3.1 <i>Write Current Influence on Flying Height Measurement</i> .....	87
5.3.2 <i>Flying Height Measurement on Deformed Disk by Clamping</i> .....	92
5.4 DRIVE-LEVEL FLYING HEIGHT STABILITY ANALYSIS .....	94
5.4.1 <i>Off-Track Tolerance of Harmonic Burst Method</i> .....	94
5.4.2 <i>Altitude Effect on Flying Height at Drive</i> .....	97
5.4.3 <i>Ambient Temperature Effect on Flying Height at Hard Disk Drive</i> .....	103

5.5 SUMMARY .....	105
<b>CHAPTER 6 CONCLUSION AND FUTURE WORK</b>	<b>106</b>
<b>REFERENCE</b>	<b>109</b>

## Summary

The developing information technology and growing requirement for massive data storage have demanded economical, reliable, rapidly accessible and high capacity data storage systems. Magnetic hard disk drives are the only high capacity storage devices which can meet all those requirements at the lowest cost. To further increase the recording density, one of the most critical approaches is to reduce the flying height between slider and recording disk.

Currently flying height has been driven down to sub 10 nm, with a variation margin of  $\pm 10\%$  or merely 1 nm. Such a low flying height and small margin makes the drive-level flying height measurement very important and necessary because undesirable flying height variation would result in data loss or even head crash.

Flying height variation in hard disk drives may be due to several sources: disk surface flatness, waviness and roughness, the design of slider air bearing surface and environmental factors. While the disk and slider could be optimized at the design stage, it is quite important to study how the environmental factors influencing the flying height. If the flying height variation due to environmental changes could be recognized and measured, the flying height of slider could be compensated to the normal value to avoid data loss or drive crash.



Existing flying height measurement methods could be classified into two groups: optical methods and in-situ flying height measurement methods. The traditional optical measurements cannot be used to measure flying height at drive level because special glass disks are required for such methods. In-situ flying height measurement methods concern that the read/write signals, which are sensed back from rotating magnetic disk, are directly utilized to characterize the head disk surface. Such implementations are hopefully applied directly at drive level to evaluate spacing fluctuation of actual head disk system.

Work presented in this thesis is focused on the exploration of suitable methodology for disk drive level analysis of flying height variation. Based on the relationship between readback signal and flying height, the formula for harmonic intensity amplitude is derived for different recording pattern and the harmonic intensity is plotted out versus channel density. A flying height error function is derived to evaluate measurement errors in existing in-situ flying height measurement methods. Based on the flying height error function, a new harmonic burst method, which selects optimum testing frequencies by minimizing measurement error, is proposed.

The proposed harmonic burst method is successfully applied to investigate the influence of environmental changes on flying height in disk drive manufacturing environment and for operating hard disk drives. The environmental factors include the altitude effect and temperature influence. Moreover, component level experiments on spinstand also discuss the writing process influence on the application of harmonic burst method and flying height variation on deformed disk caused by disk clamping. It is proved that harmonic burst method has both the advantage of high harmonic

amplitude and alternatives for testing frequencies. By choosing optimum ratio of testing frequencies and channel density, flying height error can be minimized as possible to achieve high measurement accuracy.

## Nomenclature

Unless otherwise stated, the following abbreviations and symbols are used throughout this thesis.

ABS	Air Bearing Surface
AFM	Atomic Force Microscope
BER	Bit Error Rate
BW	Bandwidth
dB	Decibels
dBm	Decibels referred to 1 milliwatt into 50 Ohms
FH	Flying height
FFT	Fast Fourier Transform
GMR	Giant Magnetoresistive
GPIB	General-Purpose Interface Bus (IEEE 488)
HDD	Hard Disk Drive
HGA	Head Gimbals Assembly
HMS	Head Medium Spacing
HTS	Hard Transition Shift
ID	Inner Diameter
IP	Internet Protocol
LDV	Laser Doppler Vibrometer
MR	Magnetoresistive

NLTS	Nonlinear Transition Shift
OD	Outer Diameter
PRML	Partial-Response Maximum Likelihood
PW <sub>50</sub>	Pulse Width at 50% of Peak Value
RAMAC	Random Access Method of Accounting and Control
RBW	Resolution Bandwidth
RMS	Root Mean Square
SMART	Self Monitoring and Reporting Technology
SNR	Signal-to-Noise Ratio
TAA	Track Average Amplitude
TMR	Track Misregistration
ZBR	Zoned Bit Recording

## List of Figures

Fig 1.1 The evolution of IBM hard disks over the past 15 years.....	4
Fig 1.2 Spacing-Areal Density Perspective .....	4
Fig 1.3 Hard disk drive structure .....	7
Fig 1.4 HMS and head-disk clearance (the flying height) of a magnetic thin-film disk	8
Fig 2.1 Schematic illustration of the working principle of the carrier current erasure method for flying height measurement. ....	16
Fig 2.2 Schematic illustration of the recording process of the flying height change with the carrier current erasure method .....	16
Fig 2.3 Work principle of the scanning carrier current method.....	19
Fig 2.4 Recorded sinusoidal waveform and non-sinusoidal waveform.....	22
Fig 2.5 PW50 of isolated pulse .....	23
Fig 2.6 Track profiles of signal amplitude and PW50 .....	25
Fig 2.7 Measurement of PW50 by oscilloscope .....	26
Fig 2.8 The change in MR transducer output with RPM.....	27
Fig 2.9 The relationship between landing RPM and flying height.....	28
Fig 3.1 Schematic of an inductive write head and a GMR read head.....	35
Fig 3.2 Square wave recording waveform and harmonics.....	38
Fig 3.3 1 <sup>st</sup> to 5 <sup>th</sup> harmonics waveform of fixed transition interval method.....	40
Fig.3.4 “111100” readback waveform and superposed waveform by harmonics .....	40
Fig 3.5 First harmonic intensity VS channel density .....	42
Fig 3.6 Harmonics of all “1” pattern and “111100” pattern .....	43

Fig 3.7 Flying height variation at different channel density.....	45
Fig 3.8 Error of flying height caused by $\delta$ variance .....	48
Fig 3.9 Flying height error by fixed transition interval method .....	50
Fig 3.10 Flying Height error by triple harmonic method.....	51
Fig 3.11 Flying height error as function of channel density and $\alpha$ .....	55
Fig 3.12 Flying height error as function of $\alpha$ and channel density.....	56
Fig 3.13 Flying height error as function of $\alpha$ at density of 1.0, 1.5, 2.0 and 2.5 .....	56
Fig 4.1 A simple illustration of the difference between dedicated servo and embedded servo:.....	62
Fig 4.2 An example of readback signal with embedded servo technique.....	62
Fig 4.3 Scheme of harmonic burst method .....	64
Fig 4.4 Partitioning and definition of aerodynamic forces .....	66
Fig 4.5 Typical eigenmodes obtained by structure-vibration analysis .....	67
Fig 4.6 Air bearing surface and dynamic characteristics of a femto slider.....	67
Fig 4.7 Readback Signal of 72 MHz and local figure.....	71
Fig 4.8 Harmonic amplitude passed by different filter bandwidth.....	71
Fig 4.10 Sinusoidal signals before and after bandpass filters.....	74
Fig 4.11 Experimental example of wide bandwidth filter .....	75
Fig 5.1 Drive-level testing setup.....	78
Fig 5.2 Functional Diagrams.....	79
Fig 5.3 Software Control Interface .....	80
Fig 5.4 Software flowchart .....	81
Fig 5.5 Command window of drive control software.....	82
Fig 5.6 NRZ coding scheme .....	83

Fig 5.7 Flying height error as function of channel density and $\alpha$ (ratio of two testing frequency) for testing disk drive .....	84
Fig 5.8 Flying height errors at recording density of ( $F_{max}/2$ ) frequency.....	86
Fig 5.9 The writing process and its influence to the flying height measurement.....	88
Fig 5.10 Correlation of ‘a’ and ‘d’” .....	89
Fig 5.11 Pole tip recess measurement at different temperature by AFM .....	92
Fig 5.12 LDV and harmonic burst method comparison .....	93
Fig 5.13 Off track tolerance of flying height measurement.....	96
Fig 5.14 Reciprocity between recording head and magnetic medium.....	96
Fig 5.15 Flying height VS altitude at different zones.....	100
Fig 5.16 Flying height variation distribution at OD zone at different altitudes.....	101
Fig 5.17 Flying height change at different ambient temperature.....	104

## **List of Tables**

Table 5.1 Zone table.....	85
Table 5.2 Pressure at different altitude.....	98
Table 5.3 Flying Height change measured by harmonic burst method.....	100
Table 5.4 Standard deviation value of flying height variation distribution at each altitude.....	102
Table 5.5 Flying height variation distribution at each ambient temperature.....	104



## **Chapter 1 Introduction**

The modern information technology consists of three parts: information acquiring, information processing, information transferring and information storage. In fact, information storage technology plays a crucial role in modern devices and systems, such as computer, entertainment systems and devices, cell phones and networks.

In this information age, the requirement to data storage devices and systems includes the followings: high capacity, high reliability, high data transfer rate as well as low cost. Magnetic hard disk drive has become the prime information storage devices for computers ranging from notebooks to mainframes because of its large storage capacity (approaching Tera-byte per drive), very high recording density (100 Gb/ in<sup>2</sup> in current commercial drives), and very low cost per megabyte. Furthermore, its data transfer rate is much faster than any of the rest possible mass storage devices, such as optical memory, tape memory and so on.

Starting from a review of the evolution of magnetic hard disk drive technologies, this chapter discusses the major technical challenges of magnetic disk drive technology in the future. After that, the objectives of the research work presented in this thesis are elaborated. Finally, the structural organization of this thesis is given in the last part.

## **1.1 Overview of Digital Magnetic Information Storage**

### **1.1.1 Evolution of Magnetic Hard Disk Drive**

Magnetic data storage technology has been playing a key role in computer development since the beginning of computer technology [1]. The history of magnetic disk drive technology started in the 1950s. The very first magnetic hard disk drive was introduced by IBM on September 13, 1956. The disk drive was of a storage capacity of 5 million characters (approximately 5 megabytes). It was really a giant with whopping 50 disks and 24 inches in diameter of each disk. The areal density was about 2,000 bits per square inch and the data transfer rate of this first drive was 8,800 bytes per second.

Over the succeeding years, the technology improved tremendously, with areal density, capacity and performance all increased greatly.

Reducing head-disk spacing will increase the achievable recording density and hence, the total capacity of the disk drives. In 1962, IBM introduced the model 1301 Advanced Disk File. The major technology breakthrough in this new disk drive was dynamic air-bearing technology, which “floated” the read/write head over the surface of high speed rotating disk. Such a dynamic air-bearing technology successfully reduced the head-disk spacing from 20  $\mu\text{m}$  to merely 6  $\mu\text{m}$  around. As the head is “floated” over the surface of high speed moving disk, the concept of “flying height” is introduced which refers to the mechanical spacing between read/write head and disk surface.

In 1973, IBM introduced the model 3340 disk drive and Winchester technology, which are commonly considered to be the father of the modern hard disk [2]. The key technology breakthrough was its vastly improved "air bearing" technology, which reduced the flying height of the slider to only 0.4  $\mu\text{m}$  above the surface of the disk.

As the introduction of mini and micro computer technology, the disk size used in disk drives was shrunk from 24 inch diameter in 1950s, to 8 ~ 12 inch in 1960s and 1970s, and 5.25 ~ 3.5 inch in 1980s, and 0.85 ~ 1 inch in recent years.

In 1980s Seagate Technology introduced the first hard disk drive for micro-computers, the ST506. It was a full height 5.25-inch drive and held 5 Mbytes. Rodime made the first 3.5-inch rigid disk drive in 1983. The 3.5-inch form factor hard drives quickly became the most popular standard for desktop and portable systems.

It has come a long way since those days, and worked down through the form factors of 5.25-inch, 3.5-inch, 2.5-inch, 1.8-inch and 1.3-inch. The smallest disk drives are of size 1 inch and 0.85 inch which were designed for personal mobile information devices and systems.

Comparing the 2  $\text{Kb/in}^2$  areal density of the disk drives in 1950s, modern disk drives are of areal density of almost 100  $\text{Gb/in}^2$  which is 50,000,000 times as high as the density 1950's. Figure 1.1 states the progress of hard disk drive in terms of capacity in the past 20 years. Other aspects of magnetic disk drives, such as reliability, data transfer rate and form factor have impressive progress during the past 20 years.

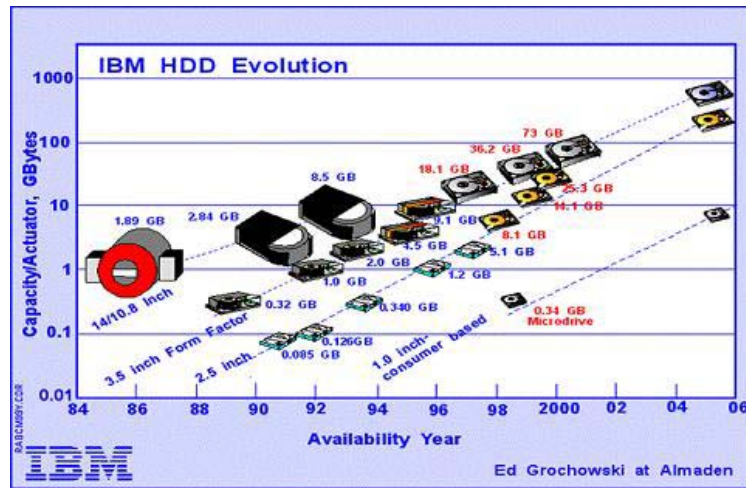


Fig 1.1 The evolution of IBM hard disks over the past 15 years [3]

Fig 1.2 shows the trend of slowing decreasing flying height with increasing areal density.

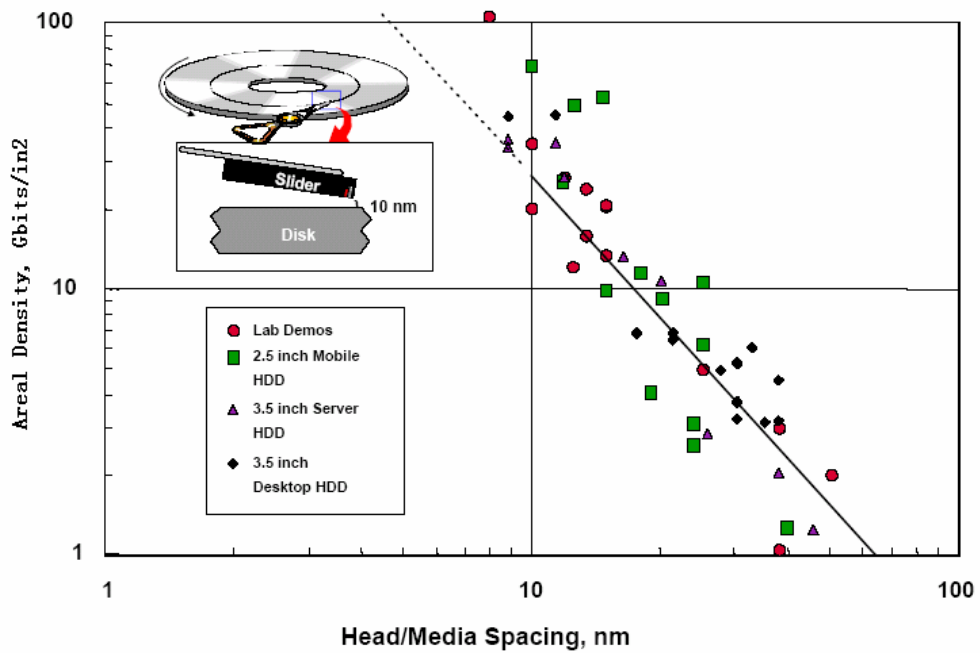


Fig 1.2 Spacing-Areal Density Perspectives [4]

### **1.1.2 Technology Trends and Challenges**

The general trend of magnetic recording and HDD technology is to further increase areal density, further reduce the cost of each mega-byte information stored in HDD and achieve high reliability.

The major challenges for future magnetic data storage industry is high sensitivity head transducer technology, highly stable data storage media with further reduced grain size and grain size distribution, and further reduced head-disk spacing or flying height.

As bit cell size decreases, the energy required to reverse the magnetization of a bit approaches the magnitude of the bit's thermal energy, causing magnetic instability problem. This behavior is called superparamagnetism and relates to the future extendibility of magnetic storage. Although proper selection of disk materials and structures can significantly delay the superparamagnetic effect, HDD technology at 100 Gbit/in<sup>2</sup> already deals with the limits of thermal stability of magnetic bits. This suggests that conventional longitudinal magnetic recording may not be able to achieve stable high density magnetic recording at 300 ~ 500 Gbit/in<sup>2</sup>. Therefore, it is expected that perpendicular magnetic recording scheme will be the solution for disk drives to further increase its areal density. Furthermore, several alternate magnetic media technologies and an alternate recording technology are being investigated to supplement the on going research on perpendicular recording technology. These alternate media technologies are Self-Organizing Magnetic Array (SOMA) and Patterned Media. Another alternate magnetic recording technology is Heat Assisted

Magnetic Recording (HAMR). With those alternative technologies, the areal density is hopeful to achieve 1T Gb/in<sup>2</sup> and beyond [5].

The rate of data retrieval from a computer's hard disk drive depends on the bit density and the speed at which the disk is spinning. Modern hard disks spin at between 4,200 and 15,000 revolutions per minute. Also, people are exploring the application of micro-electro-mechanical system (MEMs) technology and scanning probe technology for data storage, aiming to achieve further million rpm. And this should be capable of storing vast amounts of data and handling them at rates of up to 300 gigabytes a second-hundreds of times faster than the rates that are currently attainable [6].

## **1.2 Construction of Hard Disk Drive and Head-Media Interface Characterization**

A hard disk drive is basically a very compact, electronically controlled device which includes a spinning disk stack and a set of magnetic read/write recording heads positioned swiftly and accurately over magnetic disk surfaces by an electromagnetic actuator as shown in Figure 1.3.

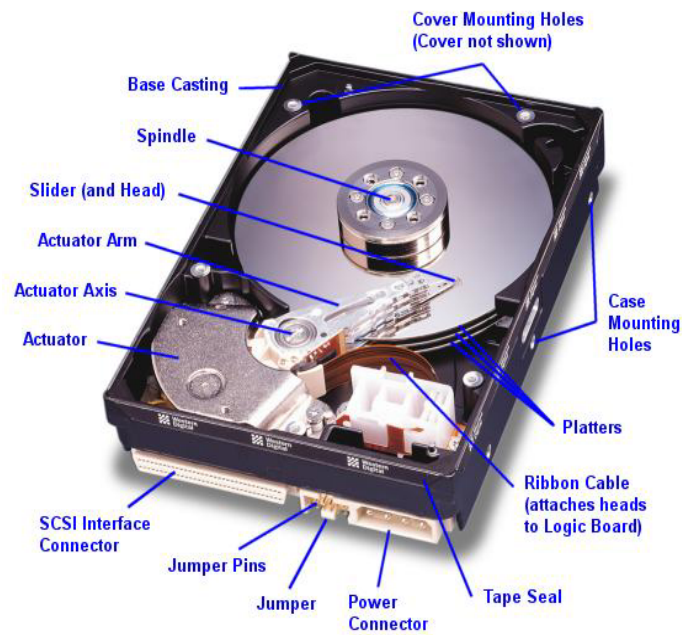


Fig 1.3 Hard disk drive structure [7]

This mechanical system is required to perform reliably and consistently for many years of operation while maintaining a nanometer positioning capability in vertical and radius directions. The drive is also required to be capable of withstanding external shocks and vibrations without jeopardizing the integrity of stored information in the device.

The interaction between slider, lubricant and disk surface is becoming the most crucial robustness concern of advanced data storage systems. It is because that the progressively increasing areal density requires a progressively decreasing magnetic spacing between the head and data recording layer of disk media. This involves the head flying closer to the disk, as well as using a thinner protective overcoat while maintaining a highly durable interface. In general, Figure 1.4 illustrates head media spacing (HMS) and head-disk clearance (the flying height).

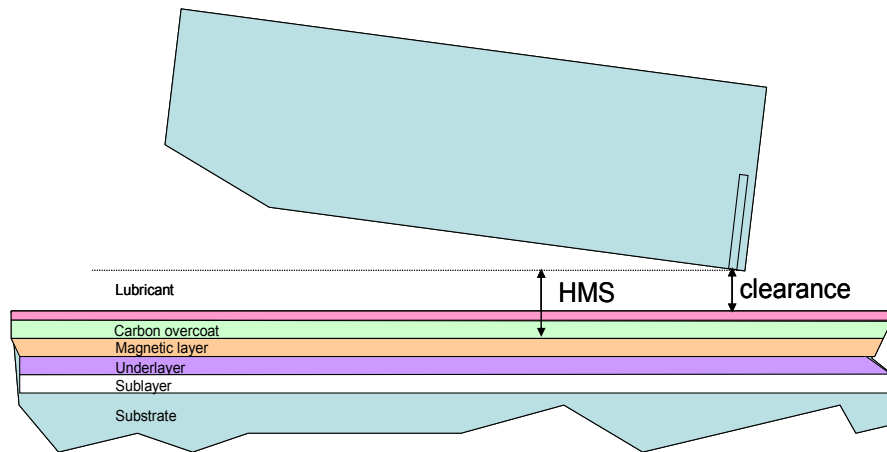


Fig 1.4 HMS and head-disk clearance (the flying height) of a magnetic thin-film disk

The term head-disk clearance is the physical clearance between the magnetic transducer slider and the magnetic recording medium surface. The spacing between the top of the magnetic layer and the bottom of the read/write element mounted on a slider is called head-media spacing and it includes the following components: disk overcoat thickness, lubricant, flying height, slider overcoat thickness and pole tip recession of the read/write transducers from slider surface. Here, flying height refers to the spacing between the mean plane of the disk surface profile and the mean plane of the slider surface profile [8].

In order to increase the recording density, it is necessary to decrease the flying height so that the signal to noise ratio obtained from the read element is within an acceptable range. Ideally, zero spacing is preferred. However, zero spacing or contact recording would lead to higher friction and wear at the head-disk interface, hence degrading the reliability of data recording and retrieval. The flying height in present days' magnetic hard disk drives is between 5 and 20 nanometers and there is disk vibration, airflow



fluctuation, slider-lubricant interaction which results in the fluctuation of the flying height [9].

As the flying height variation can strongly affect the reliability of data recording and retrieval, the flying height variation must be monitored and analyzed in real-time. Unexpected changes in flying height of a particular head, which may or may not result in deleterious head-to-disk contact, are generally indicative of a problem with the particular head or head assembly. By way of example, an appreciable decrease in flying height may be indicative of a significantly increase accumulation of lubricant over slider surface. Therefore, flying height is one of the most important parameters that control the performance and durability of a hard drive.

Furthermore, flying height is a typical characteristic in currently implemented SMART (Self Monitoring and Reporting Technology) failure prediction system, which is a reliability-prediction technology [10]. Appreciable increase of flying height both during write operation and read operation will result in data loss. Hence, monitoring flying height at disk drive level and predicting the near-term failure of an individual hard disk can let the host computer issue a backup warning to prevent data loss [11].

There are numerous parameters that affect the tribological and magnetic performance of head-disk systems, including surface morphology of disks, which includes contamination, scratches, disk micro-waviness or lubricant stick slip phenomena, and slider flying performance. They usually cause a disturbance to slider air bearing and lead to flying height variations and even slider-disk contact. Short contacts or stick slip type phenomena can even cause the slider body to resonate at its eigenfrequencies.

Moreover, the influence of intermolecular forces on the flying height of a slider can be significant and not negligible [12], when the flying height is in the range of deep sub 10 nm.

### **1.3 Research Objectives**

As the magnetic recording density goes to several hundred Gb/in<sup>2</sup>, the slider has to be flying at sub-10nm spacing over the disk surface. At nanometer head-disk spacing, there exists a high likelihood of a slider-lube and a slider-lube-disk interaction, and such interaction degrades the performance and reliability of the recording system.

Over the past years, a variety of methods have been proposed to measure flying height which can be usually classified into two categories: optical methods and in-situ flying height measurement methods. Traditional optical measurements, which use the glass disks without carbon overcoat and lubricant layer, cannot identify the problems related to in-situ head-disk interaction of actual disk drives. Moreover, the accuracy and precision achieved by this method is not reliable enough at flying height below 5 nm due to its calibration method of optical reflectivity, absorption rate and the contamination of glass disk. The most important flaw is that these methods are unable to measure flying height in a direct manner because special disks or sliders are required.

In-situ flying height measurement methods are based on the read/write signal sensed back from rotating magnetic disk. Such signal is directly utilized to characterize the

head disk system as the quality of such signal is a function of the flying height. Therefore, it is widely believed that the in-situ flying height measurement methods which are hopefully applied on drive level will play more and more important role in the evaluation of spacing fluctuation of actual head-disk systems at sub 10 nm or even deep sub 10 nm level of head-disk spacing.

As technology moves towards lower and lower flying height, it is becoming more and more important for in-situ flying height evaluation in terms of flying height control, disk drive robustness, and flying height adjustment at drive level. The requirement of drive level flying height characterization includes the followings: simple methodology and easy to implement, in addition to the general requirement to in-situ flying height analysis.

Currently, in-situ flying height measurement methods include writing-process based methods and reading-process based methods. The methodologies and working principles of in-situ flying height measurement techniques are reviewed in the first section of this thesis to identify the respective strengths as well as weakness.

The second part of this thesis evaluates the measurement error by harmonic ratio flying height methods and proposes an error function in order to investigate the optimum testing density and frequencies. Based on the error function, a new method named harmonic burst method is proposed to measure flying height of a flying slider by writing flux on a rotating disk on predetermined track with predetermined channel density. The following section deals with the experimental work to verify the

feasibility of this method and also study slider's flying stability with application of the proposed method at disk drive level as well as at component level.

## **1.4 Thesis Structure**

This thesis is divided into six Chapters. As an introduction, the chapter 1 briefly describes the background, motivation, objectives and structure of the research work.

Art of in-situ flying height measurement methods are reviewed in Chapter 2. In-situ flying height measurement can be divided into reading process-based methods and writing process-based methods. Each method is reviewed with working principle, advantages as well as weakness. A conclusion is drawn out that currently harmonic ratio method is the most promising method for in-situ characterization of hard disk drives in operation.

In Chapter 3, fundamentals of reading physics by GMR reading transducer are briefly introduced. Based on the reading principle, frequency domain expression for multi-transitions is derived and followed by spectral analysis of readback signal of two specified patterns, all "1" code and "111100" ("1" here presents a magnetic transition), which are the most frequently used patterns for harmonic ratio method. Next, issues on flying height measurement are firstly discussed from the point of readback signal sensitivity to flying height variation, good signal to noise level. A new flying height error function is proposed to describe the influence of testing conditions (recording density) to the measurement results. In order to achieve high sensitivity as well as

minimize flying height error, an enhanced harmonic ratio method named harmonic burst method is proposed for drive level applications.

Chapter 4 elaborates two embodiments of harmonic burst method on hard disk drive. The principles to choose optimum testing density and ratio of two testing frequencies are illustrated from three points: sensitivity requirements, minimum flying height error and high-density introduced nonlinearities, such as non-linear transition shift, hard transition shift, and partial erasure effects. Data group length for harmonic burst method is selected by interested flying height modulation frequencies and based on the frequency band, either a spectrum analyzer or software based wide bandwidth filter is used to extract the harmonics from the readback signal.

Experimental setup including hardware setup and software for harmonic burst method is brought up in Chapter 5. And this is followed by flying stability and media/head recording capability analysis at component level. Influence on flying height measurement of off-track reading is also investigated and harmonic burst method shows a high tolerance of off-track percentage. Moreover, environmental factors effects on flying height inside hard disk drives are studied by harmonic burst method.

Finally, Chapter 6 concludes the research work and discusses some possible topics for the future work.

## **Chapter 2 Flying Height Measurement Methods at Disk**

### **Drive Level**

As illustrated in Chapter 1, the existing flying height testing technologies can be divided into standard optical testing methods and in-situ flying height testing techniques. However, the optical techniques require replacement of magnetic disk with special glass disk. Moreover, those techniques are at component level only and do not directly measure the spacing and its variations on a production disk file. In other words, it is impossible for those methods to be implemented in disk drive for in-situ characterization of the head media spacing and description of the actual scenario in operating disk drives. As in-situ flying height testing methods directly utilize the correlation between magnetic read/write signal and the head media spacing to characterize flying height, in-situ flying height measurement techniques are becoming more promising and attractive choice.

In-situ flying height testing techniques are divided into the reading process based methods and the writing process based methods. In this chapter, the principles of in-situ flying height testing techniques are reviewed and analyzed in terms of feasibility of implementation at disk drive level according to the drive-level flying height testing which have been illustrated.

## **2.1 Drive Level Flying Height Evaluation Criteria**

Drive level flying height evaluation is important in terms of flying height control, flying height adjustment and disk drive robustness analysis. Generally, besides the requirements of repeatability and high precision for component level flying height testing, there are three additional requirements for drive level flying height testing. Firstly, there should be no modification of components in drives in terms of flying height measurement to achieve low cost and easy application. Secondly, flying height measurement process should not influence system level information on disk such as servo signal. The last but not the least, the hardware electronics for flying height data processing should be simple and easy for implementation.

## **2.2 Writing-Process Based Flying Height Measurement Techniques**

The writing process methods comprise carrier current erasure method [13] and scanning carrier current writing method [14]. These approaches, which are firstly proposed by Liu, et al, are designed to use “writing” and “erasure” operations to record the flying height variation during dynamic transient process, such as track seeking and load/unload process.

## 2.2.1 Carrier Erasure Current Method

Carrier current erasure method is proposed to analyze flying height variation caused by the dynamic operations such as seeking, dynamic load/unload, head's take-off process, and so on. The working principles of this method are illustrated in Figure 2.1 and Figure 2.2.

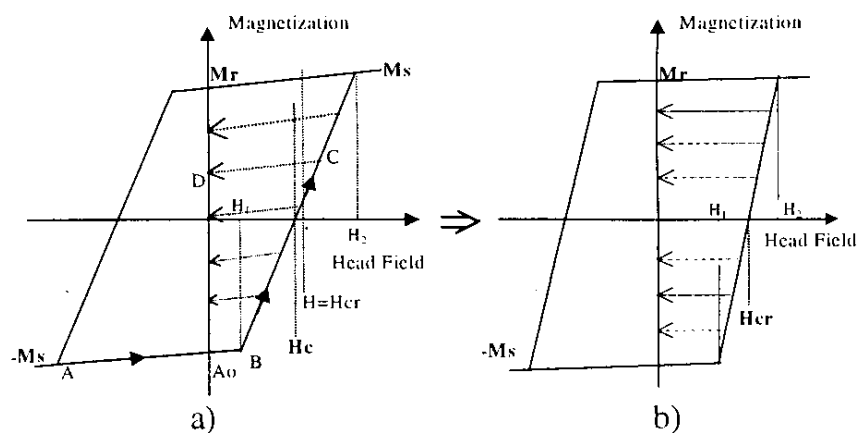


Fig 2.1 Schematic illustration of the working principle of the carrier current erasure method for flying height measurement. The carrier DC erasing current is selected so that the variation of the head-disk spacing will lead to a variation of the head field in the range between  $H_1$  and  $H_2$ .

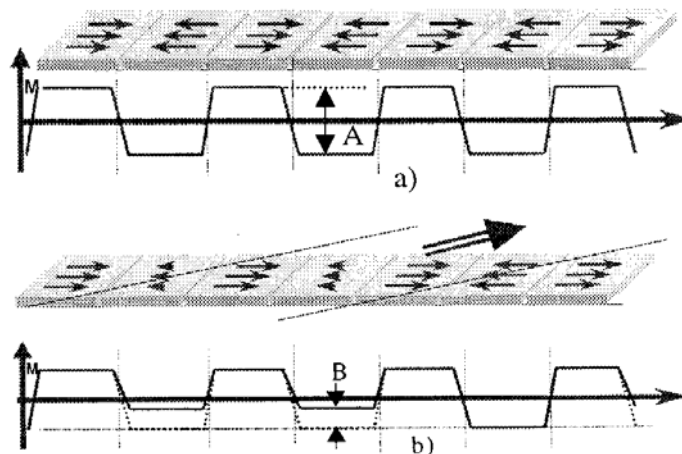


Fig 2.2 Schematic illustration of the recording process of the flying height change with the carrier current erasure method: a) magnetization before carrier current erasure (A the magnetization difference between adjacent bit cells), b) magnetization after carrier current erasure (B the change of magnetization difference caused by the erasure operation with selected carrier current)



Instead of basing the test on readback process, carrier erasure current method uses a selected carrier erasure current to record the spacing variation. Transitions are pre-recorded along the test tracks with a saturating writing current. Then, a predetermined carrier erasure current (constant value) is applied to modulate the magnetization difference between positive magnetization status and negative magnetization status, according to flying height variation. By comparing the amplitude of the original readback signal to the amplitude drop caused by the carrier erasure operation, the recorded flying height variation is retrieved as the readback amplitude is proportional to the magnetization difference in adjacent bit cells.

The magnetization difference after carrier current erasure can be estimated as:

$$M_r - M = M_r - \frac{2M_r}{H_2 - H_1}(H_e - H_{er}) \quad (2.1)$$

The readback amplitude before carrier current erasure ( $V_0$ ) and after carrier current erasure ( $V$ ) can be expressed as:

$$V_0 = 2M_r \cdot f(\beta_{head}, g, a, d_r, \delta) \quad (2.2)$$

$$V = f(\beta_{head}, g, a, d_r, \delta) \left[ M_r - \frac{2M_r}{H_2 - H_1}(H_e - H_{er}) \right] \quad (2.3)$$

where  $f(\beta_{head}, g, a, d_r, \delta)$  is a factor describing the dependence of readback amplitude on head's magnetic coefficient  $\beta_{head}$ , gap length  $g$ , transition region length  $a$ , head-disk spacing during the readback process  $d_r$  and the medium thickness  $\delta$ . Factor  $f(\beta_{head}, g, a, d_r, \delta)$  will be of the same value no matter reading the original signal ( $V_0$ ) or the residual signal ( $V$ ) after carrier current erasure. Therefore, the flying height variation  $\Delta d$  by measuring the residual to original ratio of the readback signal:

$$\frac{V}{V_0} = \frac{1}{2} + \frac{2g \cdot \Delta d}{\eta \cdot [g^2 + 4(d_0 + \delta)^2] \tan^{-1} \frac{g}{2(d_0 + \delta)}} \quad (2.4)$$

Such an approach is of the advantages of supporting all kinds of post-processing of the recorded flying height variation, high sensitivity and easy implementation as it is based on amplitude measurement. However, the spacing testing range of the proposed carrier current method is still not big enough to meet the requirement for head disk interaction analysis in the ramp load/unload process, even though the carrier current method gives larger testing range of flying height variation than the possible range of all the reading process based methods.

### **2.2.2 Scanning Carrier Current Method for In-Situ Flying Height Measurement**

The scanning carrier current method works under the same principle of the carrier current method and is proposed to further enlarge the testing range. A schematic diagram is illustrated in Figure 2.3, showing the testing process of the scanning carrier current method.

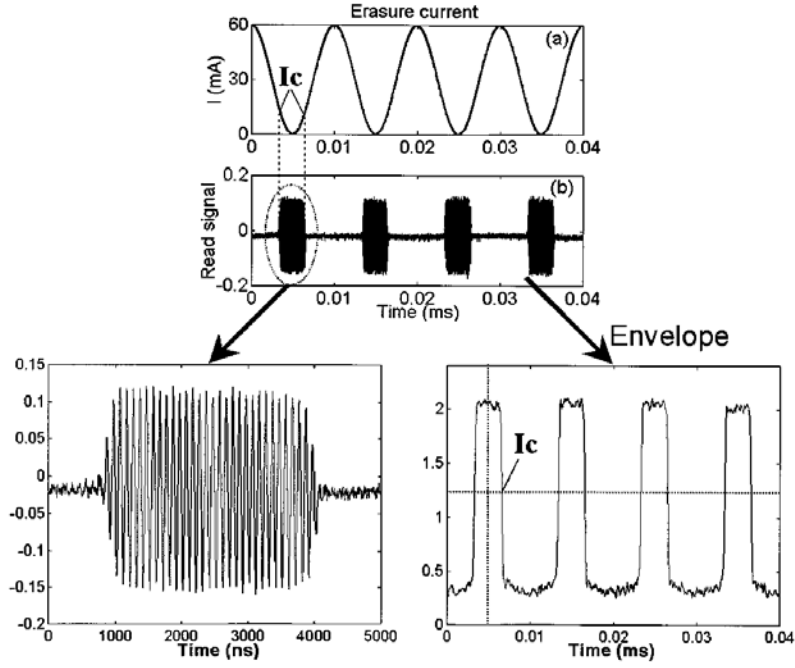


Fig 2.3 Working principle of the scanning carrier current method

Scanning the carrier current from the zero is necessary. The readback signal from the area corresponding to zero current value serves as a reference signal in the flying height retrieval process. The phase variation of the scanning current is recovered by detecting the envelope of the readback signal. As the amplitude of the scanning current is known, the current value applied in the current scanning process can be derived based on the retrieved phase information. The media coercivity is assumed to be constant and the head field can be approximated by Karlqvist equation. The flying height variation can be obtained from the following equations:

$$d = \frac{g}{2 \tan \left[ \frac{I_{c0}}{I_c} \tan^{-1} \frac{g}{2(d_0 + \delta)} \right]} - \delta \quad (2.5)$$

where  $I_{c0}$ ,  $I_c$  are the coercive current in track following status and the coercive current on the transient process,  $d_0$  and  $d$  are the head-disk spacing at track following status and the head-disk spacing in the transient process under investigation ( $d=d_0+\Delta d$ ).

The achievable testing range of flying height variation by scanning carrier current method can be up to a few hundred nanometers, depending on the writing head used. Furthermore, the scanning carrier current method can be extended to measure the flying height variation at steady flying status.

## **2.3 Art of Reading-Process Based In-situ Flying Height Testing Methods**

The reading-process based methodologies are established on the Wallace equation and Karlqvist head model [15]. The advantage of writing process based methods is its testing range. The disadvantage of such methods is its resolution.

On the other hand, the reading process based method is of the advantage of high flying height sensitivity.

The reading-processed techniques include readback signal modulation technique, pw50 method, thermal method and harmonic ratio flying height method (including fixed transition interval harmonic method and triple harmonic method).

### 2.3.1 Readback Signal Modulation Technique

W.K.SHI and D.B.Bogy etc describe a method which uses the disk file's own read head as a spacing transducer. The spacing variation is deduced from the modulation of a sinusoidal readback signal and the dependence of the readback voltage on the head disk spacing [16]. This method is based on equation (2.6) which was derived by Wallace for the readback voltage of a sinusoidally recorded signal:

$$e(t) = 4\pi(10^{-8})N\alpha W \left(\frac{\mu}{\mu+1}\right)Mv(1 - e^{-2\pi\delta/\lambda})G(\lambda)e^{-2\pi d/\lambda} \cos\left(\frac{2\pi vt}{\lambda}\right) \quad (2.6)$$

where:

e	voltage of readback signal (V)	t	time (s)
N	number of turns of the readback coil	$\alpha$	head efficiency ( $0 < \alpha < 1$ )
W	head width (cm)	$\mu$	core permeability
M	peak remanent magnetization of the medium (EMU/cc)		
v	tangential velocity (cm/s)	$\delta$	medium thickness (cm)
$\lambda$	wavelength of recorded signal (cm)	$G(\lambda)$	gap factor
d	spacing between the head and medium (cm)		

For a given disk file operating at a given track, then quantities N,  $\alpha$ ,  $\mu$ , v,  $\lambda$  are constants. Let  $E$  denote the amplitude of  $e(t)$ . Then from (2.6)

$$E = F(M, \delta) \exp(-2\pi d / \lambda) \quad (2.7)$$

where F is a function of medium thickness  $\delta$  and the maximum remanent magnetization M. Assume the fluctuation of M and  $\delta$  is negligible, let  $d_0$  denote an arbitrary reference spacing, not necessarily the steady flying height,  $y(t)$  the spacing variation, and  $A(t)$  the amplitude modulation of the readback signal resulting from the

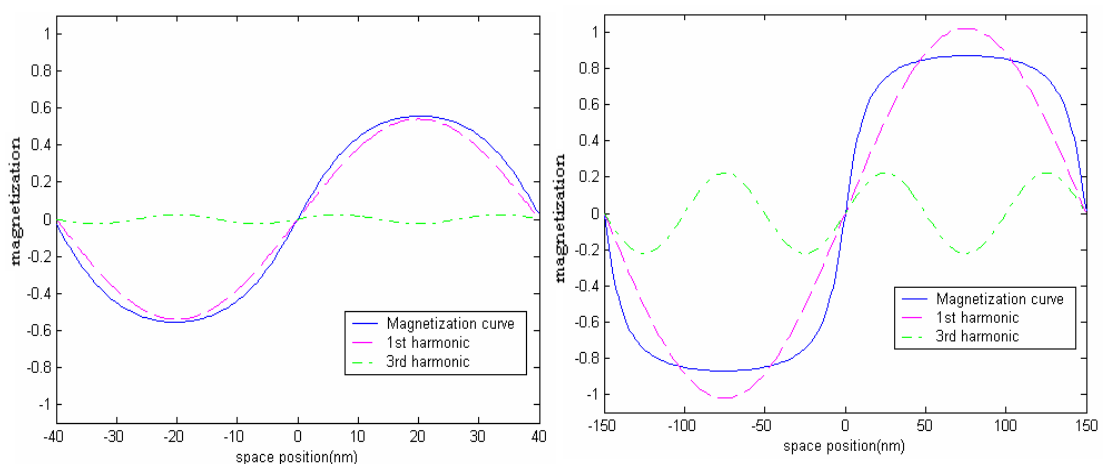
spacing variation defined by  $d = d_0 + y$  and  $A = [E(d) - E(d_0)]/E(d_0)$ . Then if  $m$ ,  $r$ , and  $f$  denote the disk rotation speed, the track radius, and the recording frequency (so that  $\lambda = 2\pi r m / f$ ), the flying height variation  $y(t)$  can be expressed as the followings:

$$y(t) = -\frac{rm}{f} \ln[1 + A(t)] = -\frac{rm}{f} \ln \frac{E(d)}{E(d_0)} \quad (2.8)$$

The spacing variation can be obtained without knowing  $d_0$  and  $E(d_0)$  if considering spacing at two different times  $t_1$  and  $t_2$ :

$$d(t_1) - d(t_2) = y(t_1) - y(t_2) = -\frac{rm}{f} \ln \frac{E[d(t_1)]}{E[d(t_2)]} \quad (2.9)$$

Therefore, the spacing variation is completely determined by (2.8) and (2.9). Although the spacing variation can be calculated by (2.8) or (2.9) for a sinusoidally recorded magnetic bits in Figure 2.4 (a), it should be noted that if the write signal is not a single frequency sinusoidal as shown in Figure 2.4 (b), consequently the state of magnetization is not necessarily sinusoidal and dominated by longitudinal component of media's magnetization, as required by (2.6).



(a) Sinusoidal Recorded Waveform; Bitlength = 40 nm      (b) Non-sinusoidal Recorded Waveform; Bitlength = 150 nm

Fig 2.4 Recorded sinusoidal waveform and non-sinusoidal waveform

Furthermore, the resolution is greatly limited by off track effect, which also results in the modulation of readback voltage and hence this technique will mistake any radial displacement of the slider (off-track) for a change in vertical flying height. Last but not the least, the measurement resolution of 5 nm is no longer suitable for present drives in which flying height has been already driven to sub 10 nm.

### 2.3.2 PW50 Method for Flying Height measurement

PW50 method is based on the detection of the pulse width of the read transducer output, where a variation in head disk space produces a proportional variation in pulse width [17]. In Figure 2.5, an example is given of the shape of the readback signal for the head that is responding to magnetic transitions written relatively wide apart (isolated pulses). The shape of this waveform will be characterized by its pulse width  $PW_x$  at x percent of the peak to base-line amplitude.

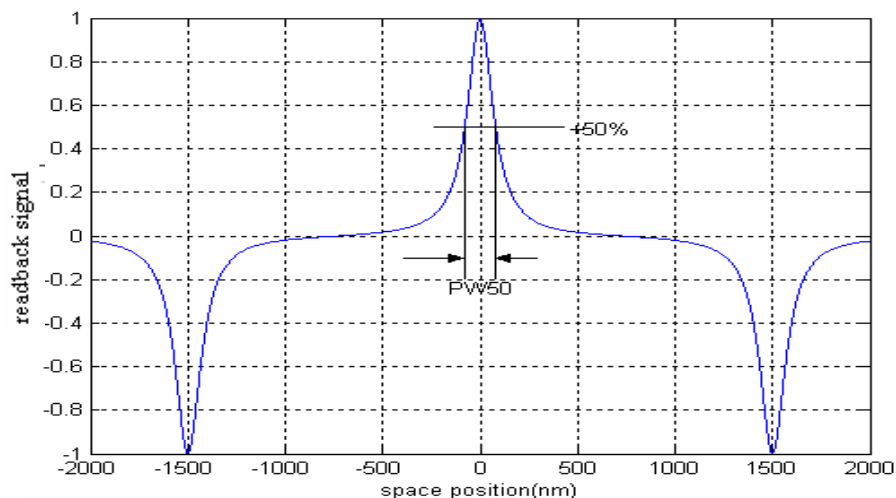


Fig 2.5 PW50 of isolated pulse

Wallace demonstrated that the magnetic spacing loss could be represented by a non-causal (no phase shift) low-pass filter, whose cutoff frequency decreases with increasing flying height. For an increase  $\Delta d$  in the flying height  $d$  this spacing loss filter has a transfer function  $H(\omega)$  given by:

$$H(\omega) = \exp\{-\Delta d|\omega|/v\} = \exp\{-2\pi\Delta d/\lambda\} \quad (2.10)$$

Here  $\lambda$  is the wavelength along the track of a sinusoidal signal at angular frequency  $\omega$ . This filter is applied to the readback signal at flying height  $d$  to arrive at the signal at flying height  $d+\Delta d$ . For pulses with a particular shape (Lorentzian) we can very easily calculate what happens to the pulse width for varying flying height in reading process.

A Lorentzian readback pulse shape is given by:

$$e(t) = \frac{e(0)}{1 + (2t/pw50)^2} \quad (2.11)$$

The Fourier transform of these Lorentzian pulses is:

$$F_i(\omega) = \frac{\pi}{2} e(0) pw50 \cdot \exp\{-|\omega|pw50/2\} \quad (2.12)$$

Filtering the Lorentzian pulse of (2.11) by the spacing loss filter (2.10) produces an output pulse whose Fourier transform  $F_0(\omega)$  is equal to the product of  $F_i(\omega)$  and  $H(\omega)$ :

$$F_0(\omega) = \frac{\pi}{2} e(0) pw50 \cdot \exp\left\{-\left(\frac{pw50}{2} + \frac{\Delta d}{v}\right)|\omega|\right\} \quad (2.13)$$

Transforming  $F_0(\omega)$  back to the time domain gives for the Wallace spacing loss weighted pulse:

$$e'(t) = \frac{e'(0)}{1 + (2t/pw'50)^2} \quad (2.14)$$

The full width at half maximum is



$$pw_{50}' = pw_{50} + 2\Delta d/v \quad (2.15)$$

Therefore, based on (2.15), monitoring the variation of pulse width, the corresponding head disk spacing variation can be calculated out.

Pulse width measurement of the readback signal in a magnetic storage device allows the in-situ, noninvasive determination of the head disk space in a fully operational device. Compared to readback signal modulation technique, this method is of small sensitivity to the track mis-registration as shown in Figure 2.6 [18].

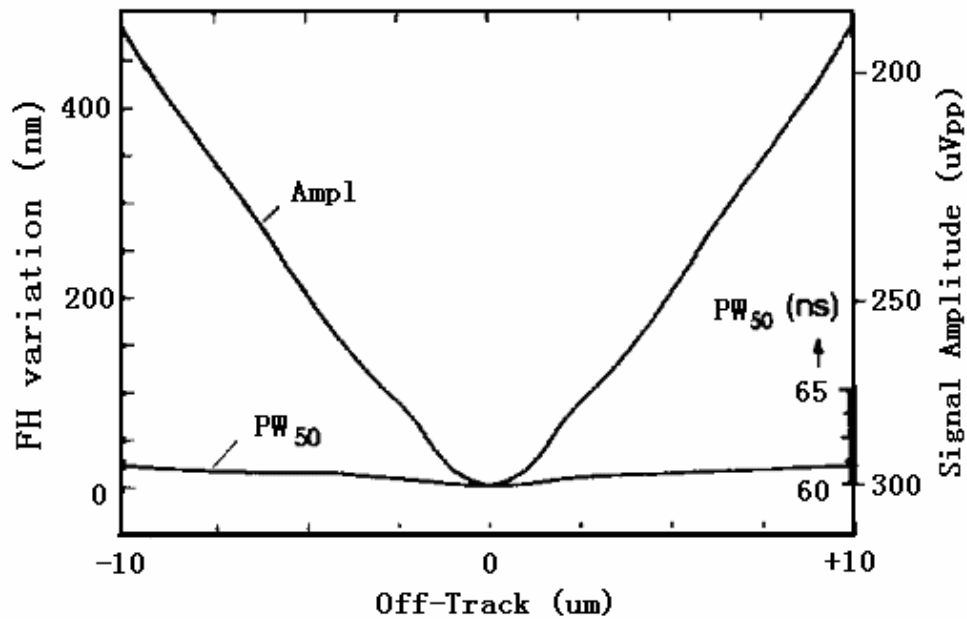


Fig 2.6 Track profiles of signal amplitude and PW50

An oscilloscope can be used to measure PW50. As shown in Fig 2.7, move the cursors to the 50% of the peak to base-line amplitude of isolated pulse and the horizontal time difference of two cursors presents the value of PW50. In this case, PW50 is 3.6 ns.

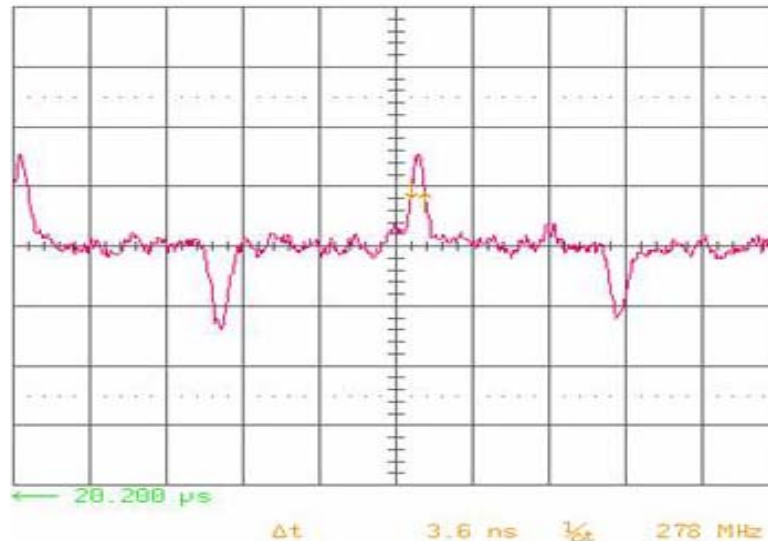


Fig 2.7 Measurement of PW50 by oscilloscope

However, electronics required to in-situ monitor the variation of PW50 are quite complicated compared with the read channel of present disk drives and are not easy to build into a disk drive system. Furthermore, because only isolated pulses are desired for testing, the sensitivity of this method is lower than other methods [19].

### 2.3.3 Thermal Method

Gordon James Smith et al describe a system and method for measuring absolute flying height using a thermal response of an MR transducer [20]. This methodology exploits a phenomenon observed by the inventor that the rate of change of the thermal response of an MR head changes significantly as the MR transducer transitions from flying above a medium to a state of contacting the medium. It computes the absolute flying height by associating a transition velocity at which the rate of change of MR signal

exceeds a pre-established threshold with absolute flying height of a slider at nominal flying state.

With reference to Figure 2.8, use a particular head of a test disk drive system, collect the data by placing the arm electronics (AE) in the MR resistance measurement mode and then monitor the MR resistance by measuring the MR voltage at constant MR bias current, the change in MR transducer signal output can be seen as a change in the slope of the curve in the figure as the curve passes from regime-1 to regime-2. The two regimes, represent different thermal transport mechanisms associated with the slider supporting the MR transducer as the slider transitions from a non-contacting flying state to a contacting state. The slope of curve in regime-1 is nearly constant and proportional to the resistance of the MR element; in regime-2, the slider is sliding on the disk surface in contrast to regime-1 wherein the slider is flying above the disk.

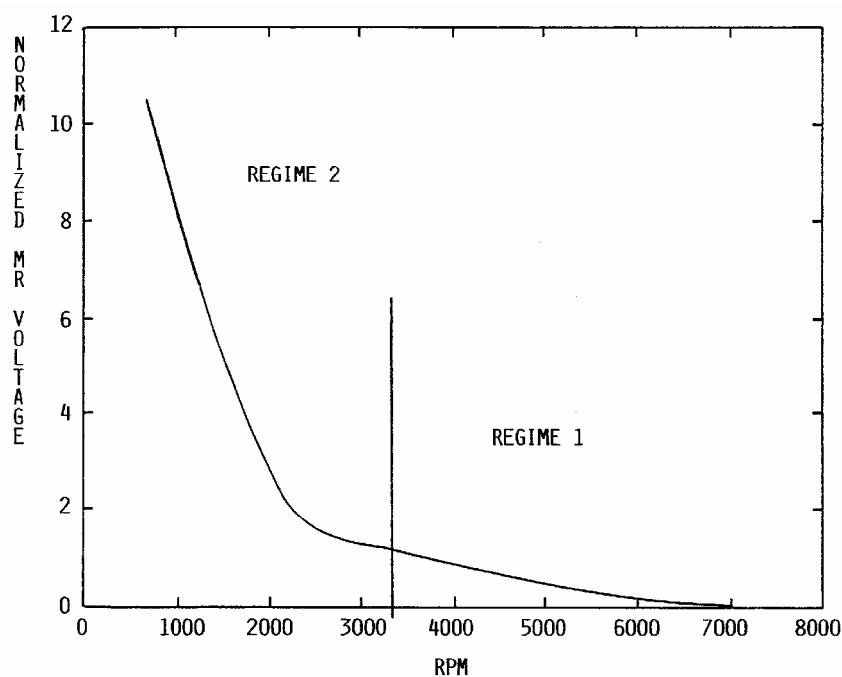


Fig 2.8 The change in MR transducer output with RPM [20]

At the time the transition from regime-1 to regime-2 is detected, which represents appreciable contact between slider and disk surface, the disk speed is stored and used to calculate absolute flying height. A head-disk flying height profile developed specifically for each head is used to relate a regime-1/regime-2 transition velocity to an absolute flying height at a full disk rotating velocity. The general relationship between full speed slider flying height and landing velocity is well-understood and could be obtained in several ways, such as through use of air bearing modeling, empirically through use of known harmonic ratio techniques and through use of acoustic emission transducers. For example, in the case of the relationship depicted in Figure 2.9, the landing velocity data was determined by use of known harmonic ratio flying height methods.

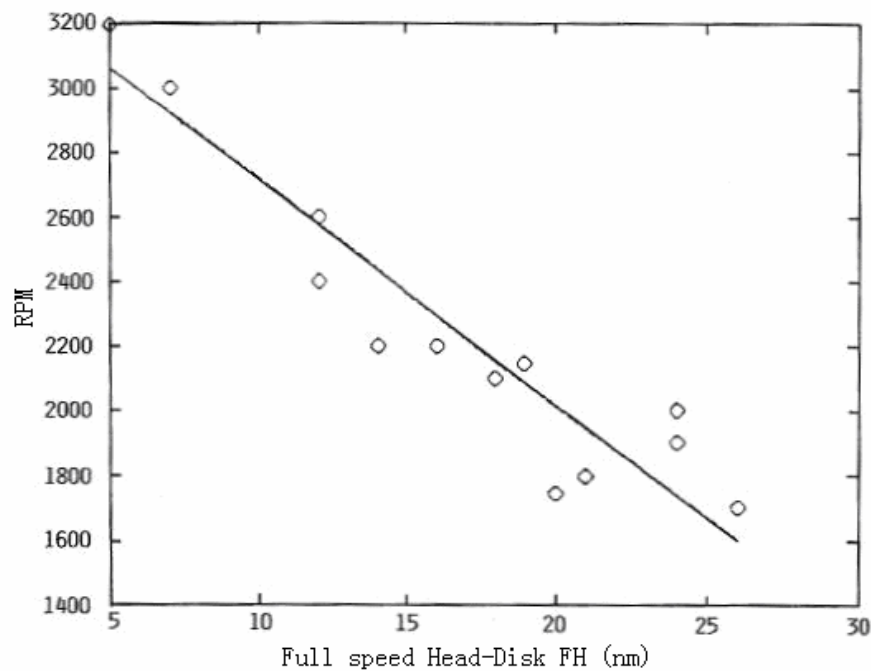


Fig 2.9 The relationship between landing RPM and flying height [20]

For purposes of illustration, and with reference to Figure 2.8 and 2.9, it may be assumed that a disk is rotating at a nominal speed of 7200 RPM, the velocity of the

disk is reduced from nominal 7200 RPM and the rate of change of the signal produced by the MR transducer is monitored. As shown in Figure 2.8, the slope of MR element voltage change curve changes appreciable at about 3200 RPM. Applies 3200 RPM to the flying height profile shown in Figure 2.9 and it corresponds to a full speed absolute flying height of 5 nm. In other words, the particular head under evaluation will be flying at approximately 5 nm at a nominal disk speed of 7200 RPM during normal operation.

This method utilizes the thermal response of an MR head to provide an estimate of absolute flying height. However, different slider may be of different relationship between its flying height and disk spinning speed (or the relative motion speed between slider and disk). If people can do the calibration of the relationship between flying height and rpm, the calibration method itself can be used for flying height testing, rather than using the thermal method plus an additional calibration. Furthermore, it is also difficult for the thermal method to give absolute fluctuation of flying height when the application is for in-situ characterization of flying height variation.

### **2.3.4 Harmonic Ratio Method for Flying Height measurement**

US patent 4,777,544 describes Harmonic Ratio Method for flying height measurement together with three implementations [21]. One implementation utilizes a recorded signal having only a single wavelength  $\lambda$ . The second concerns a dual wavelength method which requires recording two magnetic wavelengths on adjacent tracks for

measuring the changes in the head disk spacing. The third implementation of the invention is known as the harmonic ratio flying height method, and this method is based on writing a signal whose readback has a spectrum which has non-zero amplitude for at least two different frequencies. The invention uses the relationship between the amplitude of selected harmonic(s) and the head disk spacing to characterize the head disk spacing. The governing equation for the method is the Wallace equation (2.6), which shows that the harmonic readback signal reduces exponentially as the head-disk spacing increases.

Harmonic Ratio flying height measurement is a continuous, instantaneous measurement of the ratio of two spectral lines  $V(f_1)$  and  $V(f_n)$  in the spectrum of the readback signal  $V(t)$ . Both instantaneous spectral line amplitudes relate to the same volume element of the recording medium directly underneath the head. This makes the measurement inherently insensitive to such disturbances as those caused by variations in amplifier gain, head efficiency, effective track width, track-misregistration, medium velocity, magnetic moment, and medium thickness.

Commonly used recording patterns in harmonic ratio methods include all “1” code which we name as fixed transition interval harmonic method and “111100” (“1” represents a magnetic transition) code proposed by Bo Liu and Zhimin Yuan [19]. The approach using “111100” code scheme is referred to as triple harmonic method, as such a scheme provides 3 harmonics of comparable amplitude and energy intensity in a wide range of channel density. The testing process will be based on the amplitude ratio of the any 2 of the 3 harmonics, the preferred combination is the first and the third harmonics.

The harmonic amplitude ratio can be expressed by the following equation:

$$\frac{V_3}{V_1} = A_{31} k(g, \delta) \exp\left(-\frac{2\pi(d+a)}{K}\right) \quad (2.16)$$

where  $A_{31}$  is the harmonic amplitude ratio factor,  $k(g, \delta)$  is a factor determined by the gap length ( $g$ ) of the read head and the medium thickness  $\delta$ .

Zero flying height, as a reference point, is realized by spinning down the disk (to decrease the velocity between slider and disk) so that the air bearing force reduces and the slider approaches the disk. As the velocity decreases, flying height also decreases and the readback signal is sensed at each of the velocity points. When the signal ceased to increase, this indicates that the slider is in contact with the disk surface. Hence, the absolute flying height can be yielded by subtracting the harmonic amplitude ratio at zero flying height from that at working conditions and the corresponding spindle speed. Another approach is to reduce the environmental air pressure gradually until the slider contacts the disk surface.

Flying height sensitivity by this method is proportional to the channel density, which is defined as the ratio of PW50 and bitlength. A lower channel density will have lower sensitivity to the flying height variation. Therefore, it is better to have strong higher order harmonic in the testing process as it corresponds, effectively, to higher channel density. Therefore, the testing density is a critical parameter for such a flying height measurement method.

## 2.4 Summary of In-situ Flying Height Testing Techniques

The previous sections have briefly reviewed writing-process based flying height measurement techniques and reading-process based flying height testing techniques. The former include carrier erasure current method and scanning carrier current method. The reading-process based flying height measurement techniques include readback signal modulation method, PW50 method, thermal method and harmonic ratio method. Generally, these techniques are able to characterize slider's flying status in-situ and can be applied for drive level flying height monitoring.

The writing process based methods can measure the fly height in a larger range of flying height variation than all the reading process based methods. Therefore, they are suitable to characterize the flying height variation during the dynamic operations of the slider, such as the load/unload process and the track seeking process. However, as the writing process based methods are based on the nonlinear hysteresis response of the magnetic media, the accuracy achieved by these methods is not as high as the reading process based methods.

Readback signal modulation technique is, in general, based on Wallace equation and is quite intuitionistic for flying height variation. The first generation method is based on the amplitude of readback signal directly. The weakness of such a method is that its resolution can be greatly limited by off-track effect and mistakes any radial movements as vertical flying height variation. PW50 method is not as sensitive to off-track influence as readback signal modulation technique but the electronics for application can be quite complicated. Moreover, PW50 method tests flying height



variation at a low recording density which results in low sensitivity of this method. Thermal method provides estimation for flying height based on additional calibration to determine both the zero flying height and the coefficient between flying height. Thus, it is difficult to apply such a method for drive level analysis of slider's flying height.

Harmonic ratio method has high sensitivity to flying height variation at high recording density. By calculating ratio of two harmonics it removes off-track effect in a certain range. However, for drive level application we need to consider both the simplicity of methodology and testing resolution. Fixed transition interval method has low resolution at high recording density because of its low amplitude of 3<sup>rd</sup> harmonic and triple harmonic method has a complicated testing pattern for drive level applications.

Therefore, the requirement of drive level flying height measurement exerts a press for exploration of simpler, accurate, reliable and feasible in-situ flying height measurement methods for drive level analysis of flying height. As the flying stability is the main concern for drive level flying height analysis, the writing-process based techniques which are more suitable for dynamic performance analysis over large range of flying height variation (such as flying height variation during seeking and load/unload operations) are not suitable for such purpose and will not be the main research focus of this thesis.

## **Chapter 3 A New Approach for Drive Level Flying Height**

### **Analysis**

The fundamentals of reading process are analyzed in this chapter, aiming to understand how the flying height is related to the readback signal and, therefore, what are the possible directions toward better in-situ flying height analysis at disk drive level. A flying height error function is derived to evaluate the error introduced in the flying height analysis. After that, a novel harmonic burst method is proposed in the last session for drive level flying height analysis.

### **3.1 Fundamental Physics for Reading Process**

During the operation of a hard disk drive, the magnetic disk is rotated at a constant rate while data is written to or read from its surface. After the head is positioned above the track of the rotating disk specified in the access request, the requested data transferring is allowed to take place. During a read operation, data from the predetermined track is sensed by the head, after which it is processed by a read channel and delivered to the host system. In modern hard disk drives the data is read back using giant magneto-resistive (GMR) heads. The primary advantage of GMR heads is its greater sensitivity to magnetic fields from the disk, comparing the conventional magneto-resistive (MR) heads. The increased sensitivity makes it possible to detect smaller recorded bits and to read these bits at higher data rates. Larger signals from GMR heads also help

overcome electronic noise. The high areal densities attainable with GMR heads enable disk drive products to offer a maximum storage capacity with a minimum number of components including heads and disks.

A GMR read head consists of a read element located in the space between two highly permeable magnetic shields as shown in Figure 3.1. The shields help to focus the magnetic energy from the disk and reject the interference from stray fields. And the magnetoresistive element is made from a ferromagnetic alloy whose resistance changes as a function of an applied magnetic field.

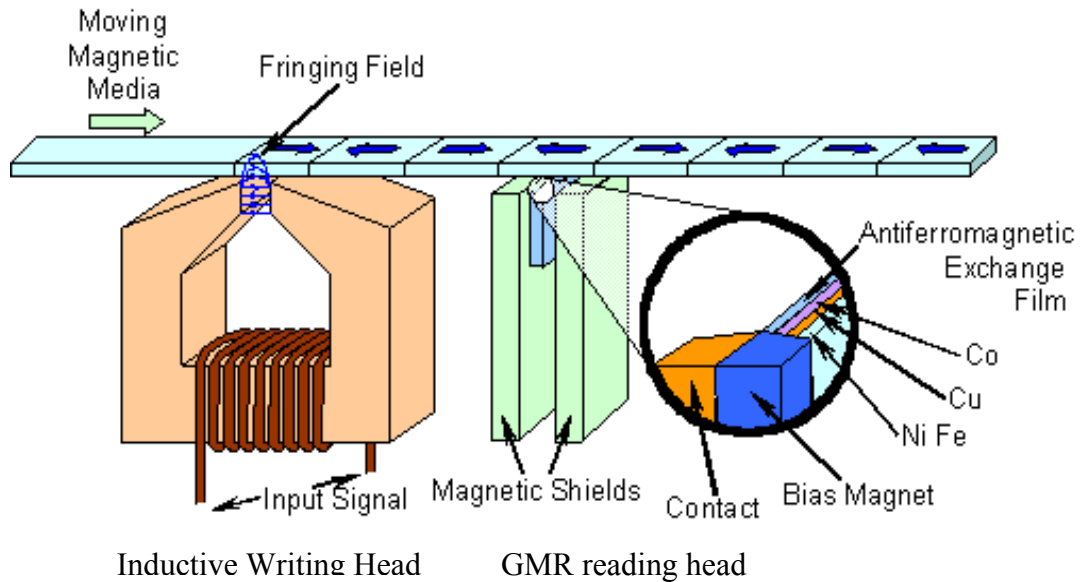


Fig 3.1 Schematic of an inductive write head and a GMR read head [22]

The essence of the magneto-resistive equivalent field is that the field is approximately that of two conventional inductive “ring” heads of opposite deep-gap field displaced by a distance of gap length and reader element thickness. The Fourier transform of an isolated pulse by GMR transducer can be expressed as [2]:

$$V_{GMR}(k) \propto e^{-k(d+a)} \frac{1-e^{-k\delta}}{k\delta} \frac{\sin(kg/2)}{kg/2} \sin\left(\frac{k(g+T)}{2}\right) \quad (3.1)$$

where variable  $k$  is the wavevector and usually holds that  $k = 2\pi/\lambda$ ,  $d$  is the head media spacing and  $a$  is the transition parameter. Here  $g$  is the read transducer gap length and  $T$  is the reader element thickness. From the above expression, it can be seen that the Fourier transform of the voltage greatly simplifies analysis of the recording process and all the information about the recorded magnetization is contained in the formula including the effect of spacing during recording process. The effect of spacing during playback is contained simply in the term “ $\exp(-k(a+d))$ ” and hence it is the basis for the in-situ flying height testing methods by measuring the readback signal.. It can also be seen that GMR heads suffer from spacing loss, thickness loss and gap loss.

### **3.1.1 Frequency Domain Expressions of the Generalized Readback Voltage of Multiple Transitions**

In order to analyze spacing effect from readback signal of multiple transitions, the analysis of the readback process is extended to consider the effects of multiple transitions. The principle of linear superposition states that the replay voltage from a sequence of step current changes is given by the sum of the playback responses of the individual transition playback voltages with regard to the spacing and polarity that comprise the current sequence [23]. Hence the Fourier transform of a given sequence is simply:

$$V_x(k) = V_{sp}(k) \sum_n (-1)^n e^{ikx_n} \quad (3.2)$$

where  $V_{sp}$  is the playback isolated transition response in formula (3.1) and  $x_n$  is the location of the  $n$  transitions written in the sequence. The Fourier transform expressions of two specific recording patterns including all “1” code and “111100” will be derived

in the next part to analyze the spacing effect. These two patterns are specially selected for analysis because they are the most popular recorded patterns used in harmonic ratio method, which are referred as fixed transition interval method and triple harmonic method.

### 3.1.2 Spectral Analysis of Square Wave Recording

Square wave recording refers to an alternating series of step record current changes at fixed transition interval. It is also referred to as an all “1” pattern. The continuous infinite Fourier transform from equation (3.2) is:

$$V_x(k) = V_{sp}(k) \sum_{n=-\infty}^{\infty} e^{-in(kB-\pi)} = V_{sp}(k) \sum_{m=-\infty}^{\infty} \delta\left(\frac{kB}{2\pi} - \frac{1}{2} - m\right) \quad (3.3)$$

Since the wavenumber of the fundamental component is related to the bitlength B by:  $k_0 = \frac{\pi}{B}$  and delta functions possess the property that:  $\delta(ax) = \frac{\delta(x)}{|a|}$ , equation (3.3)

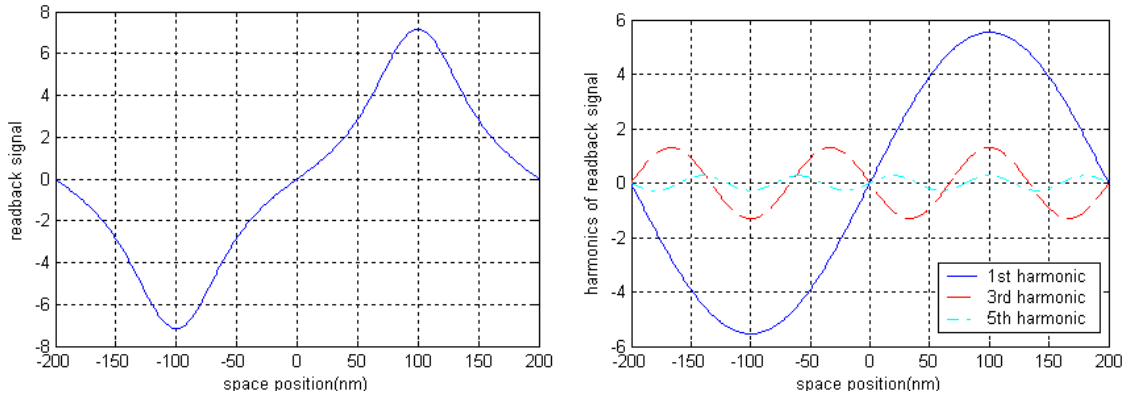
can be expressed as:

$$V_{flux}(k) = 2k_0 V_{sp}(k) \sum_{m=-\infty}^{\infty} \delta(k - (2m+1)k_0) \quad (3.4)$$

Equation (3.4) yields equally weighted pulses at all odd harmonics for both positive and negative k and the pulse weights do not decrease inversely with the harmonic number. It is useful to give equation (3.4) in a form corresponding to quantitative spectral measurements. A spectrum analyzer measures the rms power in a bandwidth  $\Delta f$  centered about frequency f.

$$V_{rms}(k = mk_0) = \frac{2k_0}{\sqrt{2\pi}} |V_{sp}(k)|, m = 1,3,5,7 \quad (3.5)$$

The spectrum differs from the Fourier transform of the isolated pulse by the factor  $\sqrt{2}k_0/\pi$ . Figure 3.2 (a) has simulated one period of square wave readback signal at 200 nm bitlength and Figure 3.2 (b) shows the 1<sup>st</sup>, 3<sup>rd</sup> and 5<sup>th</sup> harmonics whose amplitude is calculated by equation (3.5).



(a). Square Wave Readback Signal

(b). Odd Harmonics Waveform

Fig 3.2 Square wave recording waveform and harmonics

### 3.1.3 Spectral Analysis of Playback Signal of Pattern “111100”

Triple harmonic method records pattern of “111100”. By comparing spectral voltage of one period waveform voltage of “111111” and “111100”, spectral voltage expression for recording pattern “111100” can be derived based on equation (3.2). For six continuous bits written at a spacing of  $B_0$ :

$$V(k) = V_{sp}(k) \sum (1 - e^{-ikB_0} + e^{-i2kB_0} - e^{-i3kB_0} + e^{-i4kB_0} - e^{-i5kB_0})$$

$$k_1 = \frac{2\pi}{\lambda_1} = \frac{2\pi}{2B_0} = \frac{\pi}{B_0}, k_3 = \frac{2\pi}{\lambda_3} = \frac{2\pi}{2B_0/3} = \frac{3\pi}{B_0}$$

Therefore:

$$V(k_1) = V_{sp}(k_1) \cdot 3(1 - (-1)) = 6V_{sp}(k_1) \quad \text{and} \quad V(k_3) = V_{sp}(k_3) \cdot 3(1 - (-1)) = 6V_{sp}(k_3)$$

For a pattern of “111100” written at a spacing of  $B_0$ :

$$V(k) = V_{sp}(k) \sum (1 - e^{-ikB_0} + e^{-2ikB_0} - e^{-3ikB_0})$$

$$k_1 = \frac{2\pi}{\lambda_1} = \frac{2\pi}{6B_0} = \frac{\pi}{3B_0}, \quad k_3 = \frac{2\pi}{\lambda_3} = \frac{2\pi}{2B_0} = \frac{\pi}{B_0}$$

Therefore:

$$V(k_1) = V_{sp}(k_1) \sum (1 - e^{-i\frac{\pi}{3}} + e^{-i\frac{2\pi}{3}} - e^{-i\pi}) = V_{sp}(k_1)$$

$$V(k_3) = V_{sp}(k_3) \sum (1 - e^{-i\pi} + e^{-2i\pi} - e^{-3i\pi}) = 4V_{sp}(k_3)$$

Therefore, the 1<sup>st</sup> harmonic and 3<sup>rd</sup> harmonic intensity of pattern “111100” can be derived as:

$$V_{pattern}(k_1) = \frac{1}{3}k_3V_{sp}(k_1), \quad V_{pattern}(k_3) = \frac{4}{3}k_3V_{sp}(k_3)$$

$$V(k) = \frac{\sum (1 - e^{-ikB_0} + e^{-2ikB_0} - e^{-3ikB_0})}{3} k_0 V_{sp}(k) \sum_{m=-\infty}^{\infty} \delta(k - \frac{mk_0}{3}) \quad (3.6)$$

$$V_{rms}(k) = \frac{\sum (1 - e^{-ikB_0} + e^{-2ikB_0} - e^{-3ikB_0})}{3\sqrt{2\pi}} k_0 |V_{sp}(k)| \quad (3.7)$$

1<sup>st</sup> to 5<sup>th</sup> harmonics calculated by formula (3.6) are plotted out in Figure 3.3, and Figure 3.4 shows that waveform of readback signal of pattern “111100” and also the superposed waveform by harmonics waveform, the superposed waveform would accord with the original waveform better if more harmonics are superposed.

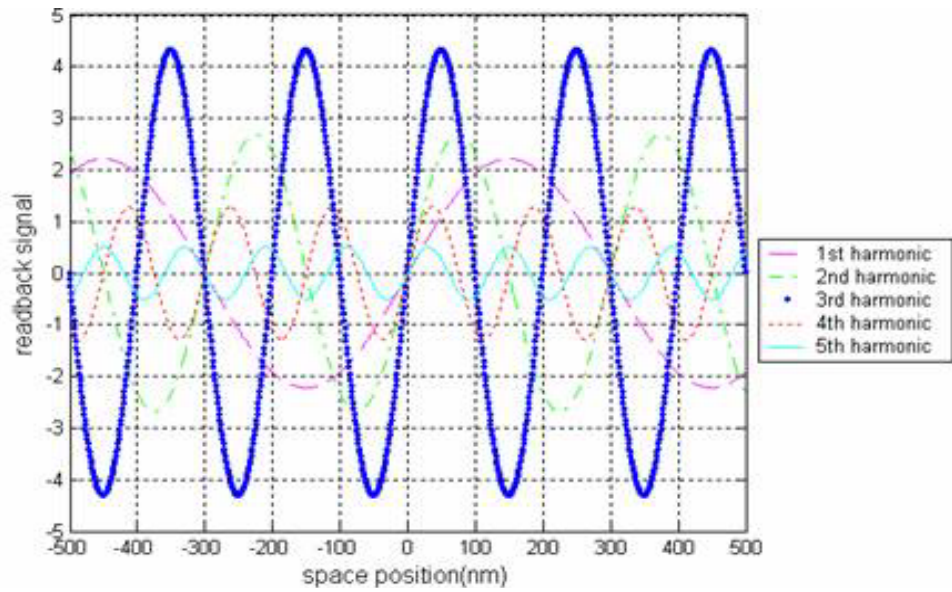


Fig 3.3 1<sup>st</sup> to 5<sup>th</sup> harmonics waveform of fixed transition interval method

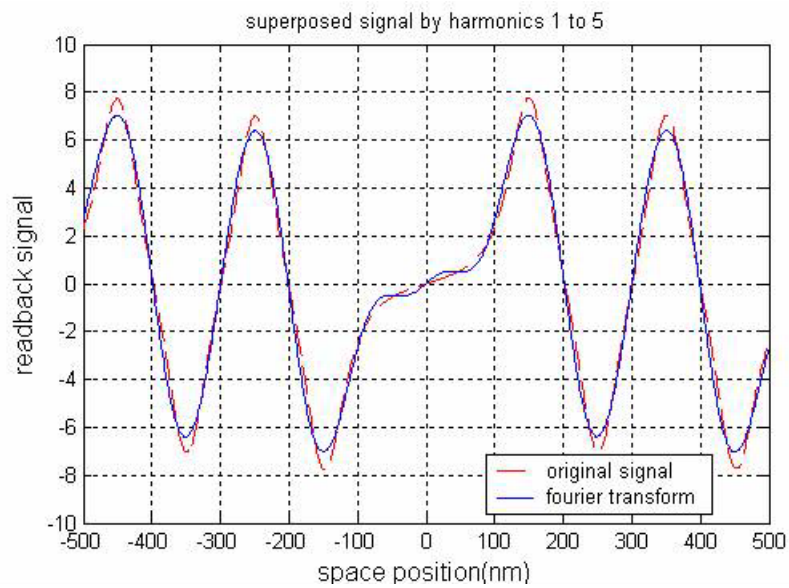


Fig.3.4 “111100” readback waveform and superimposed waveform by harmonics

### 3.2 Evaluation of Harmonic Ratio Flying Height method

As reviewed in Chapter 2, harmonic ratio method is the best in-situ solution so far to measure flying height fluctuations and characterize the lubricant related issues in the



high density magnetic recording systems. Moreover, the analysis of readback signal waveform of two special patterns (all “1” pattern and “111100”), which are referred as fixed transition interval method and triple harmonic method, are elaborated as the fundamentals of this methodology. In this part, the accuracy and sensitivity of harmonic ratio method are firstly evaluated from two conventional categories: the sensitivity of readback signal to flying height variation and readback signal amplitude. Furthermore, a new flying height error function is proposed for this evaluation.

### **3.2.1 Influencing Factors for Harmonic Ratio Method**

When slider is positioned at a predetermined track, the flying height variation is related to disk morphology and slider-medium interaction. Ideally, the error induced during measurement process should be eliminated or minimized. For flying height measurement which is at extremely small scale, it is quite important to study the measurement sensitivity, measurement precision and the measurement errors and figure out the best testing conditions to minimize the testing error.

#### **3.2.1.1 Measurement Sensitivity**

According to Wallace spacing loss theory, higher harmonic signal intensity means higher signal amplitude for flying height measurement and hence less effect from noise [24]. The sensitivity of harmonic intensity to flying height variation is investigated based on analysis of single harmonic. Simulation parameters are as following: PW50

equals to 102 nm, RPM is 5400 r/min, testing radius is at 1.0 inch, and write frequency is from 10 MHz to 150 MHz. By comparing the amplitude difference of spectral power (after logarithmic function) at two different magnetic spacing (One is 25 nm and the other is 30 nm), it can be seen from Figure 3.5 that readback signal amplitude is more sensitive to flying height variation when the channel density is high. In this case, at density of 1.0, the amplitude changes about 11%. And the sensitivity is even higher at a higher channel density. Therefore, from the ground of measurement sensitivity, the testing density should be above 1.0.

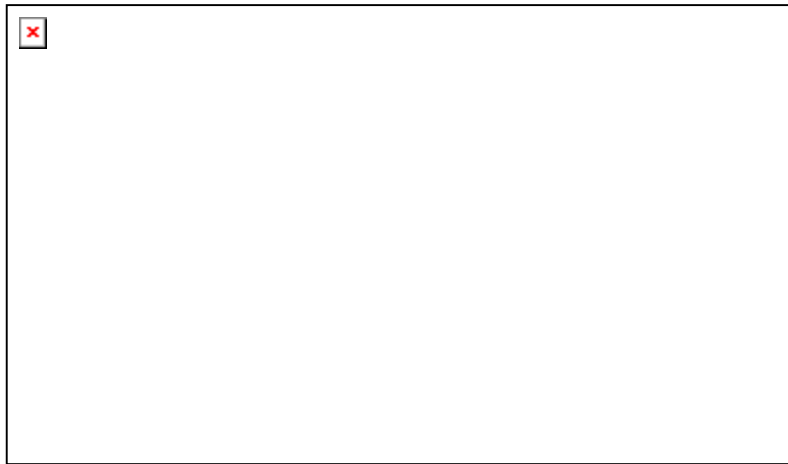


Fig 3.5 First harmonic intensity VS channel density

### 3.2.1.2 Measurement Precision

For both conventional fixed transition interval harmonic method (using all “1” data pattern) and triple harmonic method (using “111100” data pattern), the flying height can be characterized by monitoring the ratio of their 3rd harmonic to the 1st harmonic of the readback signal.

The relationship between harmonic amplitudes (before logarithmic function) and channel density of the above-mentioned two methods can be plotted by simulation as shown in Figure 3.6.

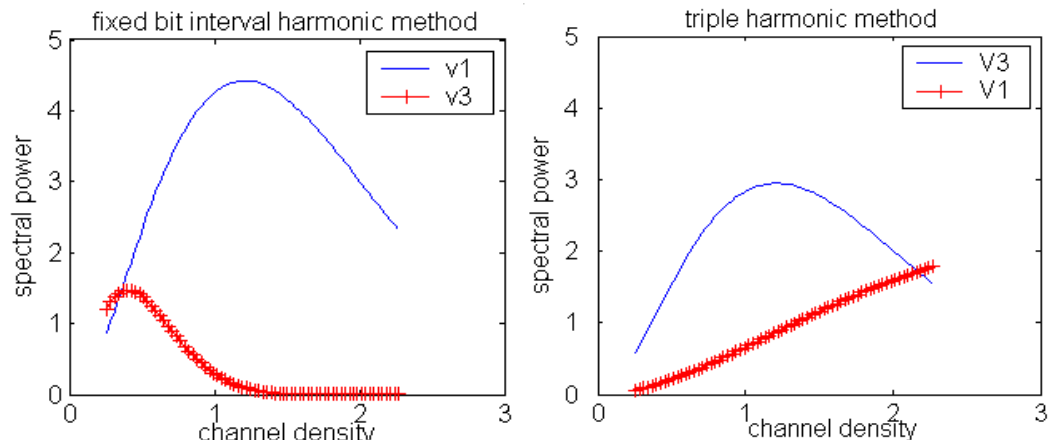


Fig 3.6 Harmonics of all “1” pattern and “111100” pattern

As mentioned before, it is preferred to test the flying height at a higher density in order to achieve higher flying height testing sensitivity. Taking SNR into consideration, the preferred channel densities for flying height measurement in the harmonic based method are those at which the harmonics to be used for flying high measurement are of strong and comparable power intensity. Compare the harmonic amplitude of two patterns, it can be seen that the amplitude of 3rd harmonic signal of all “1” pattern decreases rapidly with increased channel density, which mean lower recording density has to be used for the flying height measurement. The major advantage of triple harmonic method is its comparable power strength of two harmonics with large signal intensity. And another advantage of the method is its higher sensitivity to the flying height as it works at higher channel density. However, it can be seen that the cost of working with large amplitude of V1 signal in triple harmonic method is that the

corresponding V3 signal amplitude would be lower than the first harmonic of all “1” pattern case (the fixed transition interval method).

### **3.2.1.3 Measurement Errors**

The errors induced in the measurement process can be divided into two categories: one refers to channel noise and measuring equipments noise which are usually fixed values; the other is recording noise which is due to the media magnetic properties and varies with the recording frequency. For flying height stability measurement on a certain track, which calculates flying height variation using the average flying height of this track as the zero reference, the hardware noise is cancelled by subtracting and the measurement is only influenced by the media noise and environmental conditions. Media noise, especially the transition noise, is related to the recording frequency. As the bit aspect ratio (the ratio between bit width (radial direction) and bit length (circumferential direction)) increases, the noise from the track edge region becomes a greater percentage of the total noise of the system [25].

To investigate the transition noise effect, experiment was conducted on spinstand and different frequencies were written on radius of 1.357 inch of a disk rotating at 5400 RPM. Flying height variation was calculated by modulation of fundamental harmonic of all “1” code. Figure 3.7 shows that measurement results of flying height variation do vary with testing density, if the channel density is below 1.3.

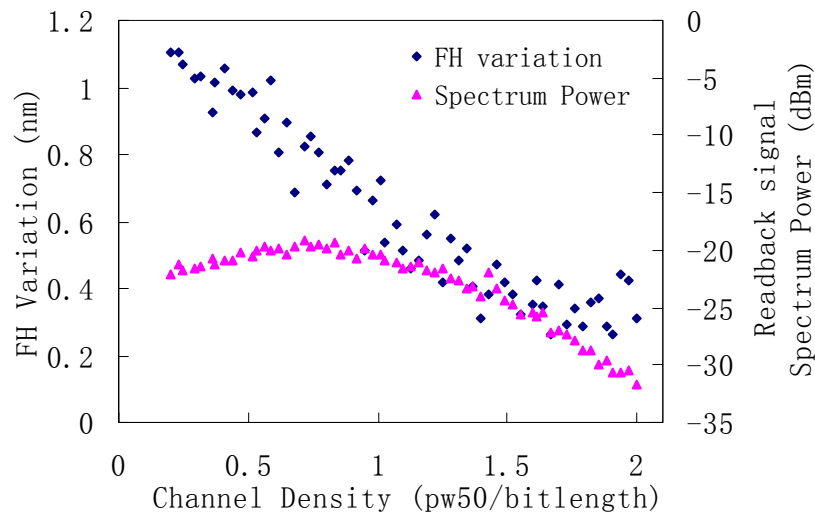


Fig 3.7 Flying height variation at different channel density

When the channel density is low, the tested value of flying height variation shows a descending trend with increasing transition noise (increasing testing channel density); while at high channel density (1.3 and above) the calculated flying height variation seems to be settling down. This discloses that increased transition noise at high density does not introduce increased measurement error and presents that in-situ reading process based methods should use high recording density in terms of less measurement error.

### 3.2.2 Flying Height Error Function

We noticed that the phenomenon illustrated in Figure 3.7 is of general meaning. Therefore, it is important to have an in-depth understanding of such phenomenon. In the engineering application, the amplitude of each harmonic signal is measured by narrow band pass filter. Although work has been reported on flying height testing sensitivity and how to achieve high and comparable harmonic amplitude, none of the

work has mentioned how to balance testing sensitivity and harmonic amplitude. For example, at channel density of 2.0, the harmonic amplitude is lower than at density of 1.0 however the testing sensitivity is much higher. Furthermore, none of the work has considered error caused by recording process and measurement equipments.

This part is focused on flying height error for fixed transition interval harmonic method and triple harmonic method.

For fixed transition interval harmonic method, assuming the recorded wavelength  $\lambda$  and according to the description of spectral voltage of formula (3.5), the amplitude of 1st and 3rd harmonic intensity can be expressed as:

$$V(k_1) = C \frac{(1 - e^{-k_1\delta})}{\delta} \frac{\sin(k_1g/2)}{k_1g/2} \sin\left(\frac{k_1(g+T)}{2}\right) e^{-k_1(d+a)} \quad (3.8)$$

$$V(k_3) = C \cdot k_1 \frac{(1 - e^{-k_3\delta})}{k_3\delta} \frac{\sin(k_3g/2)}{k_3g/2} \sin\left(\frac{k_3(g+T)}{2}\right) e^{-k_3(d+a)} \quad (3.9)$$

where C is a function of characteristic parameters of head and medium but not relevant to recorded wavelength. And,  $k_1 = \frac{2\pi}{\lambda}, k_3 = \frac{2\pi}{\lambda/3}$

Therefore, logarithmic difference of the two equations of (3.8) and (3.9) is:

$$\ln \frac{V(k_3)}{V(k_1)} = u(k, g, T, \delta) - (k_3 - k_1)(d + a) \quad (3.10)$$

$$d + a = -\frac{1}{(k_3 - k_1)} \left( \ln \frac{V(k_3)}{V(k_1)} - u(k, g, T, \delta) \right) \quad (3.11)$$

where  $u(k, g, T, \delta)$  is a factor determined by the recording wavelength, head parameters and medium magnetic layer thickness.

Equation (3.11) describes the relationship between flying height, readback signal and system parameters. To investigate flying height error, possible sources, which may be from two aspects: system parameters ( $g$ ,  $T$  and  $\delta$ ) and noise during measurement, are discussed in the following part.

### **3.2.2.1 Variation of System Parameters and Its Effect on Flying Height Measurement**

From equation (3.11), head and medium parameters, such as  $g$ ,  $T$ ,  $\delta$ , are related to flying height measurement. Read transducer gap length  $g$  and read element  $T$  are constants according to the same head. The main focus of this work is to explore methodology for the analysis of flying height fluctuation over the same track and refer its mean value of the same track. Therefore, the variation of  $g$  and  $T$  values will not affect the measurement of flying height fluctuation over the same track.

However, the industrial technique does not ensure absolute uniformity of magnetic layer thickness  $\delta$  over the track. Studies on the effect of  $\delta$  variation are necessary to investigate the variance introduced flying height error.

Assume up to 10% variation of magnetic layer thickness around 10 nm, Figure 3.8 shows the spectral voltage variation with  $\delta$  under different recording wavelength. The other parameters used are as the followings: 35 nm gap width, 45 nm for the sum of spacing  $d$  and transition length. It can be seen from Figure 3.8 that 10% variation of

magnetic layer thickness leads to a flying height testing error of up to 0.2 nm, which is less than 0.5% of the original flying height value. Compared to other error sources such as measurement equipments, this error is small and negligible. Hence the magnetic layer thickness could be assumed uniform and regarded constant in the flying height measurement process.

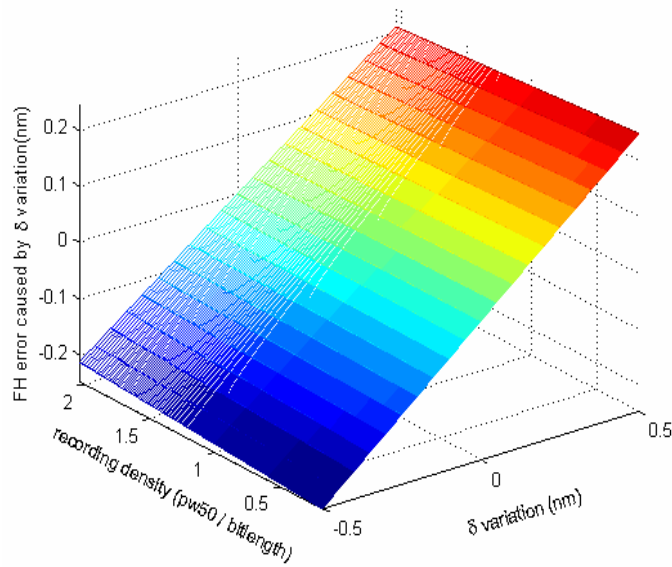


Fig 3.8 Error of flying height caused by  $\delta$  variance

### 3.2.2.2 Noise Effect on Flying Height measurement

The noise in reading of  $V(k_3)$  and  $V(k_1)$  is another possible main error source in the flying height measurement process. To study the consequent error due to the readback signal,  $\Delta V(k_3)$  and  $\Delta V(k_1)$  are used to denote noise induced fluctuation of  $V(k_3)$  and  $V(k_1)$ .

By differentiate (3.11), the factor  $u(k, g, T, \delta)$  is taken as constant and removed by differentiation. Therefore, we can deduce:



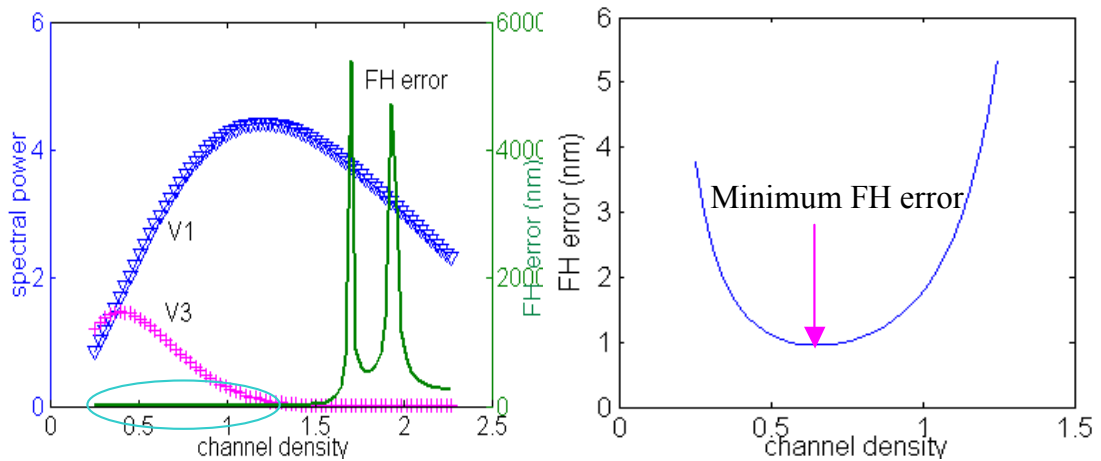
$$\Delta(d + a) = -\left(\frac{1}{k_3 - k_1}\right)\left(\frac{\Delta V(k_3)}{V(k_3)} - \frac{\Delta V(k_1)}{V(k_1)}\right) \quad (3.12)$$

This equation suggests that the noise induced error comes from the separate measurement channels of  $V(k_3)$  and  $V(k_1)$ , as shown in (3.13).

$$FH_{error} = \left| \frac{1}{k_3 - k_1} \left( \left| \frac{\Delta V(k_3)}{V(k_3)} \right| + \left| \frac{\Delta V(k_1)}{V(k_1)} \right| \right) \right| \quad (3.13)$$

where  $\Delta V(k)$  is error caused by magnetic noise, channel noise and measurement noise etc. It can be seen from (3.13) that error of the flying height measurement is also a function of testing density, other than the amplitude of harmonic intensity. Smaller recorded wavelength and higher harmonic intensity will contribute to smaller flying height error. Therefore, before flying height measurement, investigation should be done on choosing the optimum recording density to achieve high sensitivity of testing method as well as minimize testing error.

Simulation work is done based on (3.13). At RPM of 5400, fluxes of different frequencies are written at radius of 1.0 inch on disk. The channel density use in this analysis varies from 0.25 to 2.25. Considering that transition noise is linearly increased with channel density and take channel noise as a constant, we make the following supposition: the transition noise equals to  $0.01 \cdot k$  and channel noise is 1% of the maximum value  $V(k)_{max}$ . The  $\Delta V(k)$  is equal to the sum of transition noise and channel noise.



(a) Flying height error VS Channel density; (b) Flying height error at low density part

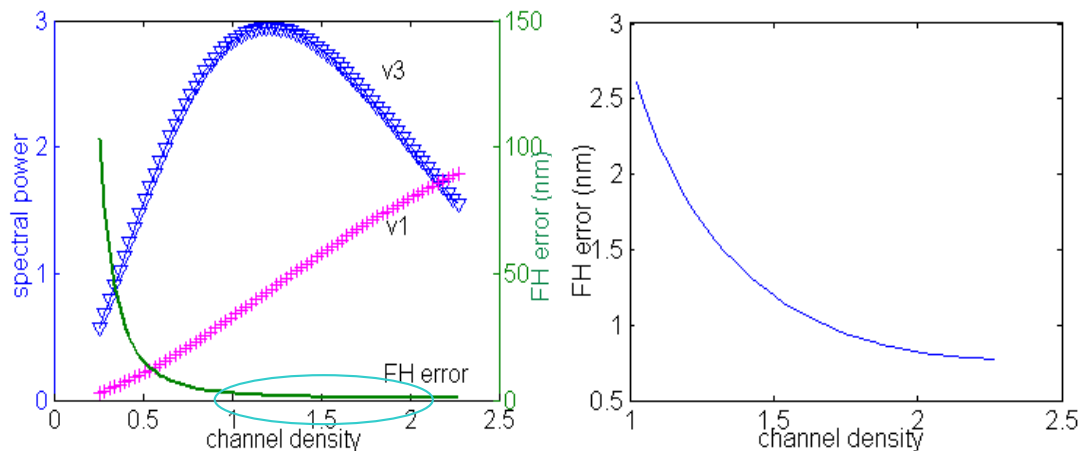
Fig 3.9 Flying height error by fixed transition interval method

Figure 3.9 (a) shows flying height error curve as well as harmonic intensity at different channel densities. Figure 3.9 (b) shows the zoom-in plot in the density range of 0.25 to 1.5. Although the amplitude of 1st harmonic intensity arrives at maximum at density around 1.2, the 3rd harmonic intensity amplitude becomes comparatively small. The flying height error decreases to minimum at the density of about 0.6.

The spike in flying height error curve occurs due to vanishing V3 value when the wavevector satisfies  $k = 2n\pi/g$ , or when the wavelengths are  $\lambda = 2\pi/k = g/n$ , where  $n = 1, 2, 3, \dots$

For triple harmonic method and under the same head-media parameters, pattern “111100” is also recorded on the same position of disk with varying channel densities. The same error  $\Delta V(k)$  is introduced and calculated by (3.13) as shown in Figure 3.10. Instead of having an optimal testing channel density as the case of fixed transition interval method, the triple harmonic method shows descending trend of flying height

error with increasing testing channel density. Furthermore, the error is reduced to 0.6 nm when the channel density is above 2.3, which is smaller than the minimum error of the fixed transition interval method (about 1 nm).



(a) Flying height error VS Channel density; (b) Flying height error at high density part

Fig 3.10 Flying Height error by triple harmonic method

In conclusion, fixed transition interval method and triple harmonic method show different characteristics of flying height error. The former method prefers testing at low density while this will decrease the sensitivity of readback signal amplitude to flying height variation; the later one is less affected by noise at high density, however nonlinearities at extremely high testing density will lead to unreliable measurement results. In other words, it is suggested for triple harmonic method to work at a channel density as high as possible unless the performance is degraded by the nonlinearity effect at extremely high channel density.

### **3.3 Methodology of Harmonic burst Method**

As discussed in last session, flying height error as described in (3.13) is a function of the two harmonics used for flying height testing. Both triple harmonic method and fixed transition interval method has a fixed relationship between two testing harmonics, that is to say, both methods measures 1st harmonic and 3rd harmonic and the ratio of two frequencies is 3. Therefore, it brings out an idea whether there is a method by which flying height error can be eliminated or minimized by choosing the optimum ratio of frequencies and optimum testing density to measure flying height. Based on this idea, harmonic burst method is proposed in the following part.

#### **3.3.1 Principles of Harmonic burst Method**

The guidelines for the exploration of new testing methodology for drive level application are the following two, in addition to the general requirement for in-situ flying height testing technology. The first is freedom of selecting harmonic frequency. The second is to increase the amplitude of the flying height testing harmonics.

Harmonic burst method relies on the relationship between readback signals and flying height. Assuming the magnetic layer is uniform on adjacent recording area, the proposed harmonic burst method writes block of data pattern at alternative frequencies on the testing tracks and uses the amplitude ratio of the readback signal from adjacent data blocks to derive flying height information. Each block is of fixed transition interval of frequency  $f_1$  or  $f_2$ , where  $f_1$  is smaller than  $f_2$ . Suppose the recorded bit-

length is  $\lambda_1$  and  $\lambda_2$ , then,  $k_1 = \frac{2\pi}{\lambda_1}$ ,  $k_2 = \frac{2\pi}{\lambda_2}$  and  $k_1 = \alpha \cdot k_2$  ( $0 < \alpha < 1$ ), the harmonic

intensity of readback signals at each recorded wavelength can be expressed as (3.1).

The logarithmic forms of the harmonic spectral voltage are as following:

$$\ln V(k_1) = \ln C + \ln\left((1 - e^{-k_1\delta}) \frac{\sin(k_1g/2)}{k_1g/2} \sin\left(\frac{k_1(g+T)}{2}\right)\right) - k_1(d + a)$$

$$\ln V(k_2) = \ln C + \ln\left((1 - e^{-k_2\delta}) \frac{\sin(k_2g/2)}{k_2g/2} \sin\left(\frac{k_2(g+T)}{2}\right)\right) - k_2(d + a)$$

Therefore, difference of the logarithmic equations is:

$$\ln \frac{V(k_2)}{V(k_1)} = u(k, g, T, \delta) - (k_2 - k_1)(d + a) \quad (3.14)$$

$$d + a = -\frac{1}{k_2(1 - \alpha)} \left( \ln \frac{V(k_2)}{V(k_1)} - u(k, g, T, \delta) \right), \quad 0 < \alpha < 1 \quad (3.15)$$

Equation (3.16) shows that the variation of flying height (also d variation) can be obtained by the ratio of  $V(k_2)$  and  $V(k_1)$  during read process.

$$\Delta FH = -\frac{1}{k_2(1 - \alpha)} \Delta \ln \frac{V(k_2)}{V(k_1)} \quad (3.16)$$

### 3.3.2 Principle for Selection of Channel Density of Flying Height Measurement for Harmonic burst Method

Flying height error function can be easily conducted from equation (3.16) that:

$$FH_{error} = \left| \frac{1}{k_2(1 - \alpha)} \right| \left( \left| \frac{\Delta V(k_2)}{V(k_2)} \right| + \left| \frac{\Delta V(k_1)}{V(k_1)} \right| \right) \quad (0 < \alpha < 1) \quad (3.17)$$

Where  $\alpha$  is the ratio of  $k_1$  and  $k_2$ .  $\Delta V(k)$  is error caused by magnetic noise, channel noise etc.

Therefore, it can be seen from (3.17) that error of the flying height measurement is also correlated to the channel density and the harmonic amplitude, similar to fixed transition interval method and triple harmonic method. Therefore, before flying height measurement, investigation should be done on choosing the optimum channel density to achieve high sensitivity of testing method as well as minimize testing error. Discussion is done in the following session to study the influence of the frequency ratio between two testing transition blocks on the accuracy of measurement result.

### **3.3.2.1 Minimization of Flying Height Error with Proper Selection of Channel Density and Frequency Ratio $\alpha$**

Based on equation (3.17), Figure 3.11 meshes out the plot of flying height error varying with the ratio  $\alpha$  and the channel density determined by  $f_2$ . The ratio of two testing frequencies varies from 0.2 to 0.8 (i.e,  $1.25f_1 < f_2 < 5f_1$ ) and the channel density for  $f_2$  varies from 0.4 to 2.5.

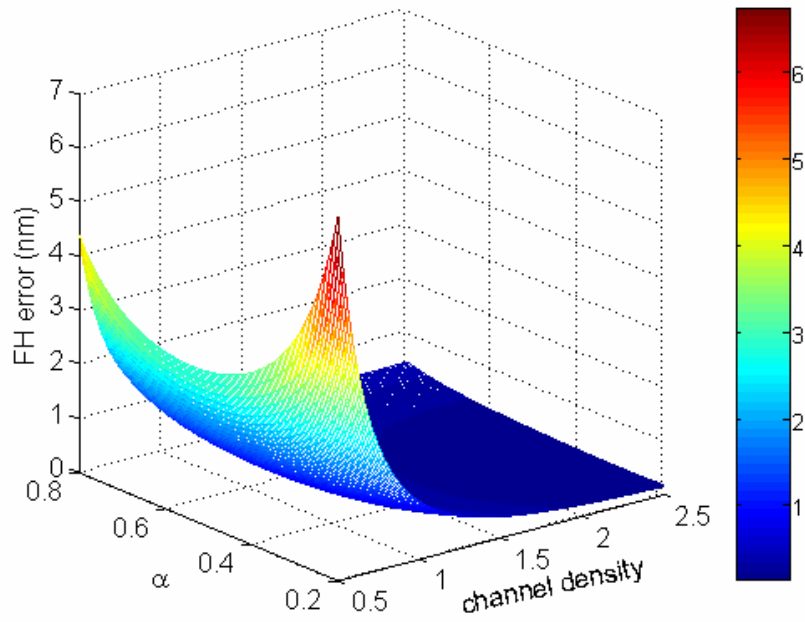
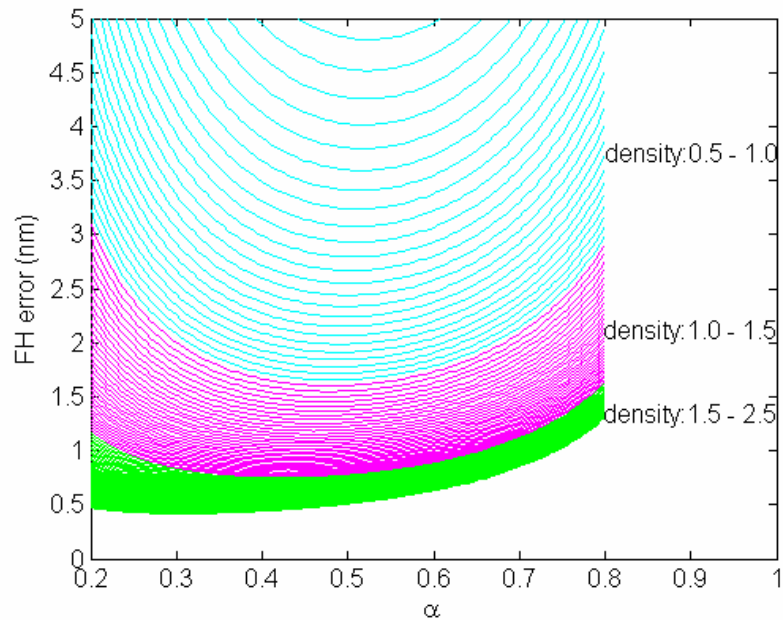
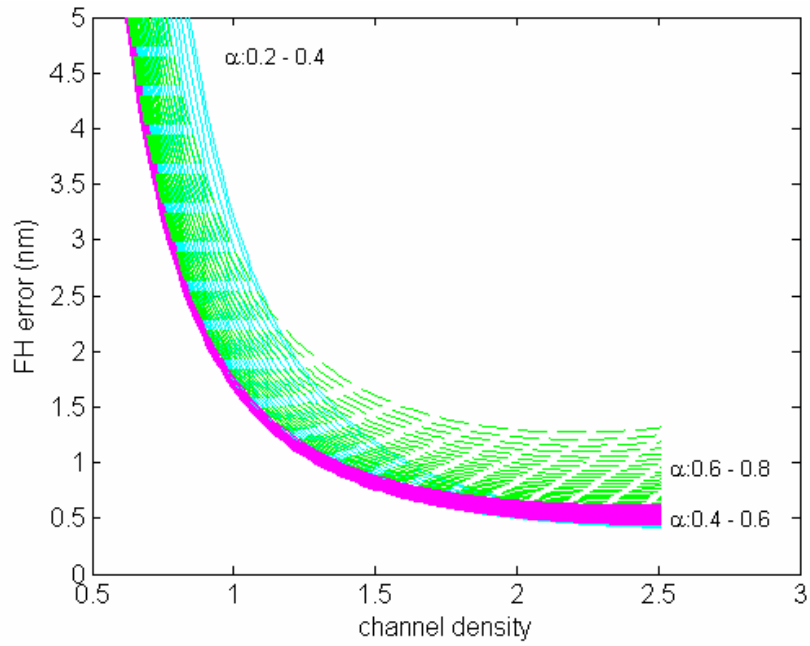


Fig 3.11 Flying height error as function of channel density and  $\alpha$

Figure 3.12 analyzes the influence of channel density and the ratio  $\alpha$  respectively. It shows that, generally, the error decreases when the channel density is higher and each channel density corresponds to an optimum ratio value.



(a) Flying height error as function of  $\alpha$ ;



(b) Flying height error as function of channel density

Fig 3.12 Flying height error as function of  $\alpha$  and channel density

Figure 3.13 illustrate the flying height error as function of  $\alpha$  at 4 different channel densities at 1, 1.5, 2 and 2.5 respectively, plot out the flying height error as function of  $\alpha$ .

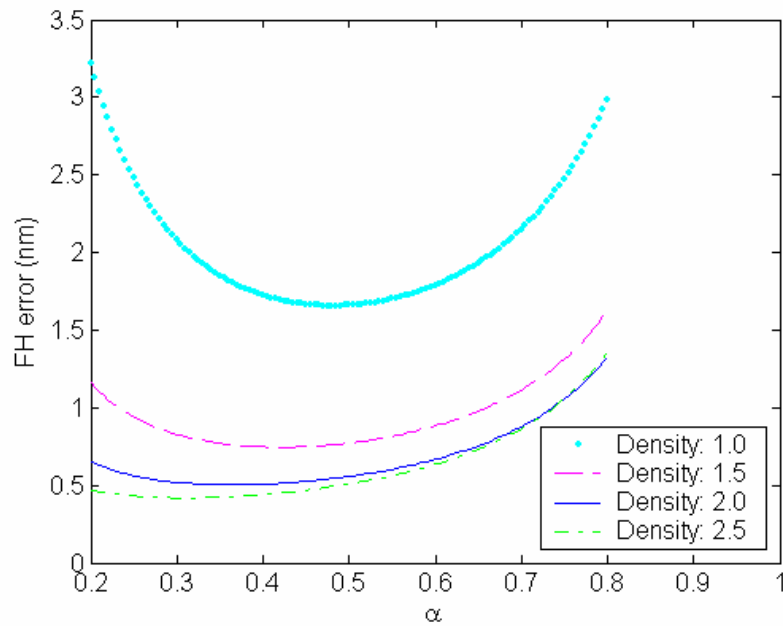


Fig 3.13 Flying height error as function of  $\alpha$  at density of 1.0, 1.5, 2.0 and 2.5



It shows that for testing density of 2.5, the optimum ratio is about 0.3, 0.4 for density of 1.5 and 2.0, and 0.45 for channel density of 1.0. The error measured at higher density is smaller than that at a lower channel density.

Therefore, to achieve high sensitivity as well as minimize the measurement error of harmonic burst method, the principle is to choose a high channel density according to head medium parameters and select an optimum ratio value at this channel density. However, it does not necessarily mean that the higher the testing frequency, the better testing result is. Nonlinearities in write and read process, which occur at high recording density, will introduce distortion in the readback signals and hence make the measurement results unreliable.

### **3.3.2.2 Nonlinearities Effect in Flying Height Measurement Process**

For rigid disk and GMR head combinations, both the write and read process can cause nonlinear distortion in the readback signals. Nonlinearities at high density are caused by strong magnetostatic interactions between transitions [26]. The nonlinearities can result in distortions in the readback signal which is no longer a linear superposition of isolated pulses. For the harmonic burst method, which is based on readback signal amplitude, the nonlinearities will obviously result in great errors in the testing results. Therefore, we should try to avoid and minimized the effects caused by nonlinearity during writing and reading process.

The nonlinear distortion generally includes both phase shift called nonlinear transition shift (NLTS) and amplitude variation called partial erasure (PE). NLTS refers to a transition position shift when two transitions are written close enough and the demagnetizing field from the previous transition affects the writing of the next transition. PE is caused by “local annihilation” of magnetic transitions and results in a reduction of the readback voltage amplitude. One of the advantages of harmonic burst method is that it is immune to NLTS. Because this method uses square wave recording pattern, i.e all “1” code, hence magnetostatic interaction causes each transition to shift towards the previous one. Since this nonlinear transition shift is applied to every transition, the distance between two adjacent transitions is unchanged. Therefore, the only waveform distortions one can observe at high density are the combination of the partial erasure and the transition broadening effect [27].

In general, selection of the channel density for flying height measurement by harmonic burst method is based on the specific head and medium parameters. Usually, we can choose the higher frequency  $f_2$  as high as possible until the signal suffers from PE obviously and thus determine  $f_1$  according to optimum ratio value to achieve minimum measurement error.

### **3.4 Summary**

In this chapter, fundamentals of reading physics by GMR transducer was elaborated in terms of GMR structure, frequency domain expression for reading back recorded transitions. Comparison between the fixed transition interval method and triple

harmonic method was made in terms of measurement sensitivity, precision and possible flying height testing errors. After that, a new flying height error function is proposed to evaluate those in-situ flying height testing methods base on harmonic ratio analysis. It is found that fixed transition interval method has to balance the amplitude between the 1<sup>st</sup> harmonic and the 3<sup>rd</sup> harmonic because the 3<sup>rd</sup> harmonic has quite low amplitude which makes it more sensitive to interference caused by possible testing noise. On the other hand, triple harmonic method suffers less influence from noise when the channel density is high. However, the harmonic amplitude of the triple harmonic method is still not high enough as its signal power scatters to three harmonics. It is worth to explore methods which can give even higher harmonic amplitude. Furthermore, it is noticed that the first harmonic amplitude of the fixed transition interval method gives the highest possible harmonic amplitude.

Thus, harmonic burst method is proposed which combines the advantage of the above mentioned two methods together. Two transition blocks are written to the testing track alternatively. Each block is of its own fixed transition interval so as to have the highest harmonic amplitude. This method has both the advantage of high harmonic amplitude and alternatives for testing frequencies. By choosing optimum ratio of testing frequencies and channel density, flying height testing error can be minimized whilst retaining the high sensitivity to flying height variation.

## **Chapter 4 Embodiments of Harmonic Burst Method on Hard Disk Drive**

In order to apply harmonic burst method at drive-level, the embodiments on hard disk drives are elaborated in this chapter. The servo mechanism on hard disk drive is illustrated firstly and followed by two embodiments of harmonic burst method on hard disk drives: one is applied at data zone and the other is at servo area. In addition, the selection of recorded data length is discussed considering system characteristic resonance frequencies and followed by studies on bandwidth effect of harmonic extractor on measurement results.

### **4.1 Servo Mechanism on Hard Disk Drive**

The servomechanism on hard disk drive is reviewed briefly here as the information recorded on and retrieved from disk surface consists of both user data and servo data.

The disk assembly of a drive usually is organized into specific structures to enable the organized storage and retrieval of data. Each platter is broken into tracks and each track is broken into sectors, which normally hold 512 bytes of information. With today's high track densities, there is an increased demand for a higher repeatability of positioning. The servo is thus introduced to solve the positioning problem caused by temperature drift, such as thermal expansion of the suspension, the disk media and the

mechanical parts. Therefore, not all the space on platters is used for data storage. Instead, there are some predetermined areas occupied by the servo information.

For hard disk drives, servo scheme is used to align the centre of the recording head to the centre of the target data track. There are three different ways that the hard disk servomechanism has been implemented: wedge servo, dedicated servo and embedded servo (also called sector servo). Each uses a different way to record and read the servo information from the disk. Wedge-servo technique was used in old generation disk drives, the servo information is recorded in a “wedge” of each platter and the remainder of the disk contains user data. The critical flaw is that the system must wait to position the sliders until the servo wedge is rotated around to where the heads are and this waiting makes the positioning performance of drives slow. In dedicated servo technique, an entire surface of one disk platter is dedicated for servo information and no servo information is recorded on the other surfaces. This design eliminates the delays associated with wedge servo designs. Unfortunately, an entire surface of the disk is wasted because it contains no data. Moreover, the heads where data is recorded may not always line up exactly with the head that is reading the servo information and hence need frequency thermal recalibration. The newest servo technique intersperses servo information with data across the entire surface of all the head disk platter surfaces. The servo information and data are read by the same heads and the heads never need wait for the disk to rotate the servo information into place as with wedge servo [28]. The need for constant thermal recalibration is greatly reduced since the servo information and data are the same distance from the centre of the disk and will expand or contract together. The difference between dedicated servo and embedded servo is shown in Figure 4.1.

*Dedicated Versus embedded Servo*

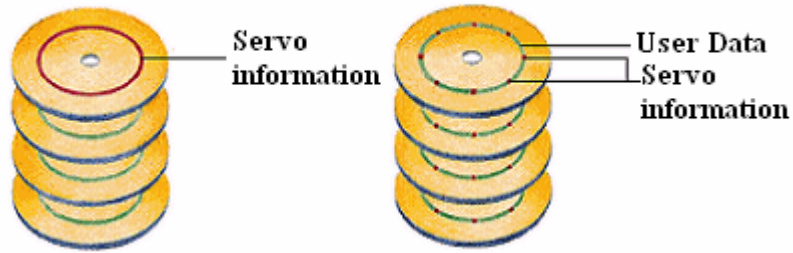


Fig 4.1 A simple illustration of the difference between dedicated servo and embedded servo: On the left, dedicated servo: one platter surface contains nothing but servo information, and the others nothing but data. On the right, embedded servo is with data and servo information together. (Note that for clarity only one track on each platter (one cylinder) is shown in this illustration; in fact every track of the servo surface has servo information in the dedicated servo design, and each track of each surface has interspersed servo information in the embedded design. [29])

All modern disk drives use sector servo in which there are fixed number of servo sectors, which are synchronized in each data zone, and more user data sectors in outer zones. The readback signal of both servo and data information with embedded servo technique is shown in Fig 4.2.

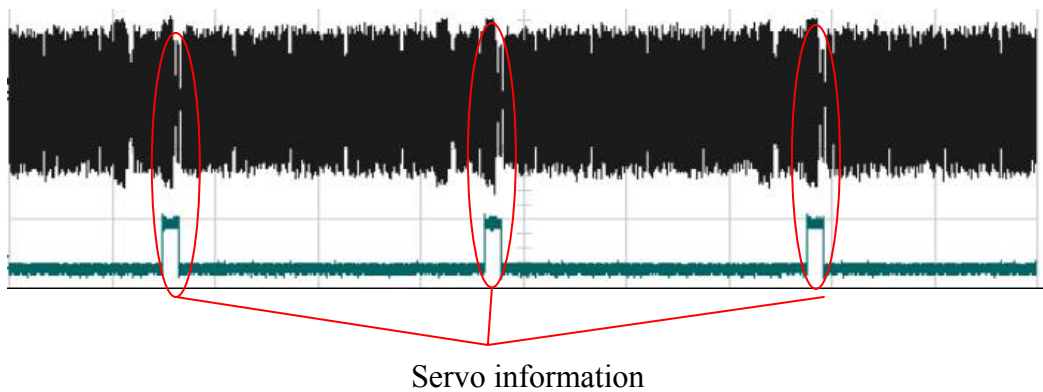


Fig 4.2 An example of readback signal with embedded servo technique

## 4.2 Two Embodiments of Harmonic Burst Method on Hard Disk Drives

Considering the servo scheme applied on hard disk drives, harmonic burst method can have two embodiments for flying height measurement. One is applied in data area and the other in servo area. The embodiment applied in data area is for flying height variation characterization. The patterns can be recorded when flying height variation measurement is requested and can be erased when the measurement is completed. The main purpose of the other embodiment in servo area is for flying height monitoring and real-time adjustment, the patterns are recorded in servo area and cannot be overwritten.

In the first embodiment which is shown in Figure 4.3 (a), a plurality of signals of constant frequency  $f_1$  and  $f_2$  are recorded alternatively on the predetermined data area of a predetermined track. Because of the space loss effect, the readback signal of two frequencies will vary on the whole track when the slider is vibrating due to disk morphology and environmental factors such as shock. By monitoring the ratio of first harmonics of the readback signals from the two different blocks, the flying height variation can be calculated. A flying height mapping can also be done from ID to OD to study characteristics of flying slider.

The second embodiment stores two patterns in one or more than one servo sectors of each track on the disk. In accordance with this embodiment, the servo pattern includes an E burst extending across the surface of the disk as shown in Figure 4.3 (b). The E burst stores two patterns with frequency  $f_1$  and  $f_2$ . In general, the method determines a

ratio of readback signals and compares this ratio to a predetermined reference value for each sector to determine whether flying height is in the proper range. If not, the host computer should issue a failure alarm and postpone read or write operations to prevent data loss.

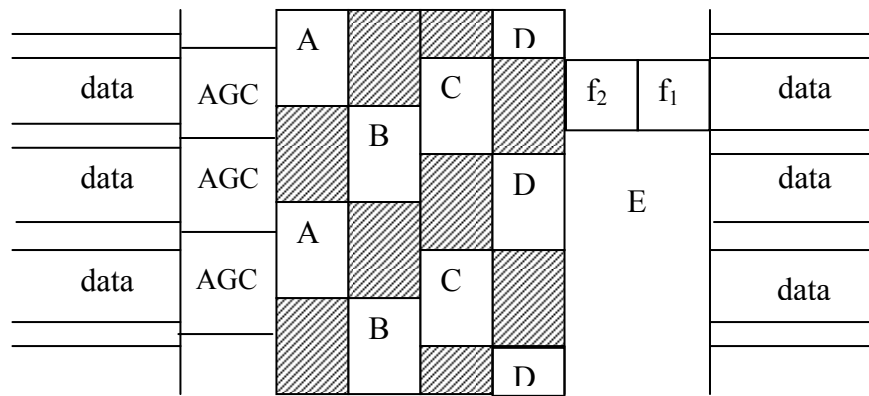
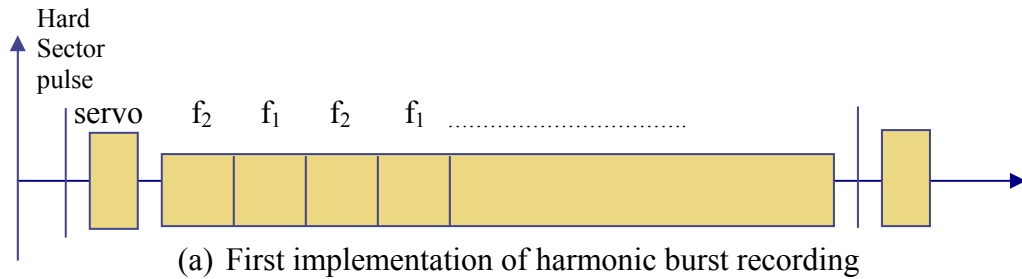


Fig 4.3 Scheme of harmonic burst method

It should be noted that there is difference between transition writing at drive level and at component testing level (such as read/write test with spinstand). Drive level testing does not allow writing with arbitrary frequencies. Modern hard disk drives employ a technique called zoned bit recording (ZBR). With this technique, tracks are grouped into zones based on their distance from the centre of the disk, and each zone is assigned a number of sectors per track. Tracks on the outside cylinders have more sectors than on the inside cylinders. The clock rate for data transfer also varies with



different zone number. Different writing clock is predetermined for different zones. Hence for drive level flying height measurement by harmonic burst method, testing frequency is limited by the writing clock and can only be multiples of the clock frequency by coding scheme. Therefore, the resolution may not be as high as on spindisk because the optimum channel density and optimum frequency ratio may not be achieved on disk drive. More details are discussed in the experimental part in chapter 5.

### **4.3 Block Length Selection and Filter Application**

Harmonic burst method writes multi-groups of data pattern at frequency of  $f_1$  and  $f_2$  on the testing tracks and the length of each data block determines the accuracy of harmonic burst method. Vibrations at slider sway mode, disk resonance mode, suspension resonance mode and air-bearing resonance mode represent slider instability in tracking direction and vertical direction. As the readback signal of each group is a function of flying height, track positioning and other factors, the length of data block should be much shorter than the wavelength of the resonance frequencies which we are interested.

### 4.3.1 Characteristic Resonance Frequencies in Hard Disk Drive

High-speed disk rotation generates strong interaction in the air-disk interface and air-slider/suspension/arm interface and leads to vibration of the disk, suspension, actuator arm, and slider. As a result, head's positioning accuracy is affected.

The resonant modes of a commercial actuator arm include arm bending, arm torsion and arm sway. The later two modes generally contribute to the track misregistration (TMR) and limit the servo bandwidth. The resonant frequencies for three modes are usually below 20 kHz [30].

The suspension has flanges, springs and gimbals portions for bending stiffness, forcing the head against the disk, and following the disk surface. And the pressure acting on the surface of a suspension obtained by the airflow modeling is integrated into the forces in every divided portion that represent fives parts (Part-A, Part-B, Part-C, Part-D and Part-E) of the HGA (see Figure 4.4).  $F$  represents normal force and  $M$  is angular momentum. Figure 4.5 shows the analyzed typical eigenmodes with corresponding eigenvalues [31].

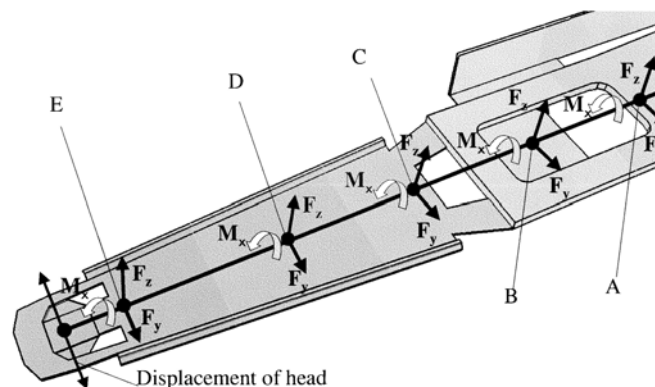


Fig 4.4 Partitioning and definition of aerodynamic forces

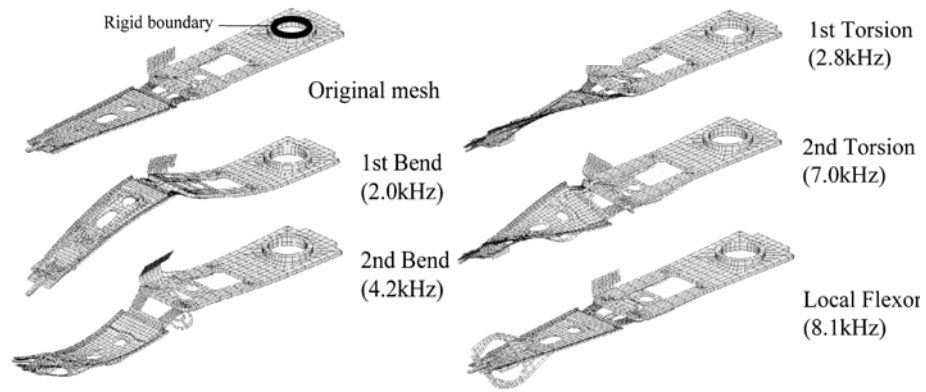


Fig 4.5 Typical eigenmodes obtained by structure-vibration analysis

The air bearing resonance may be excited by disk morphology, depending on the dynamics of mechanical system [32]. As a rigid body, a slider generally has 3 degree of freedom of vertical translation, pitch and roll angular motions. In the case of slider shown in Figure 4.6, the system has three air bearing modes. The first and third modes are coupled with vertical and pitch motion, which can be represented as a rotation of the slider with respect to the nodal lines #1 and #3 at frequencies of 134 kHz and 360 kHz respectively. The slider also has a roll mode at about 163 kHz, which is a rotational motion with respect to the nodal line of #2. And this mode usually has significant influence on the flying height modulation.

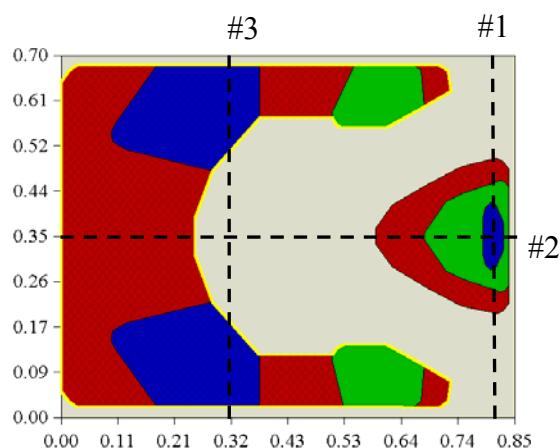


Fig 4.6 Air bearing surface and dynamic characteristics of a femto slider

### 4.3.2 Selection of the Block Length

Here, block length refers to the physical length of each harmonic burst. It is determined by bit length and total number of transitions in the burst.

Generally, considering the dynamic characteristics of actuator arm, suspension and air bearing slider, analysis of the flying height variation can be broken into three distinct frequency bandwidths: Band I: 10 to 100 kHz, Band II: 100 to 500 kHz, and Band III: greater than 500 kHz. Flying height modulation amplitude in Band I is the geometric flying height modulation and on the same order as the disk morphology. The flying height modulation in Band II is dominated by the dynamics of the air bearing slider. The Band III frequency is due to surface roughness and microwaviness. Its frequency is so high that the slider cannot follow it at all. Fortunately, the amplitude of such modulation is negligible (less than 0.1 nm). Therefore, the investigation should be focused on Bands I and II mainly [33].

For example, if we are interested in the flying height modulation below 50 kHz with the slider flying on radius of 1.7 inch of a disk which is rotating at RPM of 5400, according to sampling law, at least 1111 ( $= 2 \cdot 50k / (RPM/60)$ ) continuous harmonic burst data groups should be recorded at this selected track. Therefore, including consideration on non data area which may occupy one tenth of the whole recording surface in a typical embedded servo hard disk drive, the time for every rotation of the disk is  $\frac{1}{RPM/60}$  (s), the valid length for data recording (excluding the servo area) is

about  $\frac{9}{10} * \frac{1}{RPM / 60}$  (s); therefore, the length of each data group for flying height

characterization cannot exceed  $9 \mu s$  ( $= \frac{9}{10} * \frac{10^6}{RPM / 60} / 1111 (\mu s)$ ). If the optimum

channel density is at 2.0 (PW50 = 100 nm) and the optimum ratio is 1/3, which means the recorded wavelength is 100 nm and 300 nm respectively, the maximum number of

harmonic burst in each data group is 2196 ( $= \frac{9 \mu s}{\lambda / V}$ ) and 732 because the linear velocity

at radius of 1.7inch is about 24.4m/s ( $= 2\pi R * \frac{RPM}{60}$ ),.

Usually the spectrum analyzer can be used as narrow band-pass filter to extract harmonic amplitude from readback signal at certain frequency. However, if harmonic burst method is used to monitor high frequency modulation of flying height which means that fewer periods in each data group, the bandwidth of spectrum analyzer may be not wide enough to achieve such a rapid response to filter out harmonics of each data group because the maximum bandwidth of spectrum analyzer is 3 MHz. In this case, a software-based filter is proposed to extract harmonic signal envelope. The bandwidth of this filter is programmable and set to be wide enough to extract f1 and f2 harmonics.

### **4.3.3 Bandwidth Effect of Spectrum analyzer**

The passband of the spectrum analyzer should be subject to the requirement of the fly height modulation, e.g. whether the disk waviness, roughness or other disk feature is of interest. Simulation work is done to study how the bandwidth affects the measurement

results. The idea is to simulate square recorded waveform and a 2nd order filter with adjustable bandwidth is used to extract the 1st harmonic. Simulate flying height modulation with different modulation amplitude and frequency, and then we can find out the effect of filter bandwidth on the flying height signal.

The readback signal from each magnetization transition is approximated by the arctangent model [2], as shown in (4.1):

$$V_{amp} = a \tan \frac{\frac{g}{2} + x}{a + d} + a \tan \frac{\frac{g}{2} - x}{a + d} \quad (4.1)$$

where  $g$  represents the gap length,  $x$  refers to the moving distance of the medium relative to the head; 'a' is the transition parameter and  $d$  is referred as flying height.

If spacing  $d$  is set to be a function of time (for example, sinusoidal function), the amplitude of the read back waveform will be modulated by the flying height variation. Then, filters can be introduced to get the 1st harmonic signal. From there, the envelope will be obtained after demodulation operation so as to get the flying height modulation.

Figure 4.7 shows simulated readback signal and zoom-in plot of signal at the frequency of 72 MHz. The frequency of flying height modulation is 100 kHz.

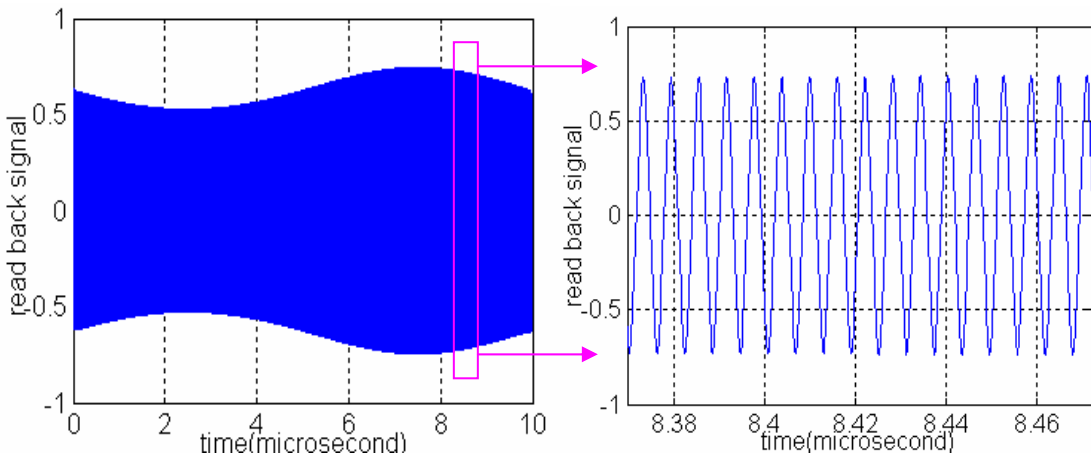


Fig 4.7 Readback Signal of 72 MHz and local figure

The 2nd order filters are used to extract the 1st harmonic waveform. Different bandwidth contributes to different response. In this numerical example, 300 kHz and 3 MHz are set respectively. From Figure 4.8, it can be seen that harmonic passed by 3 MHz bandwidth filter reflects sinusoidal modulation of flying height while the signal by 300 kHz is anamorphic. This indicates that the response time of the filter is greatly limited by the bandwidth filter. Different bandwidth can result in different transient. In this case, the transient process is slower when the bandwidth is narrower.

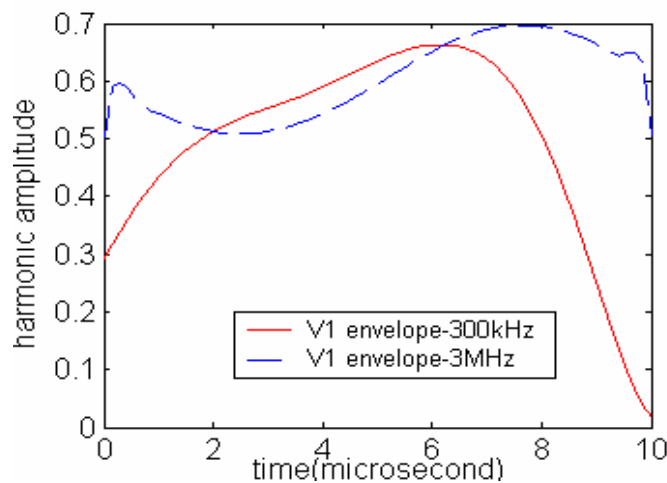


Fig 4.8 Harmonic amplitude passed by different filter bandwidth

It also can be proved that, if high frequency modulation is introduced to the value of spacing  $d$ , the narrower bandwidth may be responsible for the attenuation of the modulation amplitude in the flying height signal for its slow transient and poor following ability.

Experimental confirmation was carried out at disk drive level, as shown in Figure 4.9. It confirms that that narrow bandwidth will introduce distortion and is not a preferred choice.

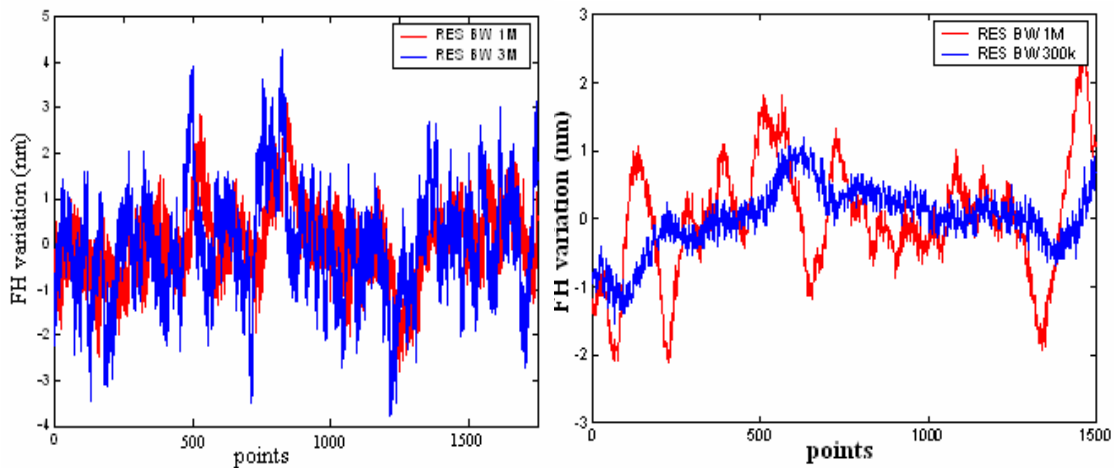


Fig 4.9 Bandwidth effect of spectrum analyzer

As can be observed from Figure 4.9, harmonic filtered by the 1 MHz bandwidth filter is similar to that filtered by 3 MHz bandwidth filter, though a small amount of time delay and smaller variation in amplitude can be observed. However, signal filtered by the bandwidth of 300 kHz is quite different from that by 1 MHz. It could be explained by the poor following ability of the narrow bandwidth as proved in the simulation part. Obviously, for extracting signals at certain frequency from spectrum analyzer, the bandwidth of 3 MHz is optimal to achieve fast transient process hence high following stability as well as less attenuation of flying height modulation.

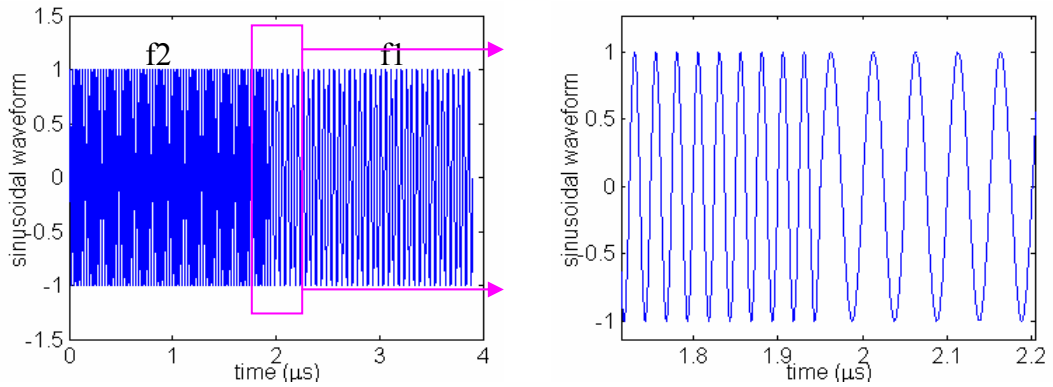


#### 4.3.4 Software-based Wide Bandwidth Filter

It is preferred to have high frequency response speed in flying height testing process. The harmonic burst method is of a limit of the highest response frequency caused by block length, as mentioned before. Therefore, it is desired to reduce transition number in each data block so as to increase the block group frequency and, thus, the response speed to flying high variation.

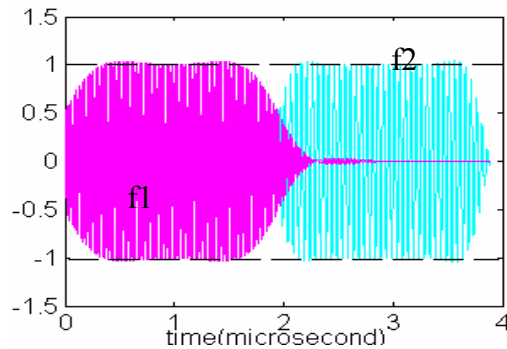
A software-based wide bandwidth filter used in the investigation. The bandwidth of the filter proposed here is set to be wide enough to extract  $f_1$  and  $f_2$  harmonics. As illustrated in the former session, square waveform is composed by odd harmonics. The bandwidth needs to cut off the 3rd harmonic and filter out 1st harmonic of readback signals. The principle is elaborated in the following part.

First of all, bandwidth effect on filtering mono frequency signal is investigated. Sinusoidal waveform of mixed frequency  $f_1$  (20 MHz) and  $f_2$  (40 MHz) is simulated as shown in Figure 4.10. Signal amplitude is generalized to be 1.



(a) Sinusoidal waveform;

(b) Local waveform



(c) Use separate filters with center frequency at 20 MHz and 40 MHz, bandwidth are set to [19MHz 21MHz] and [38MHz 42MHz] respectively.

Fig 4.10 Sinusoidal signals before and after bandpass filters

Therefore, the software-based wide bandwidth filter can filter out two harmonics with properly set bandwidth. The filter attenuates amplitude of harmonics and this attenuation quotient is related to the bandwidth of the filter. The wider the bandwidth, the smaller the attenuation quotient will be. Generally, the center frequency should be  $f_1$  and  $f_2$  respectively, and the bandwidth can be selected in this way: determine the filter bandwidth for the  $f_1$  signals first; set the cut off frequency smaller than 3<sup>rd</sup> harmonic frequency in  $f_1$  signals and the bandwidth should be wide enough not to attenuate the harmonic amplitude. Then determine the bandwidth of filter for  $f_2$  signals. For example, if  $f_2$  is two times  $f_1$ , the bandwidth for filter  $f_1$  is two times that for  $f_2$ .

Hence these wide bandwidth filters can be used to extract harmonics from both type of harmonic bursts.

Fluxes of 96 MHz and 192 MHz are written on data track at the outer diameter (OD) of disk alternatively with 10 periods in each data group. Two software-based wide bandwidth filters are used to filter out the two harmonics. Bandwidth of  $f_2$  filter is set to be [160 MHz – 224 MHz] and bandwidth for  $f_1$  filter is [80 MHz – 122 MHz]. As shown in Figure 4.11, the harmonics after filter are comparable to the amplitude of original readback signal. Because this bandwidth is selected to cut off 3<sup>rd</sup> harmonic of readback signal, hence the 3<sup>rd</sup> harmonic in readback signals has been eliminated and the extracted signal is exactly the 1<sup>st</sup> harmonic signal which can be used to calculate flying height variation.

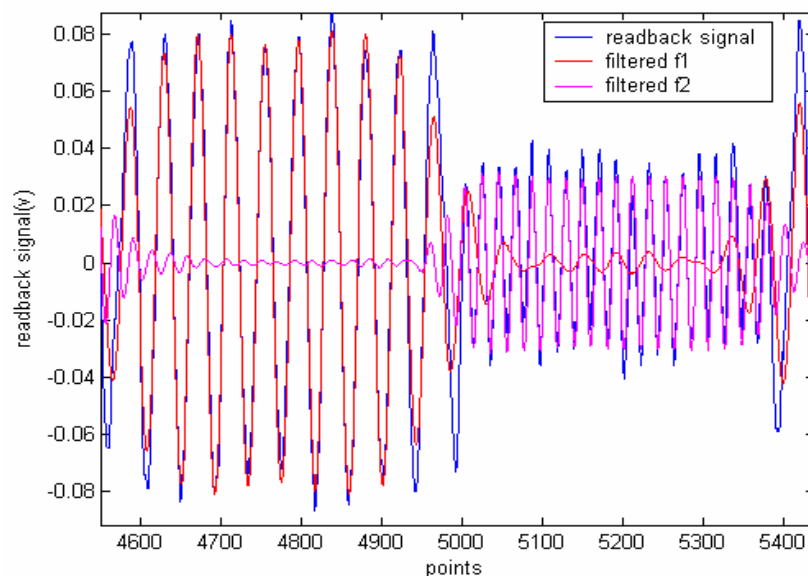


Fig 4.11 Experimental example of wide bandwidth filter: Comparison between harmonics filtered by separate filters and wide bandwidth filter

## 4.4 Summary

Thorough analysis of the harmonic burst method is presented in this chapter. Two embodiments of this method for hard disk drives application are proposed. One is to apply harmonic burst to data zone and the other is to servo area.

The response speed of the harmonic burst method can be a concern and, therefore, is discussed in this chapter. The guideline for the determination of harmonic burst length is discussed according to the resonance frequencies of mechanical parts including actuator, suspension and air bearing surface caused by unstable airflow in disk drive.

Technology for extracting primary harmonic from each harmonic block is discussed and a software based filter with a programmable bandwidth is proposed to retrieve the harmonic amplitude instead of spectrum analyzer.

Moreover, to extract harmonic out of readback signal at certain frequency, spectrum analyzer is used as the extractor. However, for high frequency modulation of flying height, the bandwidth of spectrum analyzer which is limited to be 3 MHz may be not wide enough to achieve such a rapid response to filter out harmonics of each data group. Therefore, a software-based filter with a programmable bandwidth is proposed to retrieve the harmonic amplitude instead of spectrum analyzer.

## **Chapter 5 Drive Level Slider Flying Stability Analysis**

This chapter focuses on experimental investigation of flying height change and fluctuation at disk drive level and under different working conditions. The work covers experiment setup, software and hardware implementation, cases study and comparison between the proposed harmonic burst method and other methods.

### **5.1 Experimental Setup**

#### **5.1.1 Hardware Setup**

The investigation is carried out both at disk drive level with commercial disk drives and in disk drive manufacturing environment and component level using commercial head, disk, Guzik spinstand and Guzik read/write analyzer for heads and disks.

Digital oscilloscope with differential probe is used to retrieve readback signal from drive. Spectrum analyzer is used as bandpass filter and demodulator.

Pressure box and temperature chamber are used to simulate the variable environmental conditions including altitude and ambient temperature of operating hard disk drives.

After averaging process to remove the effect of random noise to flying height, the intensity value of harmonics is displayed and saved by oscilloscope and processed by computer system.

Figure 5.1 illustrates the drive-level experimental setup.

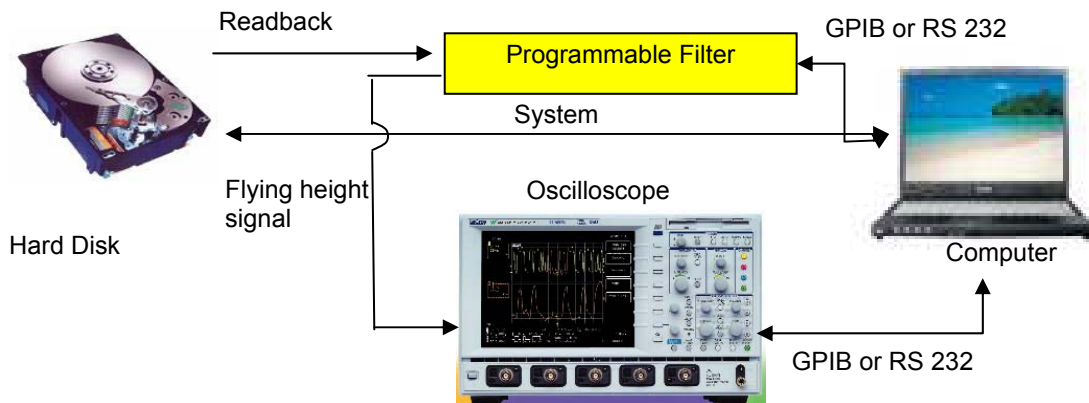


Fig 5.1 Drive-level testing setup

### 5.1.2 Software Setup for Flying Height Measurement

The software developed for the investigations is of the following functions:

- a) To be set up on the host to execute the read/write operation on rotating disk,
- b) To collect data from spectrum analyzer and oscilloscope, and
- c) To complete the algorithm for flying height measurement.

The computer interface of HDD and the interface of Guzik spinstand are different. Therefore, the author developed different software environment for HDD and Guzik spinstand.

### 5.1.2.1 Software Setup for Component-Level Testing on Spinstand

In order to make recording process on spinstand comparable to that on disk drives, each track at spinstand is divided into fixed number of sectors and servo mode is enabled.

Software is developed by VC++ language to control the testing equipments and process the readback signals. The functional diagram of the software is described in Figure 5.2.

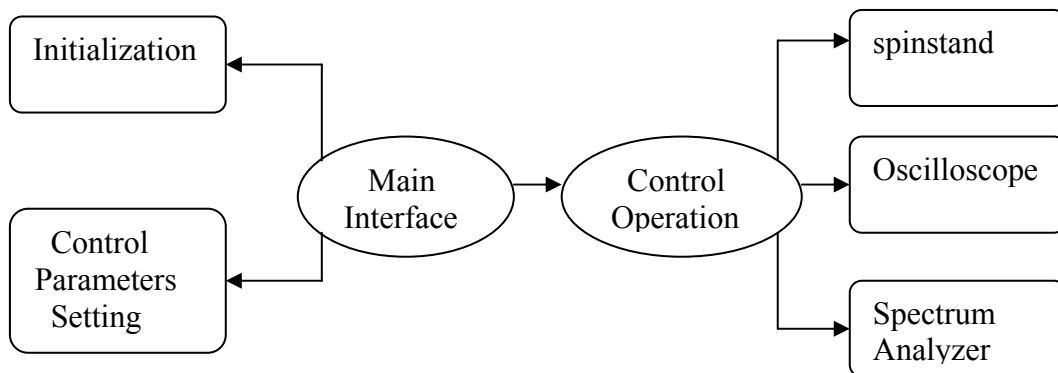


Fig 5.2 Functional Diagrams

As illustrated in Figure 5.2, the software will handle three main operations: initialization, control parameters setting and control operations. Usually there are two possible approaches to establish connection between the host and measurement equipments: by network and General Purpose Interface Bus (GPIB) which has stand-alone devices interconnected by standard cables. Configure out the unique IP (Internet Protocol) address or GPIB address of the equipments and the initialization operation could initialize the oscilloscope and spectrum analyzer to ensure they are ready to receive command from the host computer. As shown in Figure 5.3, control parameters

are set by the user to let the testing process operate at optimum write frequencies and display scaling parameters of measurement equipments for flying height variation analysis.

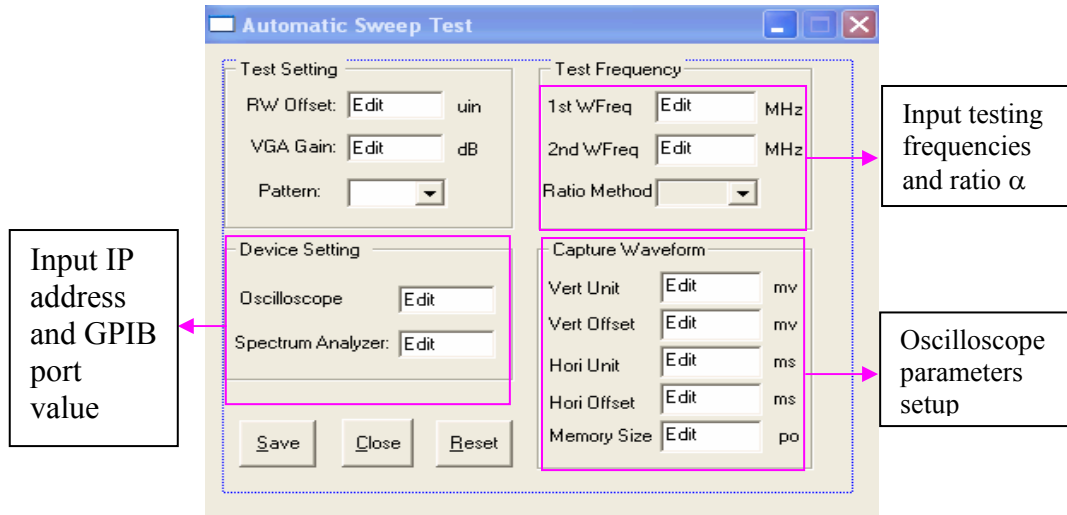


Fig 5.3 Software Control Interface

The control operations include controlling the spinstand and measurement equipments, executing operations of writing magnetic transitions in objective sectors with enabled servo, collecting readback signals, measuring harmonic intensities and calculating the flying height variation automatically and continuously. At the end of testing, operation of uninitialization is executed to release the equipments. The flowchart illustrated in Figure 5.4 presents the detailed operations.



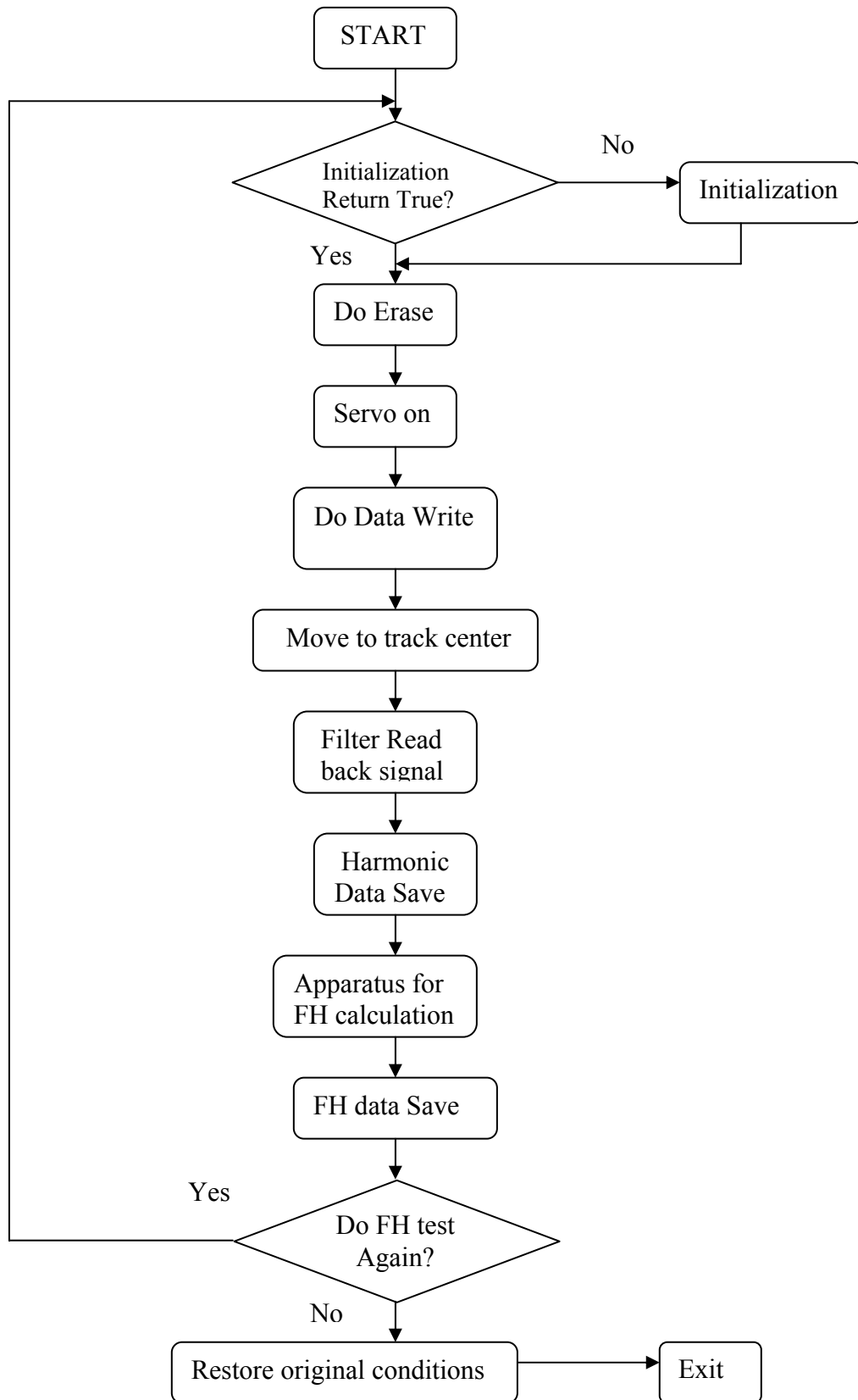
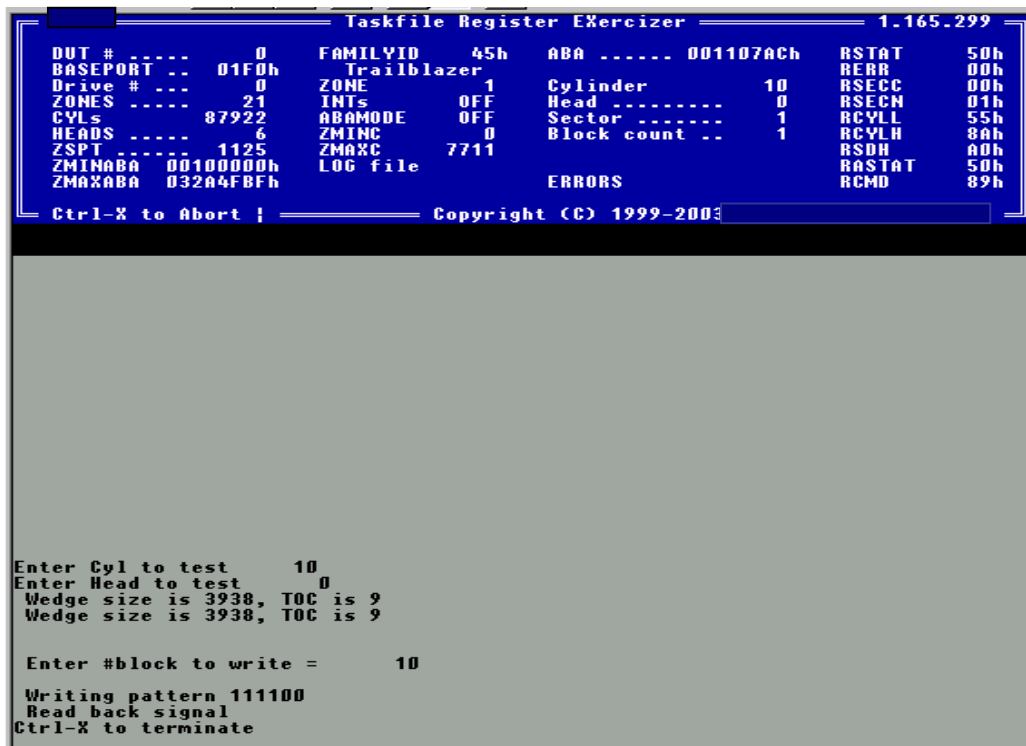


Fig 5.4 Software flowchart

### 5.1.2.2 Drive-Level Testing Software

Software for drive-level testing has to use DOS-level command and interface for reliability test and analysis. This software can help drive manufacturer to execute all sorts of operations, such as reading back, writing, and conversion between logical mode and physical mode. An example for the command window of the software is shown in Figure 5.5.



```
Taskfile Register Exercizer 1.165.299
DUT # ---- 0 FAMILIID 45h ABA ----- 0011070Ch RSTAT 50h
BASEPORT .. 01F0h Trailblazer REBR 00h
Drive # --- 0 ZONE 1 Cylinder 10 RSECC 00h
ZONES ---- 21 INTs OFF Head ----- 0 RSECM 01h
CYLS ---- 87922 ABAMODE OFF Sector ----- 1 RCYLL 55h
HEADS ---- 6 ZMINC 0 Block count -- 1 RCVLL 80h
ZSPT ---- 1125 ZMAXC 7711 RSDH 00h
ZMINABA 00100000h LOG file ERRORS RASTAT 50h
ZMAXABA 032A4FBFh RCMC 89h
Ctrl-X to Abort ! Copyright (C) 1999-2003

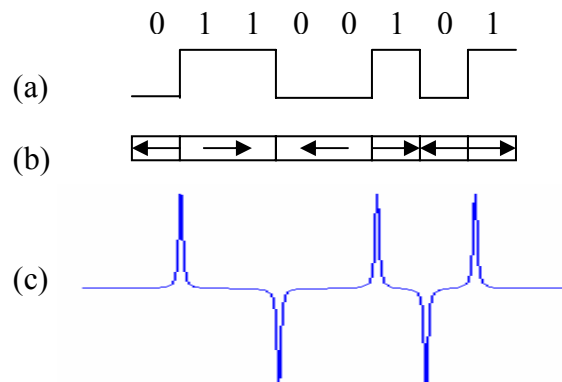
Enter Cyl to test 10
Enter Head to test 0
Wedge size is 3938, TOC is 9
Wedge size is 3938, TOC is 9

Enter #block to write = 10
Writing pattern 111100
Read back signal
Ctrl-X to terminate
```

Fig 5.5 Command window of drive control software

In order to record data on the media, this software needs to load a pattern file which specifies the recorded pattern and recording frequency. Normally, the 'NRZ' coding scheme is used for the definition of transition pattern during write-read operations. 'NRZ' is known as holding the write current to one of the two levels during one period of the write clock, with one level for binary '1' and the other level for binary '0' [30].

Figure 5.6 states the mechanism of this scheme. By ‘NRZ’ coding scheme, we can define and write any pattern on the hard disk drive.



(a) Binary digit data; (b) Magnetization on media; (c) Readback signal

Fig 5.6 NRZ coding scheme

## 5.2 Testing Frequency Selection for Harmonic Burst Method

One important step before actual flying height testing is to determine the optimum recording density to achieve high sensitivity of testing method as well as minimize testing error.

A type of 3.5” HDD with a nominal RPM of 7200 is used for this study. The skew angle ranges from  $-5^\circ$  to  $19^\circ$  from ID to OD. The gap length of the GMR heads used for this type of HDD is about 28 nm. The coercivity of the medium is 4300 Oe and the product of remanent moment to media thickness (Mrt) is about  $0.38 \text{ emu/cm}^2$ . The magnetic layer thickness is about 16 nm.

The transition noise  $\Delta V(k)$  is assumed to be 1% of the value  $V(k)$  and channel noise is also assumed to be 1% of the maximum value  $V(k)_{max}$ , in the determination process of the optimum ratio of two testing frequencies and channel density for flying height measurement. The simulation result is shown in Figure 5.7.

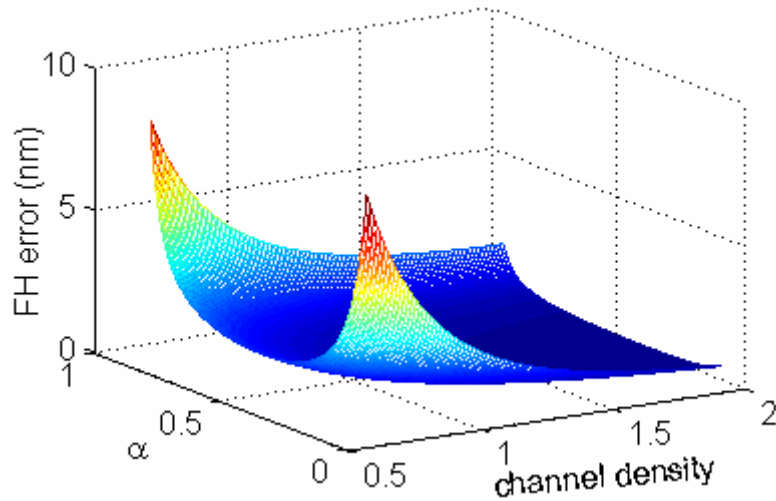


Fig 5.7 Flying height error as function of channel density and  $\alpha$  (ratio of two testing frequency) for testing disk drive

As explained in chapter 4, because of the firmware setting on the hard disk drives, testing frequency is limited by the writing clock and can only be multiples of the clock frequency. For the type of disk drives used in this investigation, the highest writing frequency for each data zone is listed in table 5.1.

Table 5.1 Zone table

Zone	Sector/track	Min cylinder	Max cylinder	Frequency (Mflux)	time (ns)
0	540	352	411	370.7	2.70
1	990	412	2854	662.7	1.51
2	972	2855	12514	654.0	1.53
3	960	12515	19231	645.0	1.55
4	945	19232	23997	636.7	1.57
5	930	23998	28051	627.5	1.59
6	900	28052	37197	600.0	1.67
7	864	37198	41320	583.3	1.71
8	840	41321	44701	566.7	1.76
9	810	44702	49261	543.8	1.84
10	780	49262	52699	526.2	1.90
11	750	52700	56498	506.7	1.97
12	720	56499	61549	480.0	2.08
13	684	61550	64779	462.5	2.16
14	660	64780	67547	446.3	2.24
15	630	67548	70992	425.5	2.35
16	612	70993	72016	415.4	2.41

The highest channel density is about 2.0 at OD, 2.4 at MD and 2.3 at ID. It is observed that readback signal at those highest possible channel densities is of low SNR and suffers from nonlinearity effects. Therefore, the channel density used in experiment is up to half of the highest channel densities. Hence the ratio value can be selected from

2/3, 2/4, 2/5, 2/6, ... and we can find out the optimum value from simulation results in Figure 5.8.

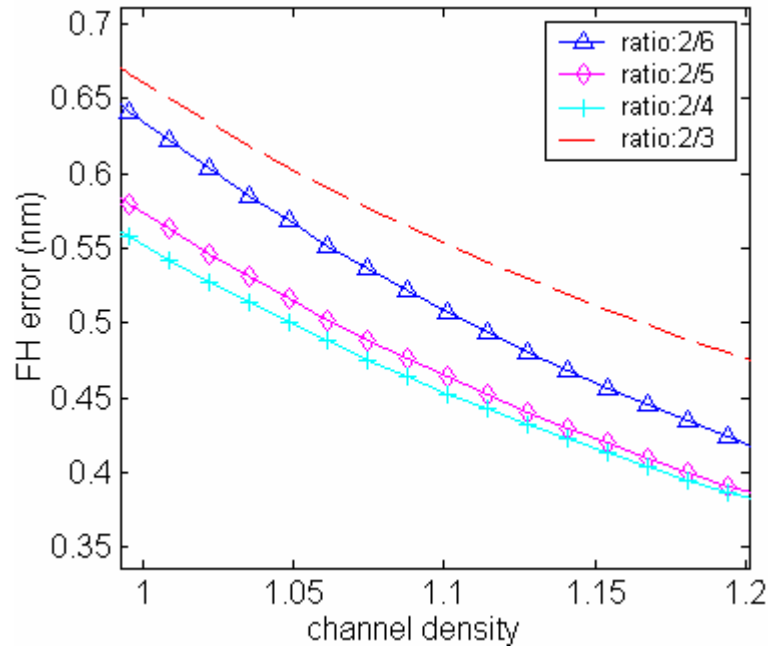


Fig 5.8 Flying height errors at recording density of ( $F_{\max}/2$ ) frequency

At channel density from 1.0 to 1.2, it can be seen that the ratio curve at (2/4) has the minimum flying height error across ID to OD area. Therefore, we choose half of the highest available channel density as the testing density and work at a ratio value of 0.5. In other words,  $F_{\max}/2$  frequency and  $F_{\max}/4$  frequency are selected as the optimum testing frequencies for the drive-level experiments. Here,  $F_{\max}$  is the read/write frequency which gives the highest possible channel density of that particular zone.

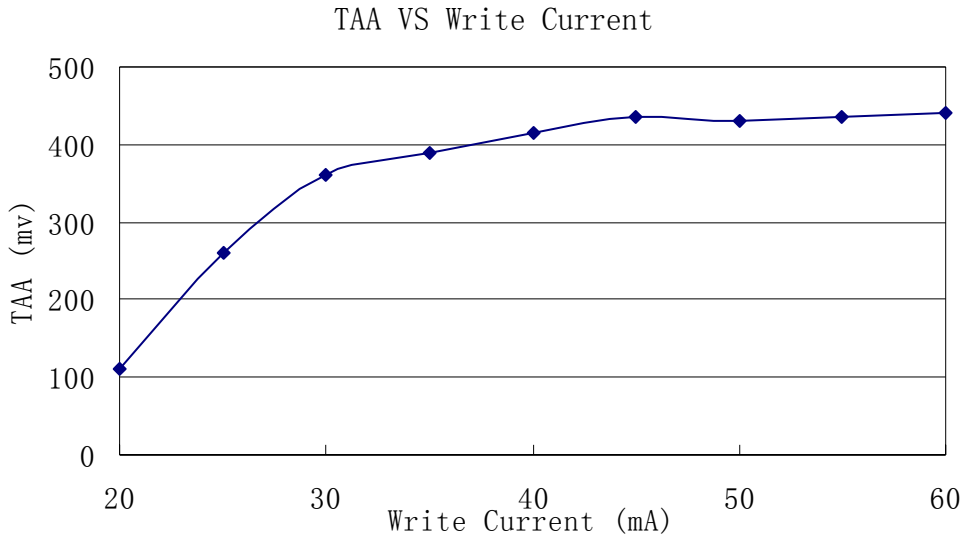
Although arbitrary frequency could be written on component level at spinstand, to keep the consistence with drive-level testing, both component level and drive level use the same testing frequencies.

## **5.3 Component-Level Flying Height Stability Analysis**

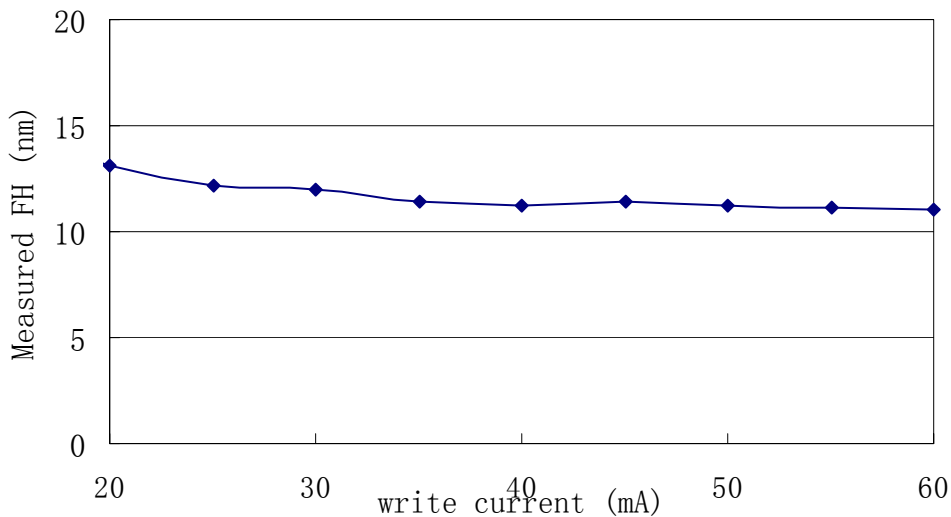
With the hardware setup and software setup introduced in the above section, the experimental work can be processed on spinstand and HDD. Before flying height measurement on the testing disk drive, writing current influence on flying height measurement is investigated by writing with different current. The sliders used for both drive level testing and spinstand level testing are the same, to make the comparison meaningful.

### **5.3.1 Write Current Influence on Flying Height Measurement**

For flying height measurement, in order to investigate flying height sensitivity to writing process, flying height was tested by harmonic burst method at 1.357 inch radius with 7200 RPM spindle rotation speed. The strength of the amplitude is related to write current directly. Increasing write current from 20 mA to 60 mA, we can plot out the saturation curve of track average amplitude (TAA) versus write current as shown in Fig 5.9 (a). The flying height dependence to the write current calculated by harmonic burst method was plotted in Figure 5.9 (b).



(a) TAA versus Write Current



(b) The effect of writing process to flying height measurement

Fig 5.9 The writing process and its influence to the flying height measurement

The results show that the measured flying height is almost a flat line and stable at the write current range of 35 ~ 60 mA. Hence harmonic burst method is not as sensitive to the writing process as the amplitude of readback signal (TAA). The measured flying height value shows a decreasing trend with increasing write current in Figure 5.9 (b), when the writing current is smaller than 35 mA. This is believed to be due to larger



transition length parameter when the writing current is not high enough. The harmonic burst method is based on equation (3.15). The flying height variation is actually calculated as the sum of variation of (d+a) and assuming transition parameter a is a constant.

The tested flying height still tends to decrease in the current range from 35 mA to 60 mA. This is believed to be related to writing induced pole tip protrusion [36]. Increased writing current leads to increased pole tip protrusion and, therefore, decreased head-disk spacing during writing operation.

A classical transition Model is:

$$a = \frac{(1 - S^*) y}{\pi Q} + \sqrt{\left[ \frac{(1 - S^*) y}{\pi Q} \right]^2 + \frac{M_r \delta}{\pi H_c} \cdot \frac{y}{Q}} \quad (5.1)$$

where  $y = d' + \delta / 2$  ( $d'$  represents magnetic space during writing-process). Suppose Q (a function of y and transition center position, with typical values of 0.65 – 0.85) equals to 0.82, coercive squareness  $S^*$  is 0.95, the relationship between a and  $d'$  could be plot out as shown in Figure 5.10. It could be seen that a increases with  $d'$ .

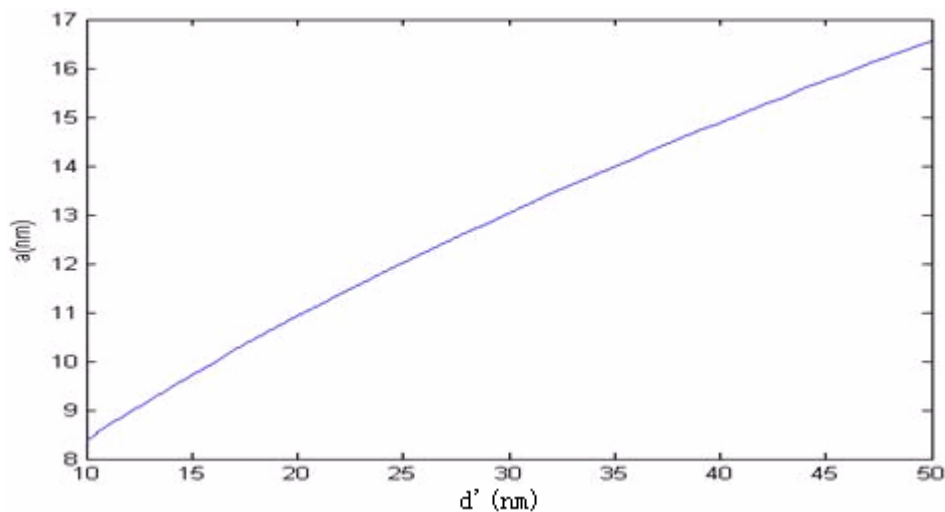
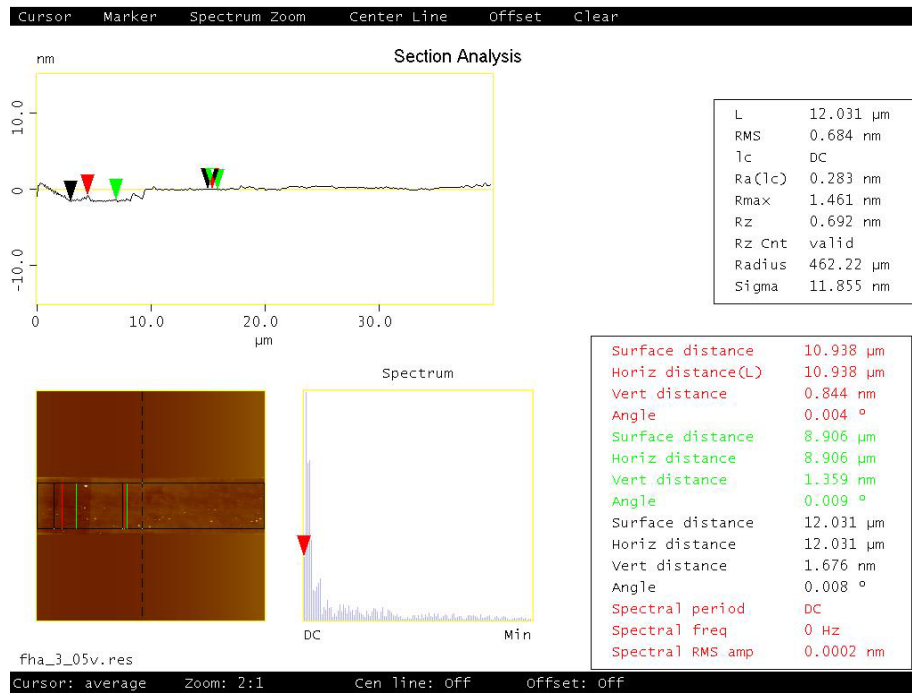


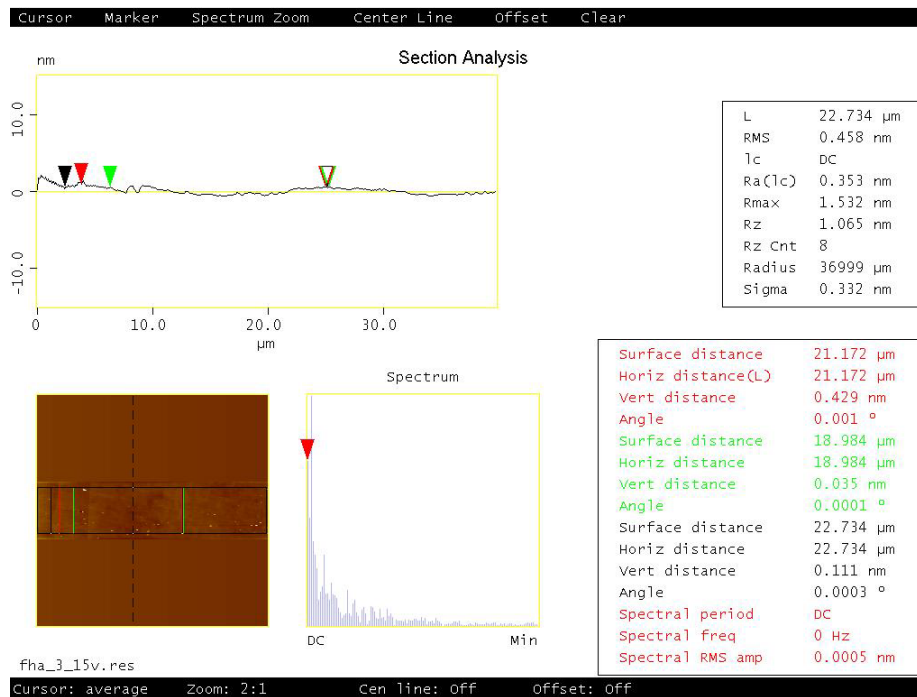
Fig 5.10 Correlation of 'a' and 'd''

In order to investigate how much is the pole tip protrusion of slider caused by writing current, static measurement is done by AFM (Atomic Force Microscopy) at different conditions: writing current equals to zero, 30 mA, and 60 mA, respectively.

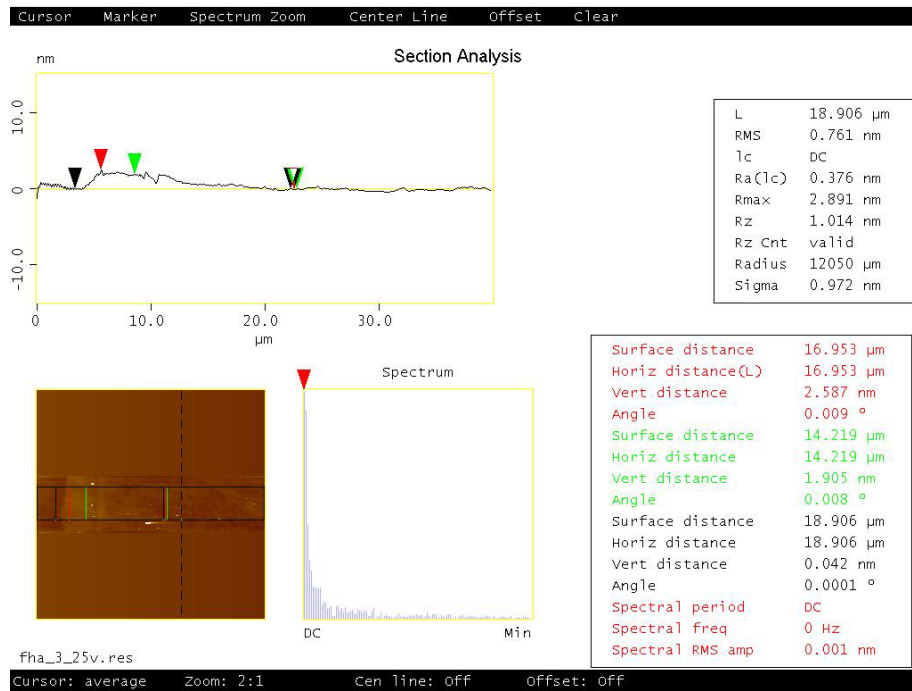
Figure 5.11 (a) shows at normal condition, the recess of GMR as the result of slider lapping process is around 1.359 nm as green mark shows. After the slider is input with 30 mA writing current, the GMR has protruded 1.395 nm as shown in Figure 5.11 (b) and protruded 3.264 nm with 60 mA in Figure 5.11 (c). Increased protrusion leads to decreased magnetic space in writing operation and forms reduced transition length parameter  $a$ . In the flying height testing process, the flying height did not change but the transition length parameter changed. Such change will be wrongly explained as flying height change if the transition length parameter is assumed to be constant. The effect of write current on pole tip protrusion at static status may be not as same as on rotating disk drive, where we should also consider other factors such as air cooling effect; however, the conclusion still make sense that that the effect of write current on flying height measurement is not negligible.



(a). Pole tip recess measurement at zero writing current;



(b). Pole tip recess measurement with 30 mA writing current input



(c). Pole tip recess measurement with 60 mA writing current input

Fig 5.11 Pole tip recess measurement at different temperature by AFM

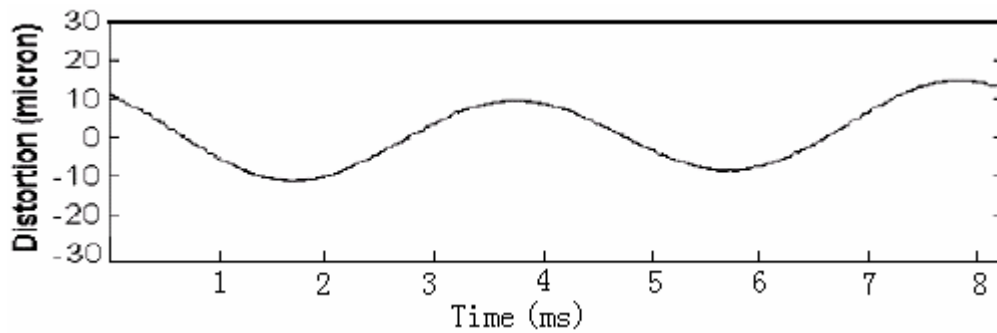
### 5.3.2 Flying Height Measurement on Deformed Disk by Clamping

The slider air bearing surfaces are designed to generate both high stiffness and high damping ratio to prevent excessive spacing fluctuation caused by various reasons, including the clamping induced disk distortion. In general, modern sliders are quite capable of following disk fluctuation.

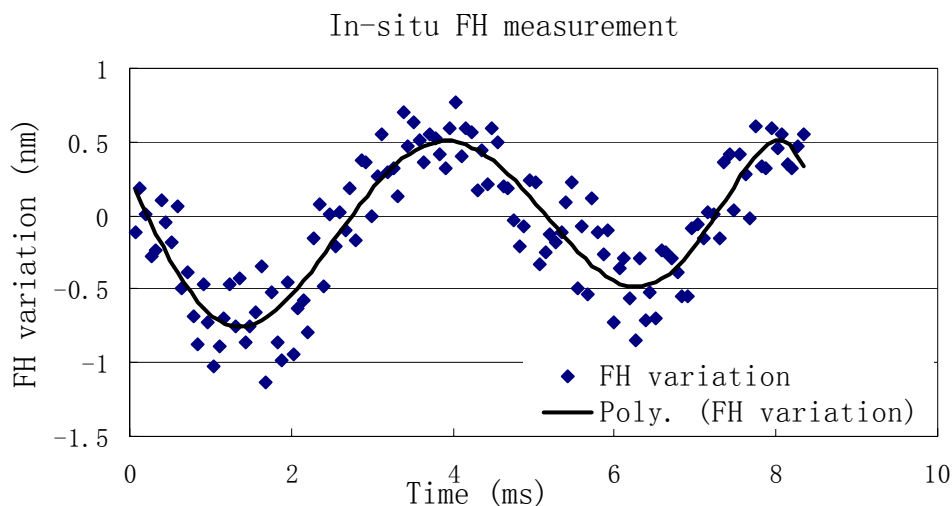
Above 10 nm flying height, the magnitude of spacing fluctuation, induced by the disk clamping distortion, is negligible when compared to the magnitude of the flying height. However, further reduction in the flying height had triggered the concerns as any spacing fluctuation could lead to head disk contact. Triple harmonic method has been

explored and used to measure the flying height variation induced by the disk clamping distortion [37]. In this session, harmonic burst method will be used to measure the flying height variation induced by the disk clamping distortion.

Various disk distortions can be generated by modifying the clamping chuck shape of the spindles. The amplitude and the types of clamping distortion used in the testing were uncommon comparing to the real drive. At RPM of 7200, harmonic burst method pattern are written at radius of 1.357 inch and the flying height variation is plotted in Figure 5.12 (b) compared with LDV measurement as shown in Figure 5.12 (a).



(a) LDV measurement of disk clamping distortion



(b) In-situ flying height measurement of flying height variation induced by disk clamping distortion

Fig 5.12 LDV and harmonic burst method comparison

The disk deformation that was used in the experiment has been identified by the LDV. The corresponding flying height variation is measured by the harmonic burst method. Results confirm that disk deformation leads to flying height variation although the slider could follow most of the disk distortion amplitude. Positive disk distortion leads to the increase in the flying height and negative disk distortion results in the reduction of flying height.

## **5.4 Drive-Level Flying Height Stability Analysis**

Reliable operation of a modern magnetic disk drive depends greatly on maintaining a pre-determined spacing between the magnetic recording head and the recording medium. In order to study slider-flying stability at varying environmental conditions, pressure-adjustable box and temperature chamber are utilized to simulate stressed environments. This section investigates the application of harmonic burst method for the analysis of flying height change caused by altitude and temperature effects at drive-level.

### **5.4.1 Off-Track Tolerance of Harmonic Burst Method**

Due to mechanical disturbances, the heads do often fly off-track in disk drives. When the head reads at a certain off-track position, the readback signal amplitude will drop. In this case, the radial movement of slider will be misunderstood as vertical fluctuation

if readback signal is used to monitor the flying height variation. In order to find out the tolerance of harmonic burst method to off track effect, the slider is set to be off track from 0% to 14% of the track width. The adjacent tracks are erased so that the interference from the adjacent track is minimized.

( $F_{max}/2$ ) frequency and ( $F_{max}/4$ ) frequency pattern is recorded group by group on the selected testing track with zero skew angle. Such an arrangement is to ensure that the off-track effect is symmetric regardless the off-track is towards inner diameter (ID) or outer diameter (OD). Set the slider flying from +14% off-track (towards ID) to -14% off-track (towards OD) and filter the 1st harmonic of each pattern, we can compare the results of harmonic burst method to the results of readback signal modulation technique using ( $F_{max}/2$ ) frequency and ( $F_{max}/4$ ) frequency pattern respectively. The percentage of flying height error is calculated with 6.6 nm nominal absolute flying height as reference.

Figure 5.13 shows the error percentage for 3 different methods. The harmonic burst method gives negligible error (less than 5% of the 6.6 nm flying height) if the off track is within 6% of the track width. On the other hand, the readback signal modulation technique is quite sensitive to off-track effect. Furthermore, readback signal modulation technique using low frequency pattern results in even higher flying height error than using high frequency pattern.

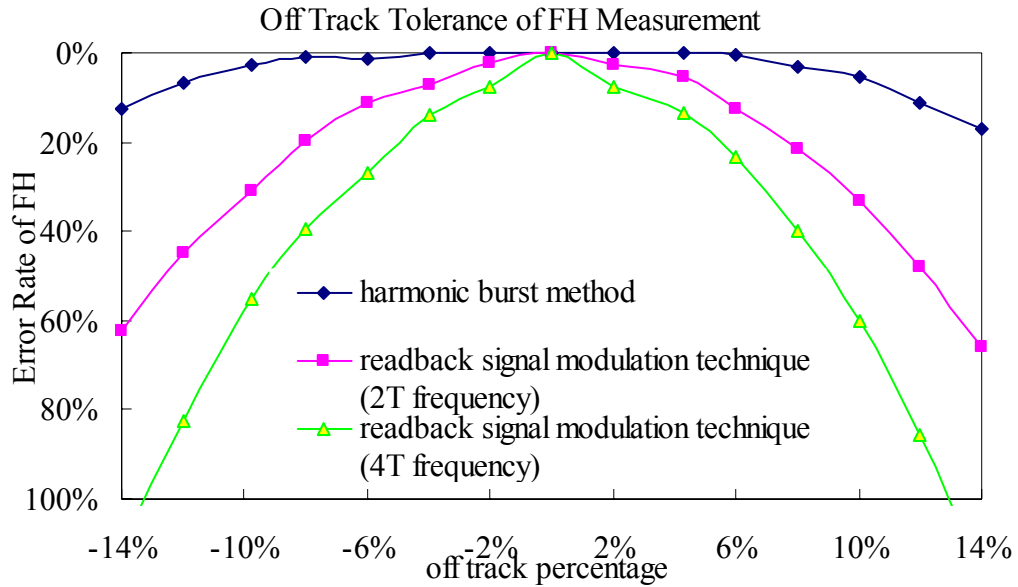


Fig 5.13 Off track tolerance of flying height measurement

The higher flying height error for low frequency pattern could be explained by side read effect. Based on the reciprocity principle, the presence of side fringing field indicates that the head will not only read the magnetic charges located at  $z \leq 0$ , but also  $z \geq 0$  (outside of the physically covered area of the head) as shown in Figure 5.14, which is referred as the side read.

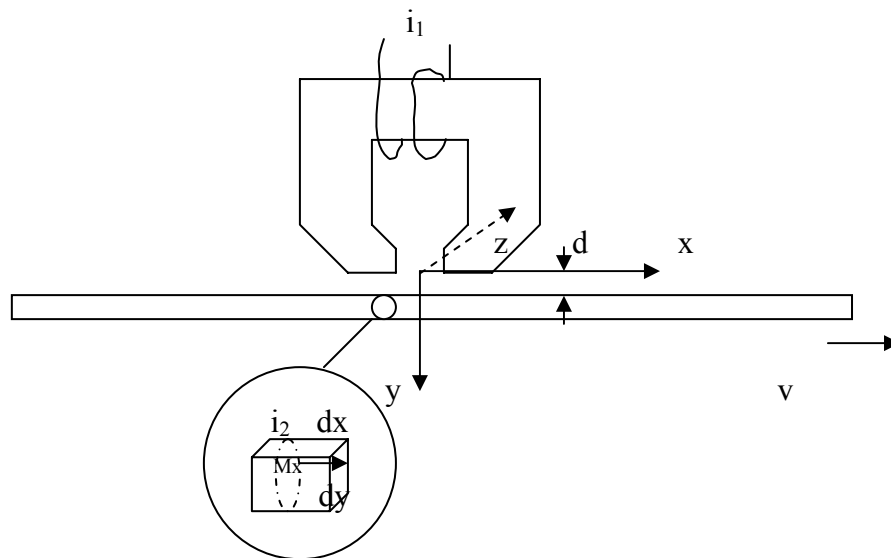


Fig 5.14 Reciprocity between recording head and magnetic medium



Extending the Wallace spacing loss to the z-direction, the Fourier transform with respect to x of the side read voltage signal from a magnetic charge at z is much bigger than y or gap length will decay exponentially:  $V(k, z) \propto e^{-kz}$ . In other words, the side read voltage signal at a wavelength of  $\lambda$  would decay as a linear function of  $1/\lambda$  [38]. Therefore, side read is more serious for low-frequency signals than for high-frequency ones.

However, for harmonic burst method, the side read influence by off-track is to some extent removed by calculating the ratio of two testing frequencies and hence harmonic burst method is of significant advantaged in terms of its tolerance to the possible track mis-registration at disk drive level.

#### **5.4.2 Altitude Effect on Flying Height at Drive**

When a drive spins up to operating speed, the high speed causes air to flow under the slider and lift the slider off the disk surface. The variation of environmental pressure (for example, the disk drive is moved from sea level altitude to 15 kfeet altitude) will cause thinner air density and hence result in decreased air bearing force between the air bearing surface of slider and disk surface. Therefore, slider will fly lower than its predetermined flying height because of this decreased lift-up force. In this case, as specified in the former chapters, reduced flying height will lead to slider-disk interaction and even slider crash which are not tolerable in terms of drive reliability.

Thus altitude effect on flying height is one thing must be evaluated and investigated at drive level.

In order to change the ambient pressure of a working hard disk drive, the testing disk drive is placed into a vacuum chamber in which air can be pumped out to reduce the air pressure gradually [39]. The reading of vacuum gauge will show the pressure inside the chamber and hence slider flying status can be investigated at simulated high altitudes. The relationship between altitude and air pressure is shown in table 5.2.

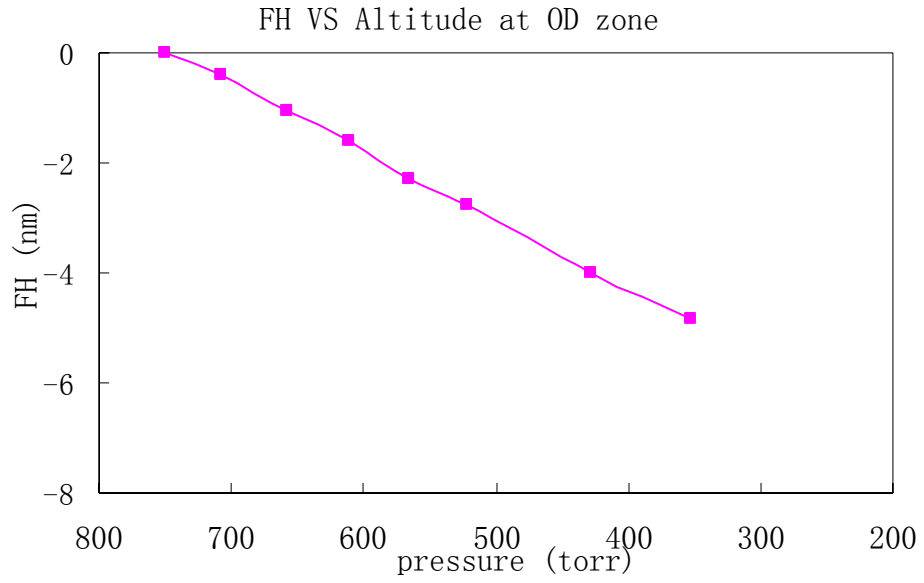
Table 5.2 Pressure at different altitude

Altitude (kfeet)	0	5	10	15	20
Pressure (Torr)	747.6	632	523	428	350

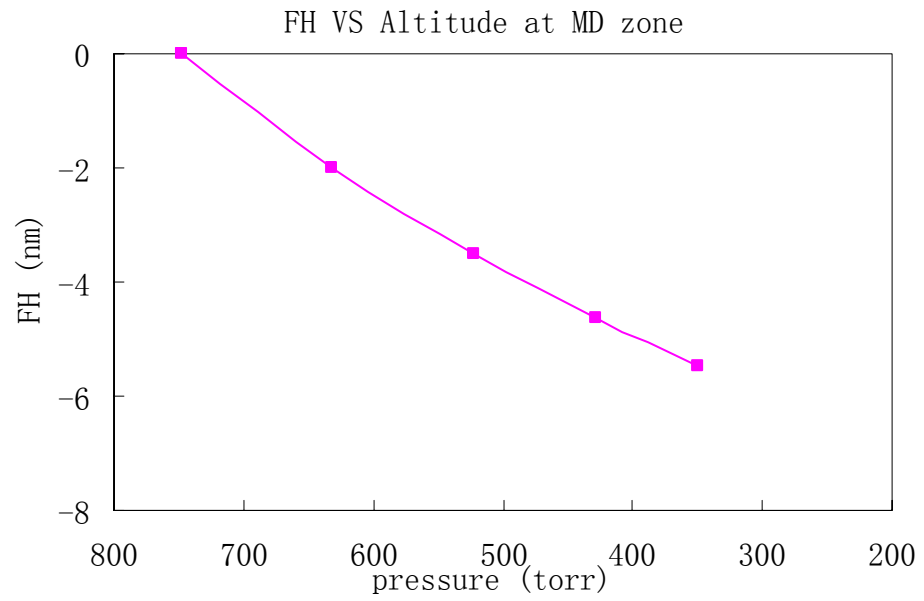
The experiment process is as following. The harmonic bursts of flux frequency ( $F_{max}/2$ ) and ( $F_{max}/4$ ) are recorded alternatively over testing tracks at ID (radius: 26.3 mm), MD (radius: 33.79 mm) and OD (radius: 45.845 mm).

The testing process is the followings:

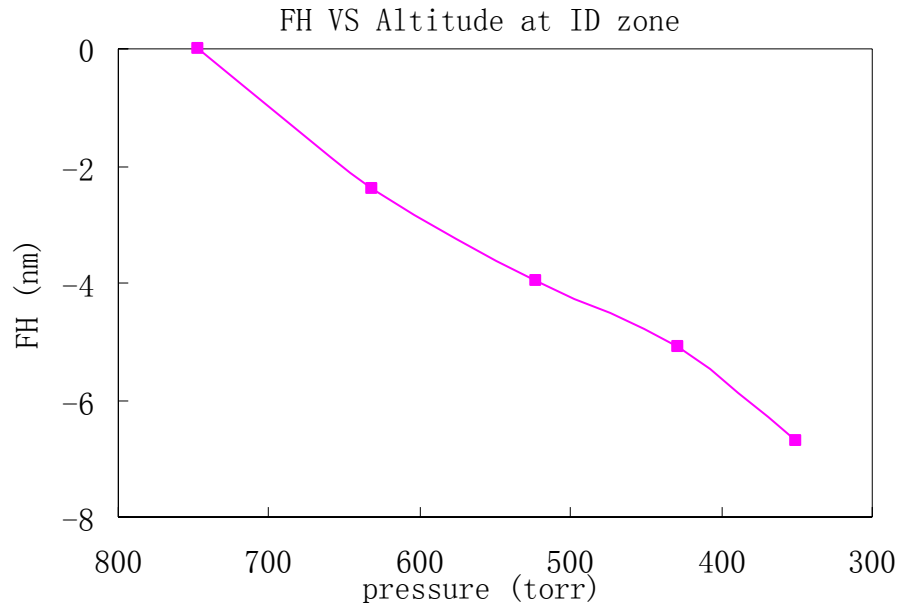
- a) increase the altitude (which also means decreasing the air pressure) from 0 kfeet to 20 kfeet at 5 kfeet each step,
- b) average the readback signal by 300 times so as to remove the effect of random noise;
- c) save the filtered  $f_1$  and  $f_2$  harmonic intensity on oscilloscope.
- d) calculate flying height value and plot out the relationship between flying height drop and altitude change.



(a) Flying height loss VS altitude at OD zone



(b) Flying height loss VS altitude at MD zone



(c) Flying height loss VS altitude at ID zone

Fig 5.15 Flying height VS altitude at different zones

From Figure 5.15, it can be seen that flying height is greatly influenced by ambient pressure of hard disk drives. All three zones show the trend of descending flying height. Table 5.3 lists the flying height variation calculated by harmonic burst method. It shows that flying height decreases faster at ID zone than at outer zones.

Table 5.3 Flying height change measured harmonic burst method

Zone	Flying height loss at different altitude (nm)				
	0 kfeet	5 kfeet	10 kfeet	15 kfeet	20 kfeet
OD	0	-1.32	-2.77	-3.99	-4.85
MD	0	-1.23	-3.6	-4.62	-5.46
ID	0	-2.4	-3.96	-4.84	-6.91

The flying height variation distribution is also calculated to analyse the altitude effect on flying stability. The histograms of flying height variation distribution at each altitude indicate that the flying height variation distribution shows a Gaussian distribution as illustrated in Figure 5.16.

The distribution at different altitude shows that flying height variation becomes larger at higher altitude. Also OD zone shows bigger standard deviation than at ID zone.

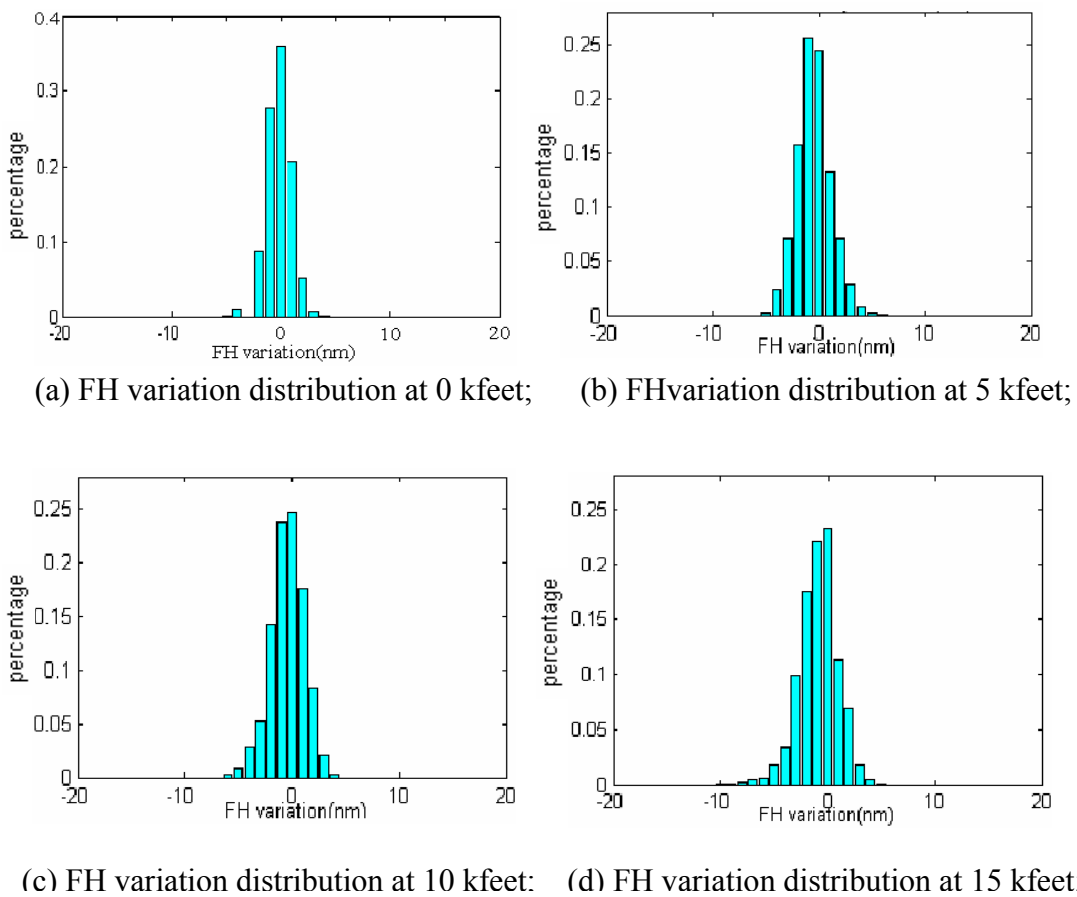


Fig 5.16 Flying height variation distribution at OD zone at different altitudes

Table 5.4 has listed the standard deviation value of flying height variation distribution histogram for each altitude at different zone.

Table 5.4 Standard deviation value of flying height variation distribution at each altitude

Altitude	Standard deviation of flying height variance distribution at different zones		
	ID	MD	OD
0 kfeet	1.0 nm	1.0 nm	1.2 nm
5 kfeet	1.4 nm	1.4 nm	1.6 nm
10 kfeet	1.4 nm	1.4 nm	1.6 nm
15 kfeet	1.4 nm	1.5 nm	1.8 nm

Another application which utilizes the dependence of flying height on the ambient pressure is absolute flying height measurement. The experiment process is as following:

- a) first of all, fluxes of harmonic burst patterns are recorded on the predetermined track and sensed back at sea level altitude;
- b) then, decrease the pressure gradually to reduce the flying height until disk-slider contact, indicated by ceased amplitude change to when ambient pressure is further reduced
- c) calculated the absolute flying height as the summation of all the  $\Delta FH$  from the zero spacing value to that calculated at the normal operating status at sea level altitude.

### **5.4.3 Ambient Temperature Effect on Flying Height at Hard Disk**

#### **Drive**

With the disks typically rotating at 7200 RPM, the operating temperature inside a disk drive can rise to more than 50 °C. The internal temperature can be even higher if more disk platters are installed into one drive to have higher data capacity per drive. Moreover, sometimes hard disk drives are required to operate in stressed environments, such as at low temperature (for example zero centigrade) or high temperature. Temperature can change many parameters of mechanical parts, such as thermal expansion of the suspension, the disk media and the mechanical parts which may result in poor tracking capability, change in slider crown, change in the air viscosity and change in the mean-free path of the air which may directly lead to flying height change [40]. As to insure the reliability of drive read/write capability, it is essential to monitor slider flying stability.

Harmonic burst method is implemented to study slider flying status in a hard disk drive at different working temperatures. A thermal chamber is used to adjust the ambient temperature of the operating drive. The chamber temperature is set to 25 °C, 45 °C and 60 °C separately and the harmonic burst pattern is written group by group on the OD, MD and ID cylinders (same as written during altitude experiment). When the temperature is increased to the set value, 10 to 15 minutes is given to settle the drive to work at the certain temperature.

It is observed that ID, MD and OD have different flying height changing trends, when the ambient temperature increased from 25 °C to 60 °C. The measured flying height

variation on each cylinder shows much wider distribution (standard deviation) at higher ambient temperature than room temperature, as can be seen in Table 5.5.

Table 5.5 Flying height variation distribution at each ambient temperature

Temperature (Celsius degree)	Standard deviation of flying height variance distribution at different zones		
	ID	MD	OD
25	1.0 nm	1.0 nm	1.2 nm
45	2.9 nm	2.4 nm	2.8 nm
60	3.1 nm	2.6 nm	3.2 nm

Absolute flying height decreases at different zones as shown in Figure 5.17.

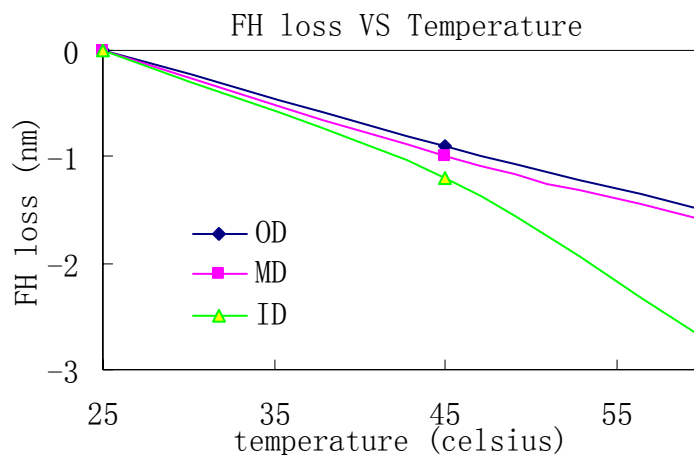


Fig 5.17 Flying height change at different ambient temperature

The flying height variation distribution and decreasing flying height at high ambient temperature both disclose that slider is more likely to fly unstably and lower at high operating temperature, which does not benefit reliability of hard disk drive.



## **5.5 Summary**

This chapter is more dedicated to experimental application of the proposed harmonic burst method and experimental investigation of drive level flying height change under various conditions.

Harmonic burst method is implemented to investigate slider flying stability under different environmental conditions. In the touch down experiment, flying height measured by harmonic burst method is compared to the results obtained from the readback signal modulation method. It can be seen that results of two methods accords well over the disk.

The great advantage of harmonic burst method over readback signal modulation method is that it removes off-track effect while the latter method suffers severely from off-track.

## **Chapter 6 Conclusion and Future Work**

The aggressive areal density growth in the disk drive requires the head-disk spacing to be further reduced to towards 2-3 nm level. At the same time, the magnetic performance and recording reliability of hard disk drives are further driven to be well under control. As a critical parameter in the magnetic head disk systems which reflects the performance of recording system, the engineering needs to characterize the drive performance require the measurements of flying height to be made at the drive level instead of at the component level. Thus, the in-situ measurement methods are needed to characterize the drive performance at higher areal density. Furthermore, the relevant in-situ techniques become more challenging with the advancement of the drive technology. Therefore, in-situ techniques to characterize the performance of the head disk systems deserve a detailed study.

This thesis is dedicated to the investigation and implementation of the useful in-situ techniques for characterizing flying height in the magnetic head disk systems with higher accuracy and better efficiency. The background of magnetic recording technology is firstly introduced to explain the importance of in-situ flying height monitoring at drive level. The detailed art of in-situ flying height techniques, including writing-process based methods and reading-process based methods, are reviewed and compared in terms of sensitivity, resolution and feasibility at drive-level. As a result, the harmonic ratio methods are identified to be the most suitable methods for characterizing the sub-10 nm flying height in the disk drives.

By deducing the expression of flying height variation with readback signal amplitude, an analytical formula is derived to characterize the possible measurement error of flying height with harmonic based in-situ testing methods.

The formula and corresponding analysis suggest that there is an obvious optimal channel density range in which the flying height testing error is the smallest.

The formula and related theoretical work also lead to a systematic approach on how to determine the optimum ratio of frequencies and optimum channel density so as to achieve minimum flying height measurement error.

A novel method, harmonic burst method, is proposed for the flying height analysis at disk drive level. The method combines the advantages of all harmonic based methods together. Furthermore, it has the unique advantage of easy to implement at disk drive level.

One thing important for the harmonic burst method is how to determine the length of each burst. The response speed must be significantly higher than the resonance frequency of those components which can affect the flying height. Therefore, the resonance frequencies of mechanical components including actuator, suspension and air bearing surface caused by unstable airflow in disk drive are analyzed and the criteria for the length determination of harmonic burst is derived. Results indicate that the transition burst method is of high enough response speed to all major factors affecting flying height variation.

The criteria and practice for filter design and bandwidth selection are proposed and confirmed both by software and experiments.

Two possible embodiment of the proposed harmonic burst method are proposed. Experimental investigation and drive level application of the proposed harmonic burst method are carried out and results are presented in the thesis. The investigations include writing process and its effect on the flying height measurement of the proposed method, flying height variation study of the proposed method for the disk fluttering effect, investigation of off-track tolerance of proposed harmonic burst method, investigations into the influence of environmental changes (altitude effect and temperature effect) on flying height variation at disk drive level and with the proposed method, and so on. Results confirmed the advantages of the proposed method for drive level investigation of flying height variation.

The authors would also like to recommend transferring of the proposed method to manufacturing line application in the future.

## Reference

- [1] Andreas Moser, Kentaro Takano, David T Margulies, “Magnetic Recording: Advancing Into the Future,” Journal of Applied Physics Vol. 35, 2002
- [2] Shan X.Wang, Alexander M.ztaratorin, “Magnetic Information Storage Technology”, Academic Press, 1998
- [3] Edward grochowski, “Emerging Trends in Data Storage on Magnetic Hard Disk Drives”, IBM Almaden research center, San Jose, CA, USA
- [4] Edward grochowski, “HDD Technology 2003”, San Jose Research Center, Hitachi Global Storage Technologies
- [5] Yoshimasa Miura, “Hard Disk Drive Technology: Past, Present and Future”, IEEE, 2002
- [6] Barry H. Schechtman, “Long term outlook for magnetic and optical disk storage technologies”, Optical Data Storage Topical Meeting, 1997. ODS. Conference Digest, 7-9 April 1997.
- [7] “Construction and Operation of the Hard Disk”, <http://www.pcguides.com/ref/hdd/op/index.htm>
- [8] Brown et al, “Method and Apparatus for in-situ measurement of head/recording medium clearance”, US patent 4,777,544, Oct.11, 1988
- [9] Talke Lab Head/Disk Interface Research, Univ. of California. San Diego, <http://talkelab.ucsd.edu/head-disk/>
- [10] Gordon F.Hughes, “Wise drives”, University of California (San Diego).

- [11] G.F.Hughes et al, "Improved Disk Drive Failure Warnings", IEEE transactions on reliability, September 2002.
- [12] Jianhua Li, Bo Liu, "Effects of intermolecular forces on sub-10nm spaced sliders", Magnetism Conference, 2002.
- [13] Bo Liu and Qisuo Chen, "Carrier Erasure Current Method for In-Situ Monitoring of Head-Disk Spacing Variation" IEEE Transactions on Magnetism, Vol. 35, No. 2, Mar 1999
- [14] Bo Liu and Zhinmin Yuan, "A Scanning Carrier Current method for the In-Situ Monitoring of Head-Disk Spacing," Patent filing
- [15] John Mallinson, "The Foundations of Magnetic Recording", Second Edition
- [16] W.K.Shi, L.Y.Zhu and D.B.Bogy, "Use of Readback Signal Modulation to Measure Head/Disk Spacing Variations in Magnetic Disk Files", IEEE Transactions on Magnetism, Vol.Mag-23, No.1, January 1987.
- [17] Klaassen et al, US patent 5,130,866, filed Jul.17, 1990.
- [18] Klaas B. Klaassen and Jack C.L. van Peppen, "Slider-Disk Clearance Measurements in Magnetic Disk Drives Using the Readback Transducer", IEEE Trans. Instrumentation and Measurement, VOL.43, NO.2, 1994
- [19] Bo Liu and Zhimin Yuan, "In-situ Characterization of Head-Disk Clearance", Proc.Symp. Interface Tribology Towards 100 Gb/in<sup>2</sup> and Beyond:ASME, 2000,pp 51-48.
- [20] Gordan James Smith, US patent 6,417,981, filed Sep.23, 1999
- [21] Brown et al, US patent 4,777,544, filed Aug.15, 1986.
- [22] Applied Alloy Chemistry Group, "Magnetic Recording", University of Birmingham
- [23] H.Neal Bertram, "Theory of magnetic recording", Cambridge University Press

- [24] Zhimin Yuan, Bo Liu, Wei Zhang and Shengbin Hu “Engineering Study of Triple-Harmonic Method for In Situ Characterization of Head-Disk Spacing,” Journal of Magnetism and Magnetic Materials, Vol. 239, PP 367-370, 2002
- [25] Choe, G et al, “Transition and DC noise characteristics”, Magnetics conference, 2003
- [26] Xinzhi Xing and H. Neal Bertram, “Experimental studies of nonlinearities in MR heads”, JAP, 1996
- [27] Xiaodong Che, “Nonlinearity Measurements and Write Precompensation Studies For a PRML Recording Channel”, IEEE Trans. Magn, November 1995
- [28] Yamaguchi, T et al, “Improvement of servo robustness for digital sector servo system (hard disk drives””, Magnetics, IEEE Transactions on Volume 28, Issue 5, Part 2, Sep 1992
- [29] “Servo Techniques and Operation”,<http://pcguide.com/ref/hdd/op/actServo-c.html>
- [30] E.H.Ong, S.P.Lim etc, “The Reduction of Actuator’s Resonant Amplitudes with Damping Material”, IEEE, 2002.
- [31] Hayato Shimizu etc, “Numerical Simulation of Positioning Error Caused by Air Flow-Induced Vibration of Head Gimbals Assembly in Hard Disk Drive”, IEEE Transactions on Manetics, VOL.39, No.2, March 2003
- [32] Suk, M. et al, “Role of disk surface roughness on slider flying height and air-bearing frequency”, Magnetics, IEEE Transactions on Volume 26, Issue 5, Sep 1990  
Pages(s): 2493-2495
- [33] Brian H. Thornton, D. B. Bogy, and C. S. Bhatia, “The Effects of Disk Morphology on Flying-Height Modulation: Experiment and Simulation”, IEEE Trans. Magn, January 2002

- [34] Eldridge, D., Audio, "Magnetic recording and reproduction of pulses", IRE Transactions on Volume 8, Issue 2, Part 1, Mar 1960 Pages(s): 42-57
- [35] Z.Yuan et al, "Tolerance of magnetic properties and its effects on in-situ flying height testing" in Proc. Intermag, 2002. Paper DP-05
- [36] Yufeng Li, "Write-Induced Pole-Tip-Protrusion and Its Effect on Head-Disk Interface Clearance", IEEE Transactions on Magnetics, VOL.40, No.4, July 2004, Pages: 3145-3147
- [37] Ka Wei Ng et al, "Spacing Fluctuation Induced by Disk Clamping Distortion", IEEE Transactions on Magnetics, Vol.39, No.5, Sep 2003
- [38] Yuan, S, W; bertran, H.N, "Off-track spacing loss of shielded MR heads", Magnetics, IEEE Transactions on Volume 30, Issue 3, May 1994 Pages(s):1267-1273
- [39] Youping Deng et al, "Drive-Level Flying Height Measurements and Altitude Effects", IEEE Transactions on Magnetics, Vol.30, No.6, Nov 1994
- [40] Cha, E et al, "Effect of temperature and altitude on flying height", Magnetics, IEEE Transactions on Vol 32, Issue 5, Part 1, Sep 1996, Page(s): 3729-3731